逆境学课程考核 · 范例 1 文献翻译（整合版）

草地退化改变植物与土壤生物多样性—生态系统多功能性的关系

Grassland degradation alters plant and soil biodiversity–multifunctionality relationships

项目	内容
期刊	Nature Plants（自然·植物）
卷期页码	2025, 11(12): 2487–2497
在线发表	2025 年 11 月 10 日
DOI	10.1038/s41477-025-02147-x
影响因子 / 分区	15.0（2025 JCR）；中科院 1 区 Top
第一作者	高晓霞、张典业（共同第一作者）
通讯作者	杨元合（中国科学院植物研究所）
课程	逆境学 · 论文翻译（范例 1）

本文档结构：一、原文（英文全文）｜二、中文翻译｜三、思维导图｜四、摘要翻译

姓名：_____　学号：_____　班级：草业 2402　日期：2026 年 11 月

目　录

一、原文（英文全文） 3

二、中文翻译 20

三、思维导图 35

四、摘要翻译 37

附：原论文完整 PDF（24 页） 38

一、原文（英文全文）

> 本节为原论文英文正文与图注的文字版，由论文 PDF 逐页提取重排（保留小节标题与全部图注）。参考文献（原 PDF 第 22–24 页）与补充材料为图像排版，未参与文本提取；斜体学名、上标引用序号在文字版中未保留，完整原文见本文档末附录 PDF（PDF 版）／原论文（Word 版按提交要求不含附录）。

Biodiversity is known to promote ecosystem multifunctionality (EMF), but how grassland degradation influences the relationship between biodiversity and EMF remains unclear. Here, using paired observations at 44 sites (a total of 792 sampling quadrats) along a 2,600 km transect, we test how moderate grassland degradation influences 20 surrogates of ecosystem functions, EMF, plant richness, soil bacterial, fungal and protist richness, and biodiversity–EMF relationships in Tibetan alpine grasslands. Our results reveal significant declines in individual ecosystem functions and EMF with moderate grassland degradation. By contrast, both plant richness and integrated soil biodiversity exhibit significant increases. The structural equation models analyses show that following degradation, the effect of soil biodiversity on EMF strengthens, whereas that of plant richness weakens. These findings offer large-scale empirical evidence that moderate grassland degradation can amplify both soil biodiversity and its functional importance, emphasizing the key role of below-ground biodiversity in supporting ecosystem functioning in degraded grasslands.

Anthropogenic activities and climate change are driving unprecedented changes in biodiversity1,2. Given the central role of biodiversity in sustaining ecosystem functioning3, such shifts may fundamentally affect key ecosystem functions including plant productivity, soil carbon (C) storage and C emission rates, ultimately influencing the overall ecosystem multifunctionality (EMF)4,5. The indirect impact of changes in biodiversity on ecosystem functioning may rival or even exceed the direct effects of anthropogenic activities and climate change6,7. Moreover, the strength of the biodiversity–ecosystem functioning (BEF) relationships can vary under changing environmental conditions8,9, even when biodiversity remains constant. Nevertheless, empirical evidence on how BEF relationships respond to real-world environmental changes remains scarce, with most current knowledge coming from biodiversity manipulation experiments conducted at small spatial scales8–10. Consequently, it remains uncertain whether the positive BEF relationships persist across natural ecosystems facing the intensified human pressures and climate change.

As anthropogenic activities and climate change intensify, there is a growing urgency to elucidate how environmental changes alter biodiversity and the BEF relationships across natural ecosystems. Theoretically, biodiversity may increase if environmental changes promote interspecific facilitation11, enhance environmental heterogeneity12 or reduce the abundance of species that monopolize resources13. Conversely, biodiversity may decline due to the intensified interspecific competition14 or habitat loss15, processes that frequently lead to species exclusion. Moreover, environmental changes can strengthen or weaken BEF relationships by enhancing or reducing the complementarity effect, because interspecific facilitation and complementarity improve community resource-use

efficiency9,16. Environmental changes can also influence BEF relationships via other community attributes, such as species composition and evenness17. Particularly, when species turnover exacerbates the differences in functions provided by individual species, the positive effect of biodiversity on EMF may strengthen markedly, even if species richness remains unchanged18. However, current understanding of how environmental changes influence the relationship between ecosystem functioning and soil biodiversity remains limited. To date, most research has focused primarily on plant diversity8,9, despite that soil biodiversity is increasingly recognized as a fundamental regulator of terrestrial ecosystem functioning19. Yet, soil communities themselves are vulnerable to anthropogenic activities and climate change20. This highlights a pressing need for large-scale empirical studies exploring how environmental changes influence the associations of ecosystem functioning with both above-and below-ground biodiversity in natural ecosystems.

Grasslands rank among the most extensive terrestrial ecosystems and are frequently subjected to degradation. Globally, ~49% of grasslands have undergone some degree of degradation, primarily due to anthropogenic disturbances such as overgrazing, overexploitation or climate change21. The Tibetan Plateau hosts the world’ s largest alpine grassland ecosystem, where degradation has accelerated in recent decades, with the moderate degradation stage now representing the most widespread form22. This degradation has often been linked to sub-stantial changes in soil environmental conditions, ecosystem functioning and the biodiversity and composition of both plant and microbial communities23–25. Consequently, the Tibetan Plateau provides a unique, large spatial-scale natural setting for investigating how environmental changes influence BEF relationships. It has been reported that following grassland degradation, there is a notable decline in plant productivity. Meanwhile, the cover of highly productive grasses and sedges, which are resource-monopolizing clonal plants26,27, decreases, while the cover of forbs increases24,25. Grassland degradation can also alter microbial community composition and interspecific interactions23. Considering these points, we hypothesize that (1) grassland degradation impairs the overall ecosystem functioning; (2) grassland degradation can promote biodiversity by providing additional niche space for the colonization of other species or decrease biodiversity following severe habitat destruction21,25; (3) biodiversity–EMF relationships may strengthen or weaken depending on how grassland degradation alters interspecific interactions and community composition.

To test these hypotheses, we conducted a field survey in paired non-degraded and degraded grasslands at 44 sites which were all located in the transition zone between non-degraded and degraded grasslands (Fig. 1). Grassland degradation status was assessed based on a comprehensive grassland degradation index (GDI) that integrated plant community cover, composition and key soil parameters. All degraded landscapes included in this study were classified as moderately degraded based on this index (Methods). At each site, three blocks were set up, each containing both non-degraded and degraded landforms (Extended Data Fig. 1). Within each block, a 30 m × 30 m plot was demarcated in both non-degraded and degraded grasslands. From each plot, three randomly selected 1 m × 1 m quadrats were used for vegetation surveys and collection of plant and soil samples. We measured 20 indicators of 9 ecosystem functions related to plant productivity; soil water holding

capacity; pools of soil C, nitrogen (N) and phosphorus (P); C hydrolases; N hydrolases; phosphatase; and oxidases for each quadrat (Methods). Based on 16S and 18S ribosomal RNA gene amplicon sequencing, we determined both above- and below-ground biodiversity, that is, species richness of plant, bacteria, fungi and protists. In total, our study comprised 792 sampling quadrats (44 sites × 2 degradation levels × 3 blocks × 3 quadrats), encompassing ~16,000 observations of ecosystem functions and ~5 million biodiversity records (averaging ~14, 5,500, 220 and 550 records for plant, soil bacteria, fungi, and protists within each quadrat). This extensive dataset provides a robust foundation to enhance our mechanistic understanding of whether and how BEF relationships shift during grassland degradation.

Reduced ecosystem function upon grassland degradation

Our results showed that most individual ecosystem functions decreased with grassland degradation ($P < 0.05$; Fig. 2a and Supplementary Table 1), supporting our first hypothesis. The average magnitude of the decline in individual ecosystem functions was 20.3 ± 2.5% (hereafter, data are shown as mean ± standard error). EMF, calculated based on a weighted approach28, also decreased markedly from 0.21 ± 0.02 to 0.15 ± 0.01 following degradation ($P = 0.0001$; Fig. 2b). These results were consistent across alternative EMF metrics, including averaged EMF28, multiple-threshold EMF29 and the EMF based on Hill numbers30 (Extended Data Fig. 2). The decrease in EMF under grassland degradation can be attributed to several factors. First, the decline in EMF upon grassland degradation is primarily driven by livestock grazing. In fact, the degraded alpine grasslands involved in the study experience overgrazing24. Herbivore grazing and trampling directly damages vegetation, leading to a substantial reduction in above- and below-ground plant biomass. This decline in plant-derived organic matter inputs corresponds to diminished soil C and N pools, accompanied by reduced rates of organic matter decomposition. These changes collectively underpin the observed deterioration in EMF.

Second, the decline in EMF is associated with alterations of the plant and soil microbial communities. Grassland degradation typically leads to remarkable alterations in plant and microbial community composition23,24. Specifically, the relative abundance of grasses and sedges decreased, whereas that of forbs increased in degraded grasslands (Extended Data Fig. 3). Forbs are typically less productive than grasses and sedges in alpine grasslands26, so the expansion of forbs tends to decrease EMF. Moreover, grassland degradation favours microbes that are less efficient in organic matter decomposition and nutrient turnover. For example, degradation increased the proportion of slow-growing, resource-conservative oligotrophic bacteria31 (Extended Data Fig. 4), which may further lead to the lower EMF observed in degraded grasslands.

Third, the weakened EMF may also be attributed to the alterations of physical processes, for example, soil erosion and evapotranspiration. Specifically, grassland degradation in alpine grasslands disrupts the above-ground vegetation and below-ground mattic layer (consisting of a dense root mat32; Supplementary Fig. 1). The surface vegetation and mattic layer serve essential functions in decelerating water flow, pre-venting soil erosion and enhancing soil water holding capacity32. The destruction of these protective layers intensifies evapotranspiration and soil erosion and further

exacerbates the decline of EMF in alpine grasslands. In addition, the enhanced compaction of soil from over-grazing24 can restrict the penetration of oxygen, consequently reducing soil organic matter decomposition and negatively impacting EMF.

Grassland degradation increases plant richness and soil biodiversity

Our results revealed that moderate degradation significantly promoted plant species richness by 2.0 ± 0.5 species across the 44 sites

> Fig. 1 | Sampling sites and vegetation community of non-degraded and degraded grasslands. a, Distributions of the 44 sampling sites in Tibetan alpine grasslands. b, Images of contrasting non-degraded and degraded grasslands show that plant productivity and the proportion of grasses and sedges (for example, S. purpurea and K. humilis) decreases, while the proportion of forbs (for example, Leontopodium nanum and Stellera chamaejasme) increases upon degradation. Photographs were taken in Sahuteng Town (32.91° N, 95.20° E,

(non-degraded versus degraded: 13.2 ± 0.9 versus 15.1 ± 1.0; P = 0.0044; Fig. 3a). The following two reasons may account for the observed increase in plant species richness: First, the reduction in the proportion of clonal plants enhances community diversity. In non-degraded alpine grasslands, dominant clonal species such as Kobresia pygmaea, K. tibetica and Stipa purpurea are able to monopolize above-ground light and below-ground nutrients through their dense ramets and unique resource-sharing strategies (interconnected ramets of a single genet can share photosynthates and nutrients via rhizomes or stolons27), thereby impeding the colonization and growth of other species. It follows that, in degraded conditions, the reduction in clonal plant cover (P < 0.001; Extended Data Fig. 5) is likely to provide additional niche space for the colonization of other plant species and thus enhance plant species richness.

Second, increased plant species richness may be linked to the alteration of environmental heterogeneity. Environmental heterogeneity is widely recognized as a fundamental driver of biodiversity, with heightened heterogeneity facilitating available habitat space for species with different niches12. As mentioned above, the degradation in alpine grasslands is largely attributable to overgrazing21,24, and

> altitude 4,109 m; marked with a red box in a) in August 2021 by Xiaoxia Gao. National boundary layer in a from the Standard Map Service Website (https://cloudcenter.tianditu.gov.cn/administrativeDivision, approval number GS(2024)0650). Elevation data are from the Shuttle Radar Topography MissionDigital Elevation Model95 and vegetation data are from a digitalized map of China’ s vegetation, scaled at 1:1,000,000 (ref. 53).

herbivore activities such as foraging, trampling and excretion typically increase environmental heterogeneity (Supplementary Fig. 2). This amplified environmental heterogeneity promotes species coexistence and augments plant richness in degraded grasslands. Nevertheless, it should be noted that, although moderate degradation (as in our study) can enhance plant richness, severe and extreme degradation have been shown to lead to biodiversity loss24,25.

Similar to plant richness, we found that moderate grassland degradation augmented soil biodiversity by analysing amplicon sequence variants (ASVs) for soil bacteria, fungi and protists (Fig. 3b–e). The richness of soil bacteria, fungi and protists increased from 5,309.3 ± 127.4, 204.8 ± 6.7 and 520.2 ± 18.3 in non-degraded grasslands to 5,757.0 ± 97.9, 238.4 ± 10.1 and 581.8 ± 27.4 in degraded grasslands (all P < 0.05; Fig. 3c–e), respectively. The integrated soil biodiversity (mean biodiversity

across the three taxa after min–max standardization33) also significantly increased from 0.45 ± 0.02 to 0.56 ± 0.03 across the 44 sites upon degradation (P = 0.0002; Fig. 3b). These increases in soil biodiversity following moderate degradation may be attributable to alterations in plant richness and soil physicochemical conditions. First, elevated plant richness likely supplies a broader

Fig. 2 | Responses of ecosystem functions to grassland degradation. a, The individual ecosystem functions' responses to grassland degradation. The response values are calculated as (FDG − FND)/FND × 100%, where FDG is the value of the corresponding functions in degraded grasslands (DG), and FND is the value of corresponding functions in non-degraded grasslands (ND). The dots and the horizontal line represent means ± standard error (n = 44 independent sites). b, Comparison of EMF in non-degraded and degraded grasslands (n = 44 independent sites). The points (main panel) are the EMF values derived from the weighted approach28 at the site level, and the dashed line is the 1:1 line. The ends of the box plot (insert panel) denote the 25th and 75th quartiles; whiskers extend to 1.5 times the standard deviation; the horizontal line inside each box shows the median value. Linear mixed models with a correction for environmental covariates were used to conduct statistical comparisons of individual functions variety of root exudates and litter inputs, which can mitigate inter-specific competition and support the coexistence of more diverse soil microbial communities34. In line with this point, our results showed significantly positive relationships between soil biodiversity and plant richness in both non-degraded and degraded grasslands (P < 0.001; Extended Data Fig. 6). Thus, soil biodiversity enhances as plant species richness increases following degradation.

Second, shifts in soil physicochemical conditions, such as pH, are also key drivers of soil biodiversity35. Previous studies suggest that, within a specific pH range, from acidic to weakly alkaline, soil biodiversity generally increases with soil pH36. Our results are consistent with this pattern, as shown by the higher soil pH observed in degraded grasslands (Supplementary Fig. 3), which may contribute to the enhanced soil biodiversity. The underlying mechanisms can be attributed to the fact that low pH accelerates the leaching of soil base cations, such as calcium ions and magnesium ions, that are essential for biological growth37. Furthermore, reduced pH can increase the mobilization of toxic heavy metals, including aluminium and manganese38, posing additional threats to microbial survival. In addition, the increased soil environmental heterogeneity within degraded grassland (Supplementary Fig. 2) probably also fosters the coexistence of soil microorganisms, thereby promoting soil biodiversity39.

Altered biodiversity–multifunctionality relationships following grassland degradation

Based on the structural equation model (SEM), we assessed the relative contributions of climate factors (mean annual temperature and precipitation), grassland degradation intensity, plant richness and soil biodiversity to EMF for both non-degraded and degraded grasslands (Fig. 4). The results showed that grassland degradation directly reduced EMF and also indirectly influenced EMF through biodiversity.

and EMF between non-degraded and degraded grasslands. Climate and soil factors were treated as covariates, site and grassland type (alpine steppe, alpine meadow or swamp meadow) were treated as random factors. The reported two-sided P value was not corrected for multiple comparisons, and detailed F-statistics are presented in Supplementary Table 1. AGB, above-ground biomass; BGB, below-ground biomass; WHC, soil water holding capacity; SOC, soil organic carbon, DOC, dissolved organic carbon; MBC, microbial biomass

carbon; TN, total nitrogen; DTN, dissolved total nitrogen; DIN, dissolved inorganic nitrogen; MBN, microbial biomass nitrogen; TP, total phosphorus; AP, available phosphorus; MBP, microbial biomass phosphorus; BG, β-1,4-glucosidase; CB, β-1,4-cellobiosidase; NAG, β-1,4-N-acetylglucosaminidase; LAP, leucine aminopeptidase; Pase, phosphatase; POX, polyphenol oxidases; PEO, peroxidase.

In non-degraded grasslands, the standardized path coefficient of plant richness on EMF was 0.26 (P = 0.0479), while that in degraded grasslands was 0.22 (P = 0.2033). Conversely, the standardized effect of soil biodiversity on EMF increased from 0.03 (P = 0.8071) in non-degraded grasslands to 0.48 (P = 0.0301) in degraded grasslands (Fig. 4). These findings indicated that grassland degradation weakened the relationship between plant richness and EMF but strengthened the relationship between soil biodiversity and EMF.

Our finding about microbial diversity being unrelated to EMF in non-degraded grasslands (Fig. 4a) conflicts with previous studies that state that both plant richness and soil biodiversity exhibit significant positive effects on ecosystem functions across Tibetan alpine grasslands40. One possible explanation is that our analyses account for key confounding factors, including covariate effects (climate factors and GDI) and the random effect associated with grassland type (Supplementary Fig. 4)41. It is worth noting that when data were pooled across degradation states, we observed a significantly positive biodiversity–EMF relationship for plants, but not for soil biota (Supplementary Fig. 4b), even though grassland degradation reduced EMF yet promoted biodiversity. This pattern aligns with the trends observed in non-degraded grasslands. These results reflect that the effects of grassland degradation on EMF and biodiversity are less than their spatial variations across the study sites.

The observed shift in the dominant driver of EMF from plant richness in non-degraded grasslands to soil biodiversity in degraded grasslands (Fig. 4) is supported by previous studies reporting that the determinants of EMF transition from above- to below-ground diversity under harsh environmental conditions42,43. Given that plant production serves as the foundation of EMF, plant richness positively influences EMF in non-degraded grasslands by affecting matter and energy inputs42. Meanwhile, microbes in Tibetan alpine grasslands

Fig. 3 | Comparisons of plant richness and soil biodiversity in non-degraded and degraded grasslands. a, Change in plant richness following grassland degradation. b–e, Changes in integrated soil biodiversity (b), and bacterial (c), fungal (d) and protist (e) richness following grassland degradation. The points (main panel) are the values for each site, and the dashed line in each panel is the 1:1 line. The white dots in insert panels in a and b represent the median values, and the points on the left-hand side show the distribution of data (n = 44 independent sites). The ends of the box in insert panels in c–e denote the 25th and 75th quartiles, and whiskers extend to 1.5 times the standard deviation; the horizontal line inside each box shows the median value (n = 44 independent sites). Plant richness was calculated as the mean number of species across exhibit functional redundancy across species44. Collectively, only plant richness significantly affects EMF in non-degraded grasslands. By contrast, plant-derived resources decline in degraded grasslands, which enhances the dependence of ecosystem functioning on micro-bial decomposers42,43. Accordingly, soil biodiversity plays a critical role in degraded grasslands by regulating decomposition and nutrient transformation processes, thereby affecting EMF.

We further investigated the specific mechanisms driving the differential changes in above- and below-ground biodiversity–EMF relationships. These differences may be attributed to the divergent responses of interspecific interactions and community compositions to grassland degradation between plants and soil biota. For plant communities, the proportion of poisonous weeds (for example, S. chamaejasme; Supplementary Fig. 5) significantly increased in degraded grasslands (Extended Data Fig. 7). Poisonous weeds can inhibit the growth of neighbouring plants through the exudation of allelochemicals such as coumarins, flavonoids and phenolic compounds45. This suggests a probable intensification in interspecific competition but decline in complementarity effect (interspecific facilitation and resource use complementarity46) during grassland degradation. Concurrently, as mentioned above, the proportion of highly productive dominant grasses and sedges declined (Extended Data Fig. 3), which were associated with enhanced plant community evenness (Extended Data Fig. 8) but decreased selection effect (highly productive species promote ecosystem functioning46). Collectively, the weakened plant richness–EMF relationship with degradation may be due to the declines

> the nine quadrats in each site, whereas the richness of soil bacteria, fungi and protists was determined as the mean number of amplicon sequence variants. Soil biodiversity is the mean of the standardized richness across the bacteria, fungi and protists33,73. Linear mixed models with a correction for environmental covariates were used to conduct statistical comparisons of biodiversity metrics between non-degraded and degraded grasslands. Climate and soil factors were treated as covariates, while site and grassland type (alpine steppe, alpine meadow or swamp meadow) were treated as random factors. ND, non-degraded grasslands; DG degraded grasslands. All the reported two-sided P values were not corrected for multiple comparisons, and detailed F-statistics are presented in Supplementary Table 1.

complementarity effect (increased interspecific competition) and/ or downward selection effect (reductions in high functioning dominants)9,46, although further experimental validation is required to identify the exact mechanisms.

For soil biota, the enhanced soil biodiversity–EMF relationship following grassland degradation arises from the following two aspects. First, grassland degradation may promote the interspecific facilitation and resource use complementarity among soil biota. To illustrate this point, we assessed the alteration of the complementarity effect following grassland degradation by examining the interspecific cohesion derived from species co-occurrence patterns (detailed determination of microbial cohesion is outlined in Supplementary Note 1). Cohesion serves as a widely adopted proxy for microbial interactions, with positive cohesion indicating potential complementary interactions among taxa and negative cohesion suggesting competitive interactions47. Our results showed that, following grassland degradation, the positive cohesion among soil microorganisms increased ($P < 0.001$; Extended Data Fig. 9), while the negative cohesion did not show a significant change ($P = 0.7464$). These results suggest that degradation promotes facilitative interactions and complementary resource use among soil microorganisms, thereby reinforcing the biodiversity–EMF relationship in degraded grasslands.

Second, the alteration in soil biodiversity–EMF relationship may result from changes in microbial community composition and evenness. Grassland degradation altered microbial community

composition, notably increasing the relative abundance of Gemmatimonadota

> Fig. 4 | SEMs illustrating the direct and indirect effects of abiotic and biotic factors on EMF. a, Pathways of abiotic and biotic factors affecting EMF in non-degraded grasslands. b, Pathways of abiotic and biotic factors affecting EMF in degraded grasslands. The rationale of the SEM is shown in Supplementary Table 2. Grassland degradation index is constructed by integrating plant community cover, composition and key soil parameters, with higher values signifying more severe degradation. Soil biodiversity is the mean of the standardized richness across the bacteria, fungi and protists33,73. Solid arrows indicate marginal significant relationships ($P < 0.1$), with blue arrows representing positive effects and red arrows representing negative effects. Dashed black arrows denote non-significant relationships ($P \geqslant 0.1$). Path coefficients (numbers adjacent to arrows) represent standardized regression weights, and values in top-right parentheses are the two-sided P values with no adjustment for multiple comparisons. During the construction of the SEM, grassland type (alpine steppe, alpine meadow or swamp meadow) was treated as the random effect. The significance of the SEMs was test using Fisher’ s C statistics. MAT, mean annual temperature; MAP, mean annual precipitation; R2 M and R2 C marginal and conditional R2; AIC, Akaike information criterion.

(Extended Data Fig. 10). This phylum is known to play a critical role in nitrogen metabolism and had the potential to accelerate nutrient cycling48. It is well established that a higher proportion of species that increase nutrient availability can enhance BEF relationships49. Thus, the rise in Gemmatimonadota abundance likely contributes to the strengthened soil biodiversity–EMF relationship in degraded grasslands. Along with the enrichment of Gemmatimonadota, microbial evenness also increased (Extended Data Fig. 8). Under this scenario, elevated community evenness can promote interspecific facilitation and resource use complementarity50 and thus enhance soil biodiversity–EMF relationship in degraded grasslands. It is important to note that, although this study linked biodiversity and EMF based on the SEM (an analysis that has been widely used in this research field40,42,51), statistical correlations do not necessarily reflect true causal relationships. To more rigorously assess changes in the biodiversity–EMF relationship and elucidate underlying mechanisms, future studies should implement experimental manipulations through dual-factor experiments that systematically vary both degradation levels and biodiversity.

In summary, through a comprehensive large-scale field survey across Tibetan alpine grasslands, this study investigated the effects of grassland degradation on EMF, above- and below-ground biodiversity and their interrelationships. Our results showed a significant decrease in EMF, alongside notable increases in both plant species richness and soil biodiversity in moderately degraded grasslands. The relationship between soil biodiversity and EMF was more pronounced in degraded grasslands than in non-degraded ones, while the effect of plant richness on EMF weakened. These findings suggest that below-ground biodiversity plays a critical role in sustaining ecosystem functioning in degraded grasslands, an observation that is consistent with empirical evidence showing that management practices that aim to enhance soil biodiversity (for example, addition of microbial fertilizer52) can effectively restore ecosystem functioning in degraded grasslands. Although previous studies have indicated that environmental changes can strengthen the relationship between plant diversity and ecosystem functioning8,9, we present large-scale evidence for the augmentation of the association between soil biodiversity and EMF following grassland degradation. This finding emphasizes the fact

that alterations in below-ground biodiversity must be considered to achieve a more comprehensive understanding of how anthropogenic activities and climate change influence ecosystem functioning.

Methods

Study area and site description This study was carried out on the Tibetan Plateau (Fig. 1a), which covers ~2.5 × 106 km2. It is the world’ s largest and highest plateau with an average elevation exceeding 4,000 m above sea level53. Alpine grasslands cover 60% of the plateau and comprise alpine steppe, alpine meadow and swamp meadow. Alpine steppe displays relatively low levels of plant productivity and soil organic carbon content, and the primarily dominating species are S. purpurea and Carex moorcroftii26,54,55. By contrast, alpine meadow and swamp meadow have relatively high levels of plant productivity and soil organic carbon content26,54,55. The dominating species are K. pygmaea and K. humilis in alpine meadow and K. tibetica in swamp meadow26,54,55. Alpine grasslands provide forage for ~13 million yak and 50 million Tibetan sheep56 that support the livelihoods of 5 million pastoralists and agropastoralists. Primarily due to overgrazing, ~40% of the alpine grasslands on the Tibetan Plateau have experienced degradation22,24,57.

To assess the impacts of grassland degradation on plant richness, soil biodiversity and ecosystem functions, we conducted an extensive field survey across the Tibetan Plateau during the peak growing seasons (July to August) of 2021 and 2022. Our study used a paired sampling design, comparing non-degraded and degraded grasslands at 44 spatially distributed sites (Fig. 1a). Details concerning geographical information and sampling year are given in Supplementary Table 3. The climate factors were similar between the two sampling years (Supplementary Fig. 6), with R2 values for 2021–2022 mean annual temperature and mean annual precipitation being 0.94 and 0.86, respectively. The 44 study sites comprised 16 alpine steppes, 24 alpine meadows and 4 swamp meadows and spanned a wide range of climatic conditions, with mean annual temperature ranging from −4.1 to 3.2 °C and mean annual precipitation from 233 to 941 mm. According to the World Reference Base for Soil Resources classification58, the major soil types at the sites were Cambisols, Cryosols, Calcisols, Chernozems and Kastanozems.

All the sampling sites were located in the transition zone between non-degraded and degraded grasslands. Livestock grazing has been continuously practiced across the study area for at least 40 years, with a mean grazing intensity of 88.2 ± 7.7 sheep unit per km2 (data extracted from ref. 59). Apart from grazing, no other management actions, such as fertilization, irrigation and sowing were observed across our study area. Both the non-degraded and degraded grasslands were grazed, but the grazing management regime at the study sites permitted winter grazing only, with no grazing allowed during the summer (the season in which samples were collected). The uneven spatial pattern of grazing (for example, degraded grasslands were typically close to the entrance of the pasture and experienced heavier grazing pressure compared to the non-degraded areas) was the primary driver for the formation of distinct patches of non-degraded and degraded grasslands within a specific site60.

Evaluation of grassland degradation We assessed the degree of grassland degradation at each study site by using a comprehensive GDI. The GDI integrated plant community cover, composition and key soil parameters, which are widely recognized indicators of grassland degradation21,61,62. The formula used to calculate GDI was as follows: where NDVI is the normalized differential vegetation index determined by CM1000-NDVI meter (Beijing Yinchitech), degeneration indicator species are shown in Supplementary Table 4, climax species are grasses and sedges for steppe and meadow, soil moisture is measured gravimetrically, and soil bulk density is determined by dividing the oven-dried mass of soil core by its volume (100 cm3). In principle, these parameters should be standardized against baseline values from undisturbed grasslands before GDI calculation. However, due to data limitations, undisturbed reference values were unavailable across the broad geographic scale. Given this situation, we established site-specific baselines by using the maximum observed value for each parameter across the non-degraded areas at each site63. The standardization for each site was performed using the following equation: where Parameterstandardized is the standardized value used for GDI computation, Parameterobserved represents the measured data, and Parameterbaseline denotes the maximum value of a given metric in any of the areas at a specific site in question.

According to the GDI-based classification system, a higher GDI indicates more intensive degradation. The grassland degradation can be then categorized into four distinct levels: non-degraded (0–0.25), moderately degraded (0.25–0.50), severely degraded (0.50–0.75) and extremely degraded (0.75–1.00)62,64. In this study, non-degraded grasslands exhibited GDI values ranging from 0.06 to 0.23, while degraded grasslands in our study area had values between 0.25 and 0.45 (Supplementary Fig. 7). According to the GDI-based classification, all our degraded grasslands were in the moderate degradation stage, which constitutes the most widespread form of grassland degradation across the Tibetan Plateau22,24,57. The GDI had no significant effect on plant richness in degraded grasslands, despite incorporating information on plant community cover and composition (Supplementary Fig. 8). Thus, the GDI-based classification system was considered objective and could be reliably used to explore the response of plant richness to grassland degradation.

were spaced ~500 m apart. Within each block, a 30 m × 30 m plot was established in both non-degraded and degraded grasslands. In each block, the non-degraded and degraded plots were separated by approximate 55 m, ranging from 50 to 100 m. Subsequently, three 1 m × 1 m sampling quadrats were randomly positioned in each 30 m × 30 m plot within which to conduct vegetation surveys and collect plant and soil samples. Thus, our study comprised 792 replicate sampling quadrats.

During the vegetation investigation, we recorded total vegetation cover and the number and cover of each species present in each 1 m × 1 m quadrat. The sward was then gathered to ground level, and three root cores were collected using a stainless auger with an 8 cm diameter from the upper 30 cm of the soil profile where ~90% of alpine grassland roots are distributed65,66. We carefully rinsed the root material and identified live roots by colour, flexibility and the presence of root hairs66. The above- and below-ground plant material was dried at 65 °C and weighed to determine above- and below-ground biomass. After sampling the plant material, we collected nine soil cores (10 cm depth) from each plot

using a stainless auger (3.5 cm diameter). Following collection, soil samples were sieved through a 2 mm mesh to remove gravel and root material, then homogenized to create composite samples for subsequent analyses.

Measurements of ecosystem functions and calculation of multifunctionality We measured 20 surrogates of ecosystem functions related to plant productivity (above- and below-ground biomass), soil water holding capacity, pools of soil C (soil organic C, dissolved organic C, microbial biomass C), N (total N, total dissolved N, dissolved inorganic N, microbial biomass N) and P (total P, available P, microbial biomass P), as well as organic matter decomposition functions (C hydrolases: β-1,4-glucosidase, β-1,4-cellobiosidase; N hydrolases: β-1,4-N-acetylglucosaminidase, leucine aminopeptidase; phosphatase; oxidases: polyphenol oxidases and peroxidase) for each of the 792 quadrats.

Above- and below-ground biomass were measured using the procedure mentioned above. Soil water holding capacity was determined by re-wetting fresh soil to saturation, followed by drying at 105 °C for 24 h. Concentrations of soil total C and N were measured using an elemental analyser (Vario EL Cube, Elementar), and soil inorganic C was measured via a solid-state infrared carbon-sulfur analyser (Multi EA 4000, Analytik Jena AG); soil organic C was then determined by subtracting inorganic C from the total C in the soil. We determined soil dissolved organic C and dissolved total N content using a multi-N/C 3100 analyser (Multi N/C 3100, Analytik Jena AG) after extraction with 0.5 M K2SO4 and removal of inorganic carbon with HCl. Soil dissolved inorganic N (ammonium and nitrate) concentration was determined using a continuous flow analyser (AutoAnalyzer 3, SEAL Analytic) after extraction with 1 M KCl. Soil total P concentration was quantified using inductively coupled plasma optical emission spectrometry (iCAP 6300, Thermo Fisher Scientific) following high-pressure acid digestion. Soil available P concentration was measured using the molybdenum–antimony colorimetric method67, following extraction with a 0.5 M NaHCO3 solution. Soil microbial biomass C, N and P were measured using the chloroform fumigation method68, following a 7 day pre-incubation at 15 °C (the average summer season temperature in the study area). Universal conversion factors of 0.45, 0.54 and 0.40 were used to calculate microbial biomass C, N and P, respectively68–70.

For the analysis of hydrolase activity, we prepared soil slurries by mixing 2.75 g of fresh soil with 91 ml of buffer (0.05 M sodium acetate). The pH of the buffer was adjusted to correspond with that of the soil. We then added 150 µl of soil slurry and 50 µl of substrate to each well of black 96-well microplates. The specific substrates for β-1,4-glucosidase, β-1,4-cellobiosidase, β-1,4-N-acetylglucosaminidase, leucine aminopeptidase and phosphatase were 4-methylumbelliferone-β-D-glucoside, 4-methylumbelliferone-β-D-cellobioside, 4-methylumbelliferone-Nacetyl-β-D-glucosaminide, L-leucine-7-amino-4-methylcoumarin and 4-methylumbelliferone-phosphate, respectively. The 96-well micro-plates were placed in a 15 °C incubator for 3 h, and the fluorescence intensity of the mixture was then measured using a microplate reader (Synergy H1MF, BioTek Instruments). The excitation and emission wavelengths were 365 and 450 nm71. Hydrolase activities were calculated as nanomoles per gram dry soil per hour using the fluorescence intensity and standard curve71. To account for quenching effects, standard curves were established for soil slurry samples and standards (4-methylumbelliferone for

β-1,4-glucosidase, β-1,4-cellobiosidase, β-1,4-N-acetylglucosaminidase and phosphatase, and 7-amino-4-methylcoumarin for leucine aminopeptidase). Oxidase activity was assayed by adding 50 µl of substrate (polyphenol oxidases: L-3,4-dihydroxy-phenylalanine; peroxidase: L-3,4-dihydroxy-phenylalanine combined with hydrogen peroxide)71, 200 µl of soil slurries and 50 µl EDTA to wells of transparent 96-well microplates. The microplates were incubated at 15 °C for 42 h, and a microplate reader was used to measure absorbance at 450 nm. The oxidase activities were calculated as micromoles per gram dry soil per hour.

To calculate EMF, we first standardized each of the ecosystem functions using min–max standardization methods29. We then calculated the weighted EMF, using agglomerative cluster analysis to down-weight highly correlated functions, following the method described by ref. 28. In addition, we calculated the averaged EMF29, multiple-threshold EMF29 and the EMF based on Hill numbers30 (detailed determinations of EMF are outlined in Supplementary Note 2). Given that the weighted EMF exhibited strong associations with the EMF calculated by other approaches (all R2 > 0.9; Supplementary Fig. 9), we selected the EMF index derived from the weighted approach to conduct the subsequent analyses.

Determination of plant richness and soil biodiversity We simultaneously assessed both plant richness and soil biodiversity. Plant richness was quantified as the total count of species present in each 1 m × 1 m quadrat. Soil biodiversity was assessed based on the ASVs for soil bacteria, fungi and protists. The species richness of soil bacteria, fungi and protists was estimated by the number of ASVs based on the package vegan v2.6-4 (ref. 72). The richness values for each taxonomic group were then standardized by the min–max standardization method33,73. The integrated soil biodiversity was calculated by averaging the standardized richness across the three groups (bacteria, fungi and protists)33,73.

To determine the richness of soil microorganisms, we first extracted soil DNA using the FastDNA SPIN Kit (Qbiogene/MP Biomedicals). DNA quality was evaluated based on absorbance ratios of optical density at 260/280 nm (1.8-1.9) and 260/230 nm (1.7–2.0) measured using a spectrophotometer (NanoDrop 2000, Thermo Fisher Scientific). Amplicon sequencing was then carried out for the V3–V4 regions of bacterial 16S rRNA and the V9 region of eukaryotic 18S rRNA genes using the Illumina PE250 platform with primers 338 F (5′- ACTCCTACGGGAGGCAGCAG-3′) and 806 R (5′-GGACTACHVGGGTWTCTAAT-3′) for 16S74,75 and Euk1391f (5′-GTACACCGCCCGTC-3′) and EukBr (5′-TGATCCTTCTGC AGGTTCACCTAC-3′) for 18S76,77, respectively.

The bioinformatics processing involved several steps using USEARCH v11.0.667 (ref. 78) and VSEARCH v2.15.2 (ref. 79). Raw reads were initially trimmed to eliminate low-quality bases (average quality score < 20 within a 10 bp moving window, and minimum length < 50 bp). Then FLASH v1.2.11 (ref. 80) was used to merge the paired-end reads with at least 10 bp overlap and fewer than 20% mismatches. Effective sequences were then distinguished based on barcode and primer sequences. Further quality control measures involved discarding sequences shorter than 200 bp and those exceeding an expected error rate of 0.01 per sequence using the -fastx_filter function81. After quality control, sequences were dereplicated and denoised using the UNOISE3 algorithm82 with USEARCH v11.0.667 (ref. 78), and

chimeric sequences were removed. Sequences were assigned into ASVs at the 100% identity level, as ASVs provide effective error control and enhance the robustness of downstream analyses83. Taxonomic information for each representative sequence (the most abundant sequence within each ASV) was annotated with a confidence threshold of ⩾0.8 using SILVA v138 (ref. 84) (16S rRNA gene, https://www.arb-silva.de/) and the NCBI Nucleotide Sequence Database85 (18S rRNA gene, annotated using BLASTN v2.14.0+ with the best hit methods, https://ftp.ncbi. nlm.nih.gov/blast/db/). ASV abundance tables were rarefied to 31,514 sequences per sample for bacteria (16S rRNA gene), 6,237 for fungi (18S rRNA gene) and 6,088 for protists (18S rRNA gene) to ensure uniform sampling depth across soil biological communities, respectively. Eukaryotic taxa, excluding fungi, metazoan and Streptophyta, were classified as protists73.

Determination of environmental variables Along with ecosystem functions and biodiversity metrics, we determined a series of climate (mean annual temperature and precipitation) and soil factors (soil pH and moisture) as predictors of ecosystem functions40,86. Among these variables, the mean annual temperature and mean annual precipitation from 2001 to 2020 were obtained from the National Tibetan Plateau Data Center of China (http://data. tpdc.ac.cn)87. Soil pH was measured using PB-10 (Sartorius) in a 1:2.5 soil-to-deionized-water suspension. Soil moisture was measured gravimetrically by oven-drying soil samples at 105°C for 24 h.

Statistical analyses Before the examination of shifts of biodiversity, ecosystem functions and their relationships upon grassland degradation, we averaged the values of each of the individual metrics across the 9 quadrats within each site. This procedure was carried out because the main aim of the study was to investigate how biodiversity–EMF relationships shift upon grassland degradation across broad spatial gradients, and ecosystem heterogeneity within sites was considerably lower than that observed among sites. Thus, averaging data from the 9 quadrats can improve site-level representativeness, reduce observation error and ensure statistical robustness. This analytical approach has been widely adopted in studies with a similar experimental design to ours40,88.

The statistical analyses were then carried out in two steps using the above site-level data. First, the differences in individual ecosystem functions, EMF, plant richness, and soil biodiversity between non-degraded and degraded grasslands were assessed using linear mixed models with a correction for environmental covariates. The formula of the linear mixed models was as follows: where climate and soil factors were treated as covariates, and site and grassland type (alpine steppe, alpine meadow or swamp meadow) were treated as random factors (|). Residuals of the linear mixed models were tested for homoscedasticity and normality.

Second, we conducted the SEM to illustrate the effects of abiotic and biological factors on EMF. Before the construction of the SEM, we assessed the significance of the interaction effect between grassland degradation and biodiversity on EMF9,16 using the following formula: where climate and soil factors were treated as covariates, and site and grassland type (alpine steppe, alpine meadow or swamp meadow) were treated as random factors. Our results showed that plant richness and soil biodiversity exhibited significant interaction effects with grassland degradation on the EMF (all $P < 0.05$).

Accordingly, we conducted separate SEM analyses for non-degraded and degraded grasslands, respectively.

The SEM considered (1) the direct effects of climate factors (mean annual temperature and precipitation), GDI, plant richness and soil biodiversity on EMF. (2) The indirect effects of climate factors on EMF via plant and soil biodiversity. We did not consider the effects of mean annual temperature on biodiversity metrics, because previous studies reported that mean annual precipitation rather than mean annual temperature was the primary driver of the spatial pattern of biodiversity across the Tibetan alpine grasslands40,89. Our data also confirmed that biodiversity metrics exhibited non-significant associations with mean annual temperature (all $P > 0.05$). (3) The indirect effects of GDI on EMF via plant and soil biodiversity. (4) The indirect effects of plant richness on EMF via soil biodiversity. For more details of the SEM, see Supplementary Table 2. During the construction of the SEM, grassland type was treated as the random effect. The standardized path coefficients derived from the SEM were used to explore whether the biodiversity–EMF relationships changed upon grassland degradation. The goodness of the SEM was assessed according to Fisher's C statistic, the Akaike information criterion and the whole-model P value90. The linear mixed model was conducted using the lme4 R package91, and the SEM was carried out using the piecewiseSEM R package90. All statistical analyses were conducted using R 4.2.3 (ref. 92).

Reporting summary Further information on research design is available in the Nature Portfolio Reporting Summary linked to this article.

Data availability

Data used in this study are available from the figshare data repository https://doi.org/10.6084/m9.figshare.30119233 (ref. 93). The sequence data generated in this study have been deposited in the Genome Sequence Archive in National Genomics Data Center, China National Center for Bioinformation https://ngdc.cncb.ac.cn/bioproject/browse/ PRJCA046361 (ref. 94). Source data are provided with this paper.

Acknowledgements

Author contributions

Competing interests

> Extended Data Fig. 1 | Schematic diagram of the sampling design. At a specific site, three blocks were selected, and within each block a 30 × 30 m plot was established in both non-degraded and degraded grasslands. Within each plot, three 1 × 1 m quadrats were randomly chosen to conduct vegetation surveys and collect plant and soil samples (9 soil cores at 0-10 cm depth). Altitude map derived from the Shuttle Radar Topography Mission (SRTM)-Digital Elevation Model (DEML)95. Drone images of contrasting non-degraded and degraded grasslands show that plant productivity and the proportion of grasses and sedges (for example, S. purpurea and K. humilis) decreases while the proportion of forbs (for example, L. nanum and S. chamaejasme) increases upon

degradation. Photos were captured by Qinlu Li in Babao Town (37.86°N, 100.44°E, altitude 3663 m), July 2021. ND, non-degraded grasslands; DG, degraded grasslands.

Extended Data Fig. 2 | Comparisons of ecosystem multifunctionality (EMF) between non-degraded (ND) and degraded grasslands (DG). a, Averaged approach; b, multiple-threshold approach; c, d, hill-number based approaches when q = 1 (c) and q = 2 (d). The open circles shown are the site-level values. The ends of a box denote the 25th and 75th quartiles, and whiskers extend to 1.5 times the standard deviation (n = 44 independent sites). The horizontal line within each box represents the median value. Linear mixed models with a correction for environmental covariates were employed to conduct statistical comparisons between non-degraded and degraded grasslands across the 44 sites. Climate and soil factors were treated as covariates, site and grassland type (alpine steppe, alpine meadow or swamp meadow) were treated as random factors. All the reported two-sided P values were not corrected for multiple comparisons, and detailed F-statistics were presented in Supplementary table 1.

Extended Data Fig. 3 | Comparisons of plant community in non-degraded (ND) and degraded grasslands (DG). a, Cover of grasses and sedges; b, cover of forbs. The dashed lines indicate median values; solid lines represent the values for each site (n = 44 independent sites). Linear mixed models with a correction for environmental covariates were employed to conduct statistical comparisons between non-degraded and degraded grasslands across the 44 sites (cover of grasses and sedges: $F_{1,46.72} = 276.01$, $P = 3.10 \times 10^{-21}$; cover of forbs: $F_{1, 44.72} = 52.66$, $P = 4.40 \times 10^{-9}$; the two-sided P values were not corrected for multiple comparisons). Climate and soil factors were treated as covariates, site and grassland type (alpine steppe, alpine meadow or swamp meadow) were treated as random factors.

Extended Data Fig. 4 | Differences in the relative abundance of copiotrophic and oligotrophic bacteria between non-degraded (ND) and degraded grasslands (DG). a, Copiotrophic bacteria; b, oligotrophic bacteria. The ends of a box denote the 25th and 75th quartiles, and whiskers extend to 1.5 times the standard deviation (n = 44 independent sites). The horizontal line within each box represents the median value. The open circles represent the values for each site. Linear mixed models with a correction for environmental covariates were employed to conduct statistical comparisons between non-degraded and degraded grasslands across the 44 sites (copiotrophic bacteria: $F_{1,51.14} = 5.69$, $P = 0.0209$; oligotrophic bacteria: $F_{1, 51.01} = 6.46$, $P = 0.0141$; the two-sided P values were not corrected for multiple comparisons). Climate and soil factors were treated as covariates, site and grassland type (alpine steppe, alpine meadow or swamp meadow) were treated as random factors. The demarcations of copiotrophic and oligotrophic bacteria were as follows31, oligotrophs: Acidobacteriota, Actinobacteriota, Planctomycetota, Chloroflexi, Verrucomicrobiota, Cyanobacteria; copiotrophs: Firmicutes, Gemmatimonadota, Bacteroidota, Proteobacteria. Copiotrophic bacteria are generally fast-slowing and resource acquisitive, while oligotrophic bacteria tend to be slow-growing and resource conservative31.

Extended Data Fig. 5 | Differences in cover of clonal and non-clonal plants in non-degraded (ND) and degraded grasslands (DG). a, Clonal plants; b, non-clonal plants. The horizontal line within each box represents the median value; the open circles represent the values for each site (n = 44 independent sites). Linear mixed models with a correction for environmental covariates were employed to conduct statistical comparisons between non-degraded and degraded grasslands across the 44 sites (cover of clonal plants: $F_{1,47.77} = 265.38$, $P = 3.89 \times 10^{-21}$; cover of non-clonal plants: $F_{1, 44.67} = 39.42$, $P = 1.24 \times 10^{-7}$; the two-sided P values were not corrected for multiple comparisons). Climate and soil factors were treated as covariates, site and grassland type (alpine steppe, alpine meadow or swamp meadow) were treated as random factors.

Extended Data Fig. 6 | Relationships between soil biodiversity and plant richness in non-degraded (ND) and degraded grasslands (DG). Soil biodiversity was calculated by averaging biodiversity across the three taxa (soil

bacteria, fungi and protists) after standardization33,73. Linear mixed models (n = 44 independent sites) were used to determine the linkages between soil biodiversity and plant richness, with grassland type (alpine steppe, alpine meadow or swamp meadow) being treated as the random factor (non-degraded grasslands: $F_{1,42} = 27.68$, $P = 4.55 \times 10{-}6$; degraded grasslands: $F_{1,41.71} = 24.97$, $P = 1.09 \times 10{-}5$; the two-sided P values were not corrected for multiple comparisons). Shaded areas are the 95% confidence intervals; the open circles are the values for each site. Soil biodiversity still exhibited significant linkages with plant richness when considering the environmental covariates (climate and soil factors).

Extended Data Fig. 7 | Differences in cover of poisonous weeds in non-degraded (ND) and degraded grasslands (DG). The ends of a box denote the 25th and 75th quartiles, and whiskers extend to 1.5 times the standard deviation. The open circles represent the values for each site (n = 44 independent sites). Linear mixed models with a correction for environmental covariates were employed to conduct statistical comparisons between non-degraded and degraded grasslands across the 44 sites ($F_{1,48.06} = 34.34$, $P = 4.08 \times 10{-}7$; the two-sided P value was not corrected for multiple comparisons). Climate and soil factors were treated as covariates, site and grassland type (alpine steppe, alpine meadow or swamp meadow) were treated as random factors.

Extended Data Fig. 8 | Comparisons of plant and microbial community evenness between non-degraded (ND) and degraded grasslands (DG). a, Plant evenness; b, bacteria evenness; c, fungi evenness; d, protist evenness. The ends of a box denote the 25th and 75th quartiles, and whiskers extend to 1.5 times the standard deviation (n = 44 independent sites). The horizontal line within each box represents the median value. The open circles represent the values for each site. Linear mixed models with a correction for environmental covariates were employed to conduct statistical comparisons between non-degraded and degraded grasslands across the 44 sites (plant: $F_{1,48.52} = 143.60$, $P = 4.15 \times 10{-}16$; bacteria: $F_{1, 42.24} = 11.05$, $P = 0.0018$; fungi: $F_{1, 48.86} = 4.45$, $P = 0.0400$; protist: $F_{1, 50.95} = 0.25$, $P = 0.6211$; the two-sided P values were not corrected for multiple comparisons). Climate and soil factors were treated as covariates, site and grassland type (alpine steppe, alpine meadow or swamp meadow) were treated as random factors.

Extended Data Fig. 9 | Comparisons of microbial interspecific cohesion between non-degraded (ND) and degraded grasslands (DG). a, Microbial positive cohesion; b, microbial negative cohesion. The ends of a box denote the 25th and 75th quartiles, and whiskers extend to 1.5 times the standard deviation (n = 44 independent sites). The open circles represent the values for each site, the horizontal line within each box represents the median value. Linear mixed models with a correction for environmental covariates were employed to conduct statistical comparisons between non-degraded and degraded grasslands across the 44 sites (positive cohesion: $F_{1,49.67} = 24.93$, $P = 7.71 \times 10{-}6$; negative cohesion: $F_{1, 41.20} = 0.11$, $P = 0.7464$; the two-sided P values were not corrected for multiple comparisons). Climate and soil factors were treated as covariates, site and grassland type (alpine steppe, alpine meadow or swamp meadow) were treated as random factors.

Extended Data Fig. 10 | Comparisons of microbial community composition between non-degraded (ND) and degraded grasslands (DG). a, Bacterial community composition; b, fungal community composition; c, protist community composition. Data shown in this figure are the relative abundance of microbes at the level of phylum. Community composition of bacteria, fungi and protist all exhibited significant changes following degradation according to permutational multivariable analysis of variance (all $P < 0.05$). Linear mixed models with a correction for environmental covariates were employed to conduct statistical comparisons of the relative abundance of each microbial group between non-degraded and degraded grasslands across the 44 sites. Climate and soil factors were treated as covariates, site and grassland type (alpine steppe, alpine meadow or swamp meadow) were treated as random factors. The plus (+) and minus (-) signs denote that

> microbial taxa significantly increase or decrease, respectively, following grassland degradation. All the reported two-sided P values were not corrected for multiple comparisons.

二、中文翻译

摘要

生物多样性已知能够促进生态系统多功能性（ecosystem multifunctionality，EMF），但草地退化如何影响生物多样性与 EMF 之间的关系，目前仍不清楚。本研究沿一条 2 600 km 长的样带，在青藏高原高寒草地的 44 个样点（合计 792 个采样样方）开展配对观测，检验中度草地退化如何影响 20 项生态系统功能替代指标、EMF、植物丰富度、土壤细菌/真菌/原生生物丰富度以及生物多样性—EMF 关系。结果表明，中度草地退化使各项生态系统功能和 EMF 均显著下降；与之相反，植物丰富度和综合土壤生物多样性却显著上升。结构方程模型分析显示，退化之后土壤生物多样性对 EMF 的作用增强，而植物丰富度的作用减弱。这些发现提供了大尺度实证证据，表明中度草地退化可同时放大土壤生物多样性及其功能重要性，凸显了地下生物多样性在支撑退化草地生态系统功能中的关键作用。

Abstract (原文)

Biodiversity is known to promote ecosystem multifunctionality (EMF), but how grassland degradation influences the relationship between biodiversity and EMF remains unclear. Here, using paired observations at 44 sites (a total of 792 sampling quadrats) along a 2,600 km transect, we test how moderate grassland degradation influences 20 surrogates of ecosystem functions, EMF, plant richness, soil bacterial, fungal and protist richness, and biodiversity–EMF relationships in Tibetan alpine grasslands. Our results reveal significant declines in individual ecosystem functions and EMF with moderate grassland degradation. By contrast, both plant richness and integrated soil biodiversity exhibit significant increases. The structural equation models analyses show that following degradation, the effect of soil biodiversity on EMF strengthens, whereas that of plant richness weakens. These findings offer large-scale empirical evidence that moderate grassland degradation can amplify both soil biodiversity and its functional importance, emphasizing the key role of below-ground biodiversity in supporting ecosystem functioning in degraded grasslands.

引言

人为活动和气候变化正以前所未有的速度改变着生物多样性。鉴于生物多样性在维持生态系统功能中的核心作用，这种改变可能从根本上影响植物生产力、土壤碳（C）储量与碳排放速率等关键生态系统功能，并最终影响生态系统多功能性（EMF）的整体水平。生物多样性变化对生态系统功能的间接影响，可能与人为活动和气候变化的直接效应相当，甚至更强。此外，即使生物多样性本身保持不变，生物多样性—生态系统功能（BEF）关系的强度也可能随环境条件的改变而变化。然而，关于 BEF 关系如何响应真实世界环境变化的实证证据仍然稀缺，现有认识大多来自小空间尺度上的人为生物多样性控制实验。因此，在人类活动压力与气候变化不断加剧的自然生态系统中，正向的 BEF 关系是否依然成立，仍存在不确定性。

随着人为活动和气候变化加剧，阐明环境变化如何改变自然生态系统中的生物多样性及 BEF 关系已日益紧迫。从理论上讲，若环境变化促进种间促进作用、增强环境异质性或降低垄断资源物种的丰度，生物多样性

可能上升；反之，若种间竞争加剧或生境丧失，生物多样性可能下降，因为这类过程往往导致物种被排除。此外，环境变化还可通过增强或削弱互补效应来改变 BEF 关系的强弱，因为种间促进和互补性能够提高群落资源利用效率。环境变化也可经由物种组成、均匀度等其他群落属性影响 BEF 关系。特别地，当物种周转加剧了个体物种所提供功能之间的差异时，即使物种丰富度不变，生物多样性对 EMF 的正效应也可能显著增强。然而，目前关于环境变化如何影响生态系统功能与土壤生物多样性之间关系的认识仍然有限。迄今为止，多数研究主要聚焦于植物多样性，尽管土壤生物多样性正日益被视为陆地生态系统功能的基本调控者。而土壤生物群落本身也易受人为活动和气候变化的影响。这凸显出开展大尺度实证研究的迫切需求，以探究环境变化如何影响自然生态系统中生态系统功能与地上、地下生物多样性之间的联系。

草地是分布最广的陆地生态系统之一，且频繁遭受退化。全球约 49% 的草地已发生不同程度的退化，主要驱动因素包括过度放牧、过度利用或气候变化等人为干扰。青藏高原拥有世界上最大的高寒草地生态系统，近几十年来其退化不断加速，其中中度退化阶段是目前分布最广的形式。草地退化往往与土壤环境条件、生态系统功能以及植物和微生物群落的多样性与组成发生显著变化相联系。因此，青藏高原为研究环境变化如何影响 BEF 关系提供了一个独特的大空间尺度天然平台。已有报道显示，草地退化后植物生产力显著下降；与此同时，具有资源垄断能力的高产禾草和莎草（克隆植物）盖度下降，而杂类草盖度上升。草地退化还可改变微生物群落组成和种间相互作用。综合上述认识，我们提出以下假设：（1）草地退化损害生态系统的整体功能；（2）草地退化可通过为其他物种定殖提供额外的生态位而促进生物多样性，也可能在生境严重破坏后导致生物多样性下降；（3）生物多样性—EMF 关系可能增强或减弱，取决于草地退化如何改变种间相互作用与群落组成。

为检验上述假设，我们在 44 个样点开展了非退化与退化草地的配对野外调查，所有样点均位于非退化与退化草地之间的过渡带（图 1）。草地退化状况依据一个综合的草地退化指数（grassland degradation index，GDI）评估，该指数整合了植物群落盖度、组成和关键土壤参数。基于该指数，本研究所涉及的退化景观均被判定为中度退化（见“方法”）。每个样点设置 3 个区组，每个区组均包含非退化与退化两种地貌（扩展数据图 1）。在每个区组内，分别于非退化草地和退化草地划定一个 30 m × 30 m 的样地；每个样地中随机选取 3 个 1 m × 1 m 的样方，用于植被调查以及植物与土壤样品的采集。我们对每个样方测定了与植物生产力、土壤持水量、土壤碳/氮/磷库、碳水解酶、氮水解酶、磷酸酶和氧化酶有关的 9 类生态系统功能的 20 项指标（见“方法”）。基于 16S 和 18S rRNA 基因扩增子测序，我们测定了地上和地下生物多样性，即植物、细菌、真菌和原生生物的物种丰富度。总体而言，本研究共包含 792 个采样样方（44 个样点 × 2 个退化水平 × 3 个区组 × 3 个样方），涵盖约 16 000 条生态系统功能观测值和约 500 万条生物多样性记录（每个样方平均约 14、5 500、220 和 550 条植物、土壤细菌、真菌和原生生物记录）。这一大规模数据集为深入理解草地退化过程中 BEF 关系是否以及如何发生转变提供了坚实基础。

结果

1. 草地退化导致生态系统功能下降

结果表明，大多数单项生态系统功能随草地退化而下降（$P < 0.05$；图 2a、补充表 1），支持我们的第一个假设。单项生态系统功能的平均下降幅度为 20.3 ± 2.5%（下文中数据均以平均值 ± 标准误表示）。基于加权法计算的 EMF 在退化后也由 0.21 ± 0.02 显著降至 0.15 ± 0.01（$P = 0.0001$；图 2b）。这一结果在多种替代

EMF 指标下均保持一致，包括平均法 EMF、多阈值 EMF 以及基于 Hill 数的 EMF（扩展数据图 2）。草地退化下 EMF 的下降可归因于以下几个方面。

第一，退化导致的 EMF 下降主要由家畜放牧驱动。事实上，本研究涉及的退化高寒草地长期处于过度放牧状态。草食动物的采食和践踏直接破坏植被，导致地上和地下植物生物量大幅减少。植物源有机质输入的下降，对应着土壤碳、氮库的缩减以及有机质分解速率的降低。这些变化共同构成了所观察到的 EMF 退化的基础。

第二，EMF 的下降与植物和土壤微生物群落的改变有关。草地退化通常会引起植物和微生物群落组成的显著变化。具体而言，退化草地中禾草和莎草的相对多度下降，而杂类草上升（扩展数据图 3）。在高寒草地中，杂类草的生产力通常低于禾草和莎草，因此杂类草的扩张往往会降低 EMF。此外，草地退化更有利于那些在有机质分解和养分周转中效率较低的微生物。例如，退化提高了生长缓慢、资源保守的寡营养型细菌的比例（扩展数据图 4），这可能进一步导致退化草地中较低的 EMF。

第三，EMF 的减弱也可能归因于物理过程的改变，例如土壤侵蚀和蒸散。具体而言，高寒草地的退化破坏了地上植被和地下草毡层（由密集根系交织而成；补充图 1）。地表植被和草毡层在减缓水流、防止土壤侵蚀和提高土壤持水量方面具有重要功能。这些保护层遭到破坏后，蒸散和土壤侵蚀加剧，进一步加重了高寒草地 EMF 的下降。此外，过度放牧引起的土壤压实增强会限制氧气下渗，从而降低土壤有机质分解，对 EMF 产生负面影响。

2. 草地退化提高植物丰富度与土壤生物多样性

结果表明，中度退化在 44 个样点上使植物物种丰富度显著增加 2.0 ± 0.5 种（非退化与退化草地分别为 13.2 ± 0.9 种与 15.1 ± 1.0 种；P = 0.0044；图 3a）。以下两方面原因可能解释所观察到的植物物种丰富度上升。

第一，克隆植物比例的下降提高了群落多样性。在未退化的高寒草地中，Kobresia pygmaea、K. tibetica 和 Stipa purpurea 等优势克隆物种能够通过其密集的分株和独特的资源共享策略（同一基株相互连接的分株可经由根状茎或匍匐茎共享光合产物和养分）垄断地上光照与地下养分，从而阻碍其他物种的定殖和生长。由此可以推断，在退化条件下，克隆植物盖度的降低（P < 0.001；扩展数据图 5）很可能为其他植物物种的定殖提供了额外的生态位空间，进而提高了植物物种丰富度。

第二，植物物种丰富度的增加可能与环境异质性的改变有关。环境异质性被广泛认为是生物多样性的基本驱动因素，异质性提高可为具有不同生态位的物种提供更多可利用的生境空间。如前所述，高寒草地的退化在很大程度上归因于过度放牧，而采食、践踏和排泄等草食动物活动通常会提高环境异质性（补充图 2）。这种被放大的环境异质性促进了物种共存，从而提高了退化草地中的植物丰富度。但需要指出的是，尽管中度退化（如本研究所见）能够提高植物丰富度，已有研究表明严重和极度退化会导致生物多样性丧失。

与植物丰富度类似，我们通过分析土壤细菌、真菌和原生生物的扩增子序列变体（ASVs）发现，中度草地退化提高了土壤生物多样性（图 3b–e）。土壤细菌、真菌和原生生物的丰富度分别由非退化草地的 5 309.3 ± 127.4、204.8 ± 6.7 和 520.2 ± 18.3 上升至退化草地的 5 757.0 ± 97.9、238.4 ± 10.1 和 581.8 ± 27.4（均 P < 0.05；图 3c–e）。综合土壤生物多样性（三类群丰富度经极差标准化后的平均值）在 44 个样点上也由 0.45 ± 0.02 显著上升至 0.56 ± 0.03（P = 0.0002；图 3b）。中度退化后土壤生物多样性的提高，可能归因于植物丰富度和土壤理化条件的改变。

第一，植物丰富度的提高可能提供了更丰富的根系分泌物和凋落物输入，从而缓解种间竞争并支持更多样化的土壤微生物群落共存。与这一观点一致，我们的结果显示，在非退化与退化草地中，土壤生物多样性与植物丰富度均呈显著正相关（$P < 0.001$；扩展数据图 6）。因此，退化后土壤生物多样性随植物物种丰富度的增加而提高。

第二，土壤理化条件（如 pH）的变化也是土壤生物多样性的关键驱动因素。已有研究表明，在酸性至弱碱性的特定 pH 范围内，土壤生物多样性通常随土壤 pH 升高而增加。我们的结果与这一规律一致：退化草地中观测到更高的土壤 pH（补充图 3），这可能有助于土壤生物多样性的提高。其潜在机制在于，低 pH 会加速对生物生长至关重要的土壤盐基离子（如钙离子和镁离子）的淋失；此外，pH 降低还会增加铝、锰等有毒重金属的活化，对微生物生存构成额外威胁。另外，退化草地内土壤环境异质性的增加（补充图 2）也可能促进土壤微生物的共存，从而提升土壤生物多样性。

3. 草地退化后生物多样性—多功能性关系的改变

基于结构方程模型（SEM），我们评估了气候因子（年均温与年降水量）、草地退化强度、植物丰富度和土壤生物多样性对非退化与退化草地 EMF 的相对贡献（图 4）。结果表明，草地退化不仅直接降低 EMF，还通过生物多样性间接影响 EMF。在非退化草地中，植物丰富度对 EMF 的标准化路径系数为 0.26（$P = 0.0479$），而在退化草地中为 0.22（$P = 0.2033$）；相反，土壤生物多样性对 EMF 的标准化效应由非退化草地的 0.03（$P = 0.8071$）升高至退化草地的 0.48（$P = 0.0301$）（图 4）。这些发现表明，草地退化削弱了植物丰富度与 EMF 之间的关系，但增强了土壤生物多样性与 EMF 之间的关系。

讨论

我们发现，非退化草地中微生物多样性与 EMF 无关（图 4a），这与以往认为青藏高原高寒草地中植物丰富度和土壤生物多样性均对生态系统功能具有显著正效应的研究结论不一致。一种可能的解释是，我们的分析纳入了关键的混杂因素，包括协变量效应（气候因子和 GDI）以及与草地类型相关的随机效应（补充图 4）。值得注意的是，当把不同退化状态的数据合并分析时，我们观察到植物存在显著为正的生物多样性—EMF 关系，而土壤生物则没有（补充图 4b），尽管草地退化降低了 EMF 却提高了生物多样性。这一格局与非退化草地中观察到的趋势一致。这些结果表明，草地退化对 EMF 和生物多样性的影响小于研究样点间的空间变异。

所观察到的 EMF 主导驱动因子由非退化草地的植物丰富度转向退化草地的土壤生物多样性（图 4），得到了以往研究的支持——那些研究报道，在严酷环境条件下，EMF 的决定因素会由地上多样性转向地下多样性。鉴于植物生产是 EMF 的基础，植物丰富度通过影响物质和能量输入而在非退化草地中对 EMF 产生正效应。与此同时，青藏高原高寒草地的微生物在物种间存在功能冗余。综合来看，在非退化草地中只有植物丰富度显著影响 EMF。相反，在退化草地中植物源资源减少，这增强了生态系统功能对微生物分解者的依赖。因此，土壤生物多样性通过调控分解和养分转化过程，在退化草地中发挥关键作用，进而影响 EMF。

我们进一步探究了驱动地上与地下生物多样性—EMF 关系差异变化的具体机制。这些差异可能归因于植物与土壤生物在种间相互作用和群落组成上对草地退化的响应不同。对于植物群落而言，退化草地中毒杂草（例如 Stellera chamaejasme；补充图 5）的比例显著增加（扩展数据图 7）。毒杂草可通过分泌香豆素、黄酮类和酚类化合物等化感物质抑制邻近植物的生长。这提示草地退化过程中种间竞争可能加剧，而互补效应（种间促进与资源利用互补）可能下降。同时，如前所述，高产的优势禾草和莎草比例下降（扩展数据图 3），这

与植物群落均匀度提高（扩展数据图 8）但选择效应减弱（高产物种促进生态系统功能）相联系。综合来看，随退化而减弱的植物丰富度—EMF 关系，可能源于互补效应下降（种间竞争加剧）和/或选择效应减弱（高功能优势种减少），尽管确切的机制仍需进一步的实验验证。

对于土壤生物而言，草地退化后土壤生物多样性—EMF 关系的增强源于以下两方面。第一，草地退化可能促进土壤生物之间的种间促进和资源利用互补。为说明这一点，我们通过检验由物种共现格局推导出的种间凝聚力（微生物凝聚力的具体测定见补充说明 1），评估了退化后互补效应的变化。凝聚力是微生物相互作用被广泛采用的替代指标：正凝聚力表示类群之间潜在的互补性相互作用，负凝聚力则表示竞争性相互作用。我们的结果显示，草地退化后土壤微生物之间的正凝聚力增强（$P < 0.001$；扩展数据图 9），而负凝聚力无显著变化（$P = 0.7464$）。这些结果提示，退化促进了土壤微生物之间的促进性相互作用和互补性资源利用，从而强化了退化草地中的生物多样性—EMF 关系。

第二，土壤生物多样性—EMF 关系的改变可能源于微生物群落组成和均匀度的变化。草地退化改变了微生物群落组成，尤其提高了 Gemmatimonadota 的相对多度（扩展数据图 10）。该门已知在氮代谢中发挥关键作用，并具有加速养分循环的潜力。已有充分证据表明，提高养分有效性的物种比例越高，BEF 关系越强。因此，Gemmatimonadota 丰度的上升很可能有助于退化草地中土壤生物多样性—EMF 关系的增强。伴随 Gemmatimonadota 的富集，微生物均匀度也上升（扩展数据图 8）。在此情形下，群落均匀度的提高可促进种间促进和资源利用互补，从而增强退化草地中的土壤生物多样性—EMF 关系。需要强调的是，尽管本研究基于 SEM（该分析在研究领域中被广泛使用）将生物多样性与 EMF 联系起来，但统计相关并不必然反映真实的因果关系。为更严谨地评估生物多样性—EMF 关系的变化并阐明其内在机制，未来研究应通过双因子实验开展系统的实验操控，同时改变退化水平和生物多样性。

结论

总之，本研究通过在青藏高原高寒草地开展大规模野外调查，系统考察了草地退化对 EMF、地上与地下生物多样性及其相互关系的影响。结果表明，在中度退化草地中，EMF 显著下降，而植物物种丰富度和土壤生物多样性均显著上升；土壤生物多样性与 EMF 之间的关系在退化草地中比在非退化草地中更为明显，而植物丰富度对 EMF 的效应则减弱。这些发现提示，地下生物多样性在维持退化草地生态系统功能中发挥着关键作用，这一观察与以下实证证据相一致：以提高土壤生物多样性为目标的管理措施（例如施用微生物菌肥）能够有效恢复退化草地的生态系统功能。尽管以往研究表明环境变化可以增强植物多样性与生态系统功能之间的关系，我们提供了草地退化后土壤生物多样性与 EMF 关联增强的大尺度证据。这一发现强调，为实现对人为活动和气候变化如何影响生态系统功能的更全面理解，必须将地下生物多样性的变化纳入考量。

方法

1. 研究区与样点概况

本研究在青藏高原开展（图 1a），该区域面积约 2.5×10^6 km^2，是世界最大、最高的高原，平均海拔超过 4 000 m。高寒草地覆盖高原面积的 60%，包括高寒草原、高寒草甸和沼泽化草甸三种类型。高寒草原的植物生产力和土壤有机碳含量相对较低，优势种主要为 Stipa purpurea 和 Carex moorcroftii；相比之下，高寒草甸和沼泽化草甸的植物生产力和土壤有机碳含量相对较高，高寒草甸的优势种为 Kobresia pygmaea 和 K.

humilis，沼泽化草甸的优势种为 K. tibetica。高寒草地为约 1 300 万头牦牛和 5 000 万只藏羊提供饲草，支撑着 500 万牧民和农牧民的生计。主要由于过度放牧，青藏高原约 40% 的高寒草地已经发生退化。

为评估草地退化对植物丰富度、土壤生物多样性和生态系统功能的影响，我们于 2021 年和 2022 年生长旺季（7—8 月）在青藏高原开展了大规模野外调查。研究采用配对采样设计，在 44 个空间分布的样点上比较非退化与退化草地（图 1a）。地理位置和采样年份的详细信息见补充表 3。两个采样年份的气候因子相近（补充图 6），2021—2022 年年均温和年降水量的 R^2 分别为 0.94 和 0.86。44 个研究样点包括 16 个高寒草原、24 个高寒草甸和 4 个沼泽化草甸，跨越较宽的气候范围，年均温为 −4.1 至 3.2 °C，年降水量为 233 至 941 mm。根据世界土壤资源参比基础分类，样点主要土壤类型为 Cambisols、Cryosols、Calcisols、Chernozems 和 Kastanozems。

所有采样点均位于非退化与退化草地之间的过渡带。研究区至少连续放牧 40 年，平均放牧强度为 88.2 ± 7.7 羊单位/km^2（数据引自文献 59）。除放牧外，研究区内未观察到施肥、灌溉和播种等其他管理措施。非退化与退化草地均进行放牧，但研究样点的放牧管理制度仅允许冬季放牧，夏季（即采样季节）禁止放牧。放牧的空间不均衡格局（例如退化草地通常靠近牧场入口，承受比非退化区域更重的放牧压力）是同一地点内形成非退化与退化草地斑块的主要驱动因素。

2. 草地退化程度的评估

我们采用综合草地退化指数（GDI）评估各研究样点的草地退化程度。GDI 整合了植物群落盖度、组成和关键土壤参数，这些均为公认的草地退化指标。GDI 的计算公式如下：

GDI = 1 − [(0.5 × 植被盖度 + 0.5 × NDVI) × 1/3 + (0.5 × 1/退化指示种相对盖度 + 0.5 × 顶极种相对盖度) × 1/3 + (1/3 × 土壤含水量 + 1/3 × 1/容重 + 1/3 × 1/土壤 pH) × 1/3]　　(1)

式中，NDVI 为采用 CM1000-NDVI 仪（北京依科泰克）测定的归一化植被指数；退化指示种见补充表 4；顶极种在草原和草甸中分别为禾草和莎草；土壤含水量采用重量法测定；土壤容重由环刀土样的烘干质量除以其体积（100 cm^3）计算。原则上，这些参数在计算 GDI 之前应以未受干扰草地的基线值进行标准化。然而，由于数据限制，在大尺度地理范围内无法获得未受干扰的参考值。为此，我们以每个样点非退化区域内各参数的最大观测值作为该样点的基线值进行标准化。各样点的标准化公式为：

参数标准化值 = 参数观测值 / 参数基线值　　(2)

式中，参数标准化值用于 GDI 计算，参数观测值为实测数据，参数基线值为特定样点内任一区域某一指标的最大值。

根据基于 GDI 的分类系统，GDI 越高表示退化越严重。草地退化可划分为四个等级：未退化（0—0.25）、中度退化（0.25—0.50）、重度退化（0.50—0.75）和极度退化（0.75—1.00）。本研究中，非退化草地的 GDI 为 0.06—0.23，退化草地为 0.25—0.45（补充图 7）。按照基于 GDI 的分类，本研究所有退化草地均处于中度退化阶段，这也是青藏高原分布最广的草地退化形式。尽管 GDI 纳入了植物群落盖度和组成信息，但其对退化草地中的植物丰富度无显著影响（补充图 8）。因此，基于 GDI 的分类系统被认为是客观的，可可靠地用于探讨植物丰富度对草地退化的响应。

3. 植物与土壤采样

在每个样点选择 3 个同时包含非退化与退化地貌的区组（扩展数据图 1）。区组间距约 500 m。每个区组内，在非退化与退化草地各建立一个 30 m × 30 m 的样地；同一区组内非退化与退化样地相距约 55 m（范围 50—100 m）。随后，在每个 30 m × 30 m 样地中随机设置 3 个 1 m × 1 m 的采样样方，用于植被调查以及植物和土壤样品采集。因此，本研究共包含 792 个重复采样样方。

植被调查中，我们记录每个 1 m × 1 m 样方的总植被盖度以及每个物种的株数和盖度。随后将草层齐地面剪下；并用直径 8 cm 的不锈钢土钻在 0—30 cm 土层（约 90% 的高寒草地根系分布于此）采集 3 个根系土芯。根系材料经仔细冲洗后，依据颜色、柔韧性和根毛有无鉴定活根。地上和地下植物材料在 65 °C 下烘干并称重，以测定地上和地下生物量。植物样品采集后，用直径 3.5 cm 的不锈钢土钻在每个样地采集 9 个土芯（深度 10 cm）。土壤样品过 2 mm 筛去除砾石和根系后混匀，制成复合样品用于后续分析。

4. 生态系统功能测定与多功能性计算

我们对 792 个样方分别测定了 20 项生态系统功能替代指标，涉及植物生产力（地上和地下生物量）、土壤持水量、土壤碳库（土壤有机碳、可溶性有机碳、微生物生物量碳）、氮库（全氮、可溶性总氮、可溶性无机氮、微生物生物量氮）、磷库（全磷、速效磷、微生物生物量磷）以及有机质分解功能（碳水解酶：β-1,4-葡萄糖苷酶、β-1,4-纤维二糖苷酶；氮水解酶：β-1,4-N-乙酰葡糖胺糖苷酶、亮氨酸氨基肽酶；磷酸酶；氧化酶：多酚氧化酶和过氧化物酶）。

地上和地下生物量按上述方法测定。土壤持水量通过将新鲜土壤复水至饱和后在 105 °C 下烘干 24 h 测定。土壤全碳和全氮浓度采用元素分析仪（Vario EL Cube，Elementar）测定；土壤无机碳采用固态红外碳硫分析仪（Multi EA 4000，Analytik Jena AG）测定；土壤有机碳由全碳减去无机碳得到。土壤可溶性有机碳和可溶性总氮采用 Multi N/C 3100 分析仪（Analytik Jena AG）测定，样品先用 0.5 M K_2SO_4 提取并用 HCl 去除无机碳。土壤可溶性无机氮（铵态氮和硝态氮）浓度采用连续流动分析仪（AutoAnalyzer 3，SEAL Analytical）测定，样品用 1 M KCl 提取。土壤全磷浓度经高压酸消解后采用电感耦合等离子体发射光谱仪（iCAP 6300，Thermo Fisher Scientific）测定；土壤速效磷采用钼锑抗比色法测定，样品用 0.5 M $NaHCO_3$ 溶液提取。土壤微生物生物量碳、氮、磷采用氯仿熏蒸法测定，样品在 15 °C（研究区夏季平均温度）预培养 7 天后进行；微生物生物量碳、氮、磷的换算系数分别为 0.45、0.54 和 0.40。

水解酶活性分析中，将 2.75 g 新鲜土壤与 91 ml 缓冲液（0.05 M 乙酸钠）混合制备土壤悬浊液，缓冲液 pH 调至与土壤一致。随后在黑色 96 孔微孔板的每孔中加入 150 µl 土壤悬浊液和 50 µl 底物。β-1,4-葡萄糖苷酶、β-1,4-纤维二糖苷酶、β-1,4-N-乙酰葡糖胺糖苷酶、亮氨酸氨基肽酶和磷酸酶的底物分别为 4-甲基伞形酮-β-D-葡萄糖苷、4-甲基伞形酮-β-D-纤维二糖苷、4-甲基伞形酮-N-乙酰-β-D-葡糖胺糖苷、L-亮氨酸-7-氨基-4-甲基香豆素和 4-甲基伞形酮-磷酸。微孔板置于 15 °C 培养箱中培养 3 h，随后用酶标仪（Synergy H1MF，BioTek Instruments）测定荧光强度，激发光和发射光波长分别为 365 nm 和 450 nm。水解酶活性依据荧光强度和标准曲线计算，单位为纳摩尔/（克干土 · 小时）。为校正淬灭效应，分别对土壤悬浊液样品和标准品（β-1,4-葡萄糖苷酶、β-1,4-纤维二糖苷酶、β-1,4-N-乙酰葡糖胺糖苷酶和磷酸酶用 4-甲基伞形酮，亮氨酸氨基肽酶用 7-氨基-4-甲基香豆素）建立标准曲线。氧化酶活性测定时，向透明 96 孔板每孔加入 50 µl 底物（多酚氧化酶：L-3,4-二羟基苯丙氨酸；过氧化物酶：L-3,4-二羟基苯丙氨酸 + 过氧化氢）、200 µl 土壤悬浊液和 50 µl EDTA；微孔板在 15 °C 下培养 42 h，用酶标仪测定 450 nm 吸光度。氧化酶活性单位为微摩尔/（克干土 · 小时）。

EMF 计算时，首先采用极差标准化方法对各项生态系统功能进行标准化；随后按文献 28 所述方法，利用凝聚层次聚类分析对高度相关的功能降权，计算加权 EMF。此外，我们还计算了平均法 EMF、多阈值 EMF 和基于 Hill 数的 EMF（EMF 的具体测定见补充说明 2）。鉴于加权 EMF 与其他方法计算的 EMF 高度相关（所有 $R^2 > 0.9$；补充图 9），我们选择加权法得到的 EMF 指数进行后续分析。

5. 植物丰富度与土壤生物多样性的测定

我们同步评估了植物丰富度和土壤生物多样性。植物丰富度以每个 1 m × 1 m 样方中出现的物种总数计。土壤生物多样性基于土壤细菌、真菌和原生生物的 ASVs 评估；细菌、真菌和原生生物的物种丰富度以 ASV 数目表示，使用 vegan v2.6-4 软件包计算。随后对各分类类群的丰富度进行极差标准化；综合土壤生物多样性为三个类群（细菌、真菌、原生生物）标准化丰富度的平均值。

为测定土壤微生物丰富度，首先使用 FastDNA SPIN Kit（Qbiogene/MP Biomedicals）提取土壤 DNA。DNA 质量依据分光光度计（NanoDrop 2000，Thermo Fisher Scientific）测定的 OD260/280（1.8—1.9）和 OD260/230（1.7—2.0）吸光度比值评估。随后利用 Illumina PE250 平台对细菌 16S rRNA 基因 V3—V4 区和真核生物 18S rRNA 基因 V9 区进行扩增子测序；16S 引物为 338F（5′-ACTCCTACGGGAGGCAGCAG-3′）和 806R（5′-GGACTACHVGGGTWTCTAAT-3′），18S 引物为 Euk1391f（5′-GTACACCGCCCGTC-3′）和 EukBr（5′-TGATCCTTCTGCAGGTTCACCTAC-3′）。

生物信息学处理使用 USEARCH v11.0.667 和 VSEARCH v2.15.2 完成。原始 reads 先经修剪去除低质量碱基（10 bp 滑动窗口内平均质量分数 < 20，最短长度 < 50 bp）；再用 FLASH v1.2.11 以至少 10 bp 重叠、错配率低于 20% 的标准拼接双端 reads；依据 barcode 和引物序列区分有效序列。进一步质控包括：利用 -fastx_filter 功能剔除长度短于 200 bp 及每条序列期望错误率超过 0.01 的序列。质控后，使用 UNOISE3 算法在 USEARCH v11.0.667 中对序列去重和降噪，并去除嵌合序列。序列在 100% 相似度水平上归为 ASVs，因为 ASVs 能有效控制错误并提高下游分析的稳健性。每条代表性序列（各 ASV 中丰度最高的序列）的分类信息以 ⩾0.8 的置信阈值注释：16S rRNA 基因使用 SILVA v138，18S rRNA 基因使用 NCBI 核酸序列数据库（BLASTN v2.14.0+，最佳命中法）。ASV 丰度表分别抽平至每样品细菌 31 514 条序列、真菌 6 237 条序列和原生生物 6 088 条序列，以保证土壤生物群落的采样深度一致。除真菌、后生动物和链型植物外的真核类群被归类为原生生物。

6. 环境变量的测定

除生态系统功能和生物多样性指标外，我们还测定了系列气候因子（年均温和年降水量）和土壤因子（土壤 pH 和含水量）作为生态系统功能的预测变量。其中，2001—2020 年的年均温和年降水量取自国家青藏高原科学数据中心（http://data.tpdc.ac.cn）；土壤 pH 采用 PB-10（Sartorius）在土壤与去离子水 1:2.5 悬浊液中测定；土壤含水量采用重量法，将土样在 105 °C 下烘干 24 h 测定。

7. 统计分析

在检验草地退化后生物多样性、生态系统功能及其关系的变化之前，我们先将每个样点内 9 个样方的各项指标取平均值。这样做是因为本研究的主要目的是探究生物多样性—EMF 关系如何在较大空间梯度的草地退化过程中发生转变，而样点内的生态系统异质性远低于样点间异质性。因此，对 9 个样方的数据取平均可提高样点代表性、减少观测误差并保证统计稳健性；这一分析方法在实验设计类似的研究中已被广泛采用。

随后，利用样点水平数据进行两步统计分析。第一步，采用校正环境协变量的线性混合模型评估非退化与退化草地之间单项生态系统功能、EMF、植物丰富度和土壤生物多样性的差异。线性混合模型公式如下：

Y ~ 退化 + 年均温 + 年降水量 + 土壤 pH + 土壤含水量 + (1|样点) + (1|草地类型)　　(3)

式中，气候和土壤因子作为协变量，样点和草地类型（高寒草原、高寒草甸或沼泽化草甸）作为随机因子（|)。对线性混合模型的残差进行了方差齐性和正态性检验。

第二步，构建 SEM 以阐明非生物和生物因子对 EMF 的影响。构建 SEM 之前，我们采用下式评估草地退化与生物多样性对 EMF 的交互效应显著性：

EMF ~ 退化 × 生物多样性 + 年均温 + 年降水量 + 土壤 pH + 土壤含水量 + (1|样点) + (1|草地类型)　　(4)

式中，气候和土壤因子作为协变量，样点和草地类型作为随机因子。结果表明，植物丰富度和土壤生物多样性均与草地退化对 EMF 存在显著交互效应（均 $P < 0.05$）。据此，我们分别对非退化草地和退化草地构建 SEM。

SEM 考虑了：（1）气候因子（年均温和年降水量）、GDI、植物丰富度和土壤生物多样性对 EMF 的直接效应；（2）气候因子经由植物和土壤生物多样性对 EMF 的间接效应——我们未考虑年均温对生物多样性指标的影响，因为已有研究报道年降水量而非年均温是青藏高原高寒草地生物多样性空间格局的主要驱动因子，且我们的数据也证实生物多样性指标与年均温无显著关联（均 $P > 0.05$）；（3）GDI 经由植物和土壤生物多样性对 EMF 的间接效应；（4）植物丰富度经由土壤生物多样性对 EMF 的间接效应。SEM 的更多细节见补充表 2。构建 SEM 时，草地类型作为随机效应。利用 SEM 得到的标准化路径系数探讨生物多样性—EMF 关系是否随草地退化而改变。SEM 的拟合优度依据 Fisher’s C 统计量、赤池信息量准则（AIC）和整体模型 P 值评估。线性混合模型使用 R 语言 lme4 软件包完成，SEM 使用 piecewiseSEM 软件包完成；所有统计分析均在 R 4.2.3 中进行。

8. 数据可用性

本研究数据可从 figshare 数据仓库获取（https://doi.org/10.6084/m9.figshare.30119233）。本研究产生的序列数据已存入国家基因组科学数据中心（NGDC）的 Genome Sequence Archive（https://ngdc.cncb.ac.cn/bioproject/browse/PRJCA046361）。论文附有源数据。

图表中文翻译

图 1｜非退化与退化草地的采样点与植被群落

图注译文：a，青藏高原高寒草地 44 个采样点的分布。b，非退化与退化草地的对比影像显示，退化后植物生产力以及禾草和莎草（例如 S. purpurea 和 K. humilis）的比例下降，而杂类草（例如 Leontopodium nanum 和 Stellera chamaejasme）的比例上升。照片由高晓霞于 2021 年 8 月在萨呼腾镇（32.91° N，95.20° E，海拔 4 109 m；a 中红框所示）拍摄。a 中界线数据来自标准地图服务网站（https://cloudcenter.tianditu.gov.cn/administrativeDivision，审图号 GS(2024)0650）。高程数据来自航天飞机雷达地形测绘任务数字高程模型（SRTM-DEM），植被数据来自 1:1 000 000 中国植被数字化图。

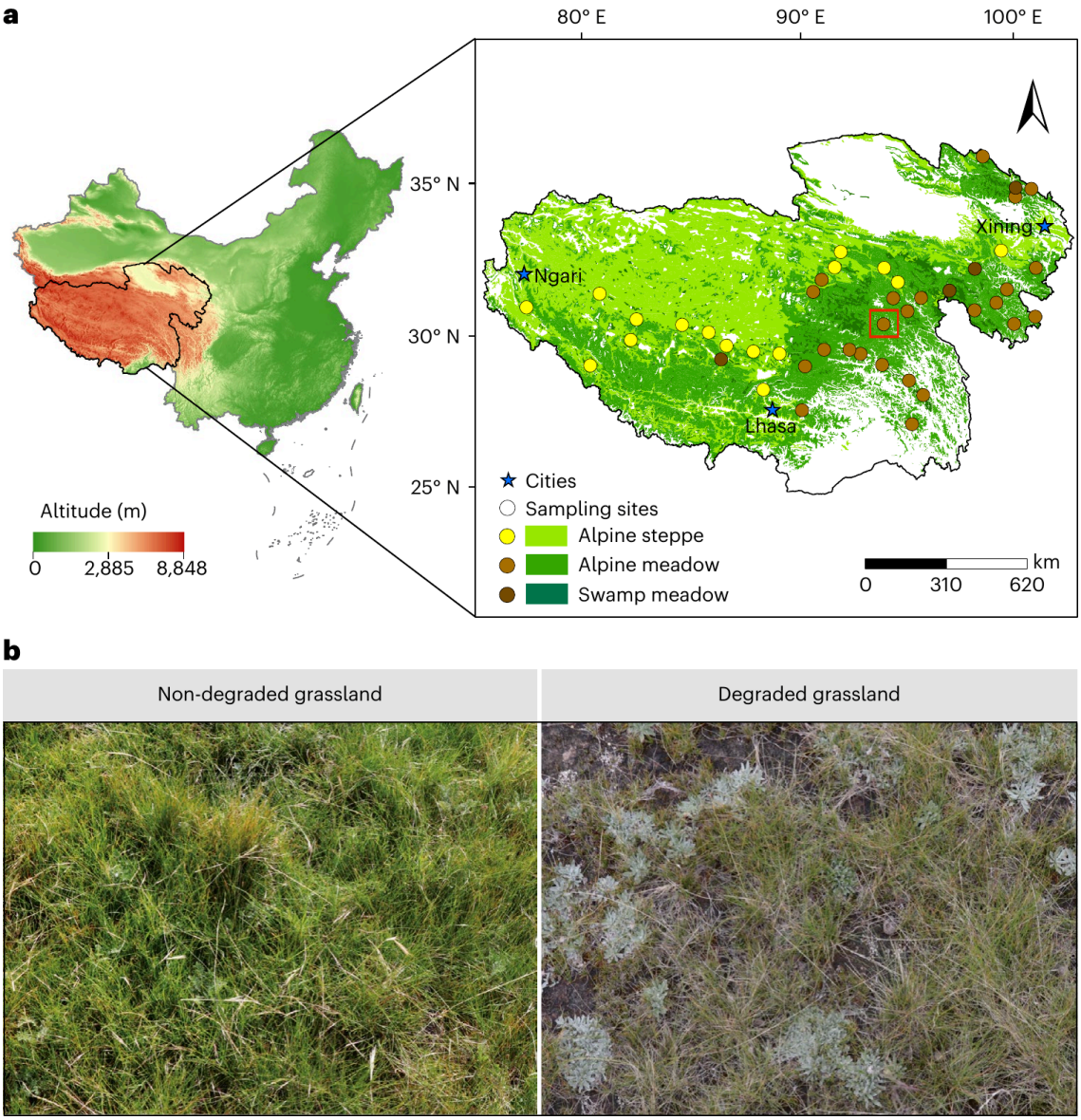


图 1

图 2 | 生态系统功能对草地退化的响应

图注译文：a，各单项生态系统功能对草地退化的响应。响应值按 (F_DG − F_ND)/F_ND × 100% 计算，其中 F_DG 为退化草地（DG）中相应功能的值，F_ND 为非退化草地（ND）中相应功能的值。圆点与水平线分别表示平均值 ± 标准误（n = 44 个独立样点）。b，非退化与退化草地 EMF 的比较（n = 44 个独立样点）。主图中的点为依据加权法得到的样点水平 EMF 值，虚线为 1:1 线；插图箱线图的两端表示第 25 和第 75 四分位数，须线延伸至标准差的 1.5 倍，箱内水平线为中位数。采用校正环境协变量的线性混合模型对非退化与退化草地的单项功能和 EMF 进行统计比较：气候和土壤因子作为协变量，样点和草地类型（高寒草原、高寒草甸或沼泽化草甸）作为随机因子。报告的双侧 P 值未进行多重比较校正，详细 F 统计量见补充表 1。AGB，地上生物量；BGB，地下生物量；WHC，土壤持水量；SOC，土壤有机碳；DOC，可溶性有机碳；MBC，微生物生物量碳；TN，全氮；DTN，可溶性总氮；DIN，可溶性无机氮；MBN，微生物生物量氮；TP，全磷；AP，速效磷；MBP，微生物生物量磷；BG，β-1,4-葡萄糖苷酶；CB，β-1,4-纤维二糖苷酶；NAG，β-1,4-N-乙酰葡糖胺糖苷酶；LAP，亮氨酸氨基肽酶；Pase，磷酸酶；POX，多酚氧化酶；PEO，过氧化物酶。

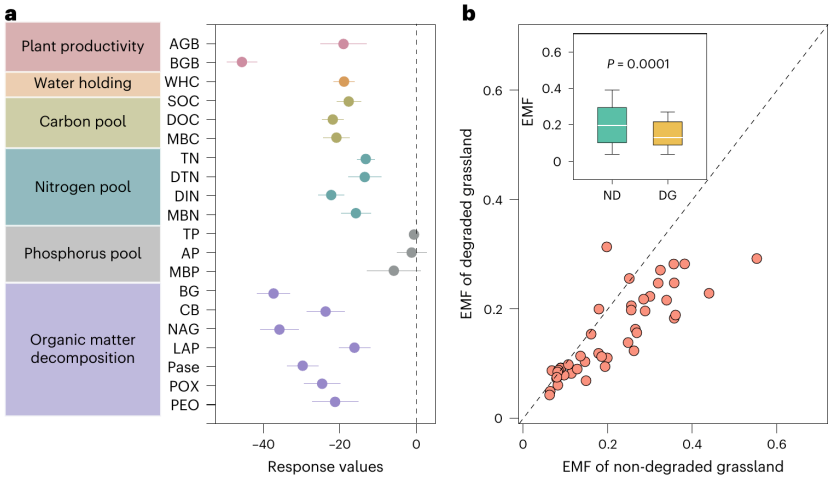


图 2

图 3｜非退化与退化草地植物丰富度和土壤生物多样性的比较

图注译文：a，草地退化后植物丰富度的变化。b–e，草地退化后综合土壤生物多样性（b）以及细菌（c）、真菌（d）和原生生物（e）丰富度的变化。主图中的点为各样点的值，各面板中虚线为 1:1 线。a 和 b 插图箱线图中的白色圆点表示中位数，左侧的点表示数据分布（n = 44 个独立样点）。c–e 插图箱线图的两端表示第 25 和第 75 四分位数，须线延伸至标准差的 1.5 倍，箱内水平线为中位数（n = 44 个独立样点）。植物丰富度为每个样点 9 个样方物种数的平均值；土壤细菌、真菌和原生生物的丰富度以扩增子序列变体数目的平均值确定。土壤生物多样性为细菌、真菌和原生生物标准化丰富度的平均值。采用校正环境协变量的线性混合模型对非退化与退化草地的生物多样性指标进行统计比较：气候和土壤因子作为协变量，样点和草地类型作为随机因子。ND，非退化草地；DG，退化草地。报告的双侧 P 值均未进行多重比较校正，详细 F 统计量见补充表 1。

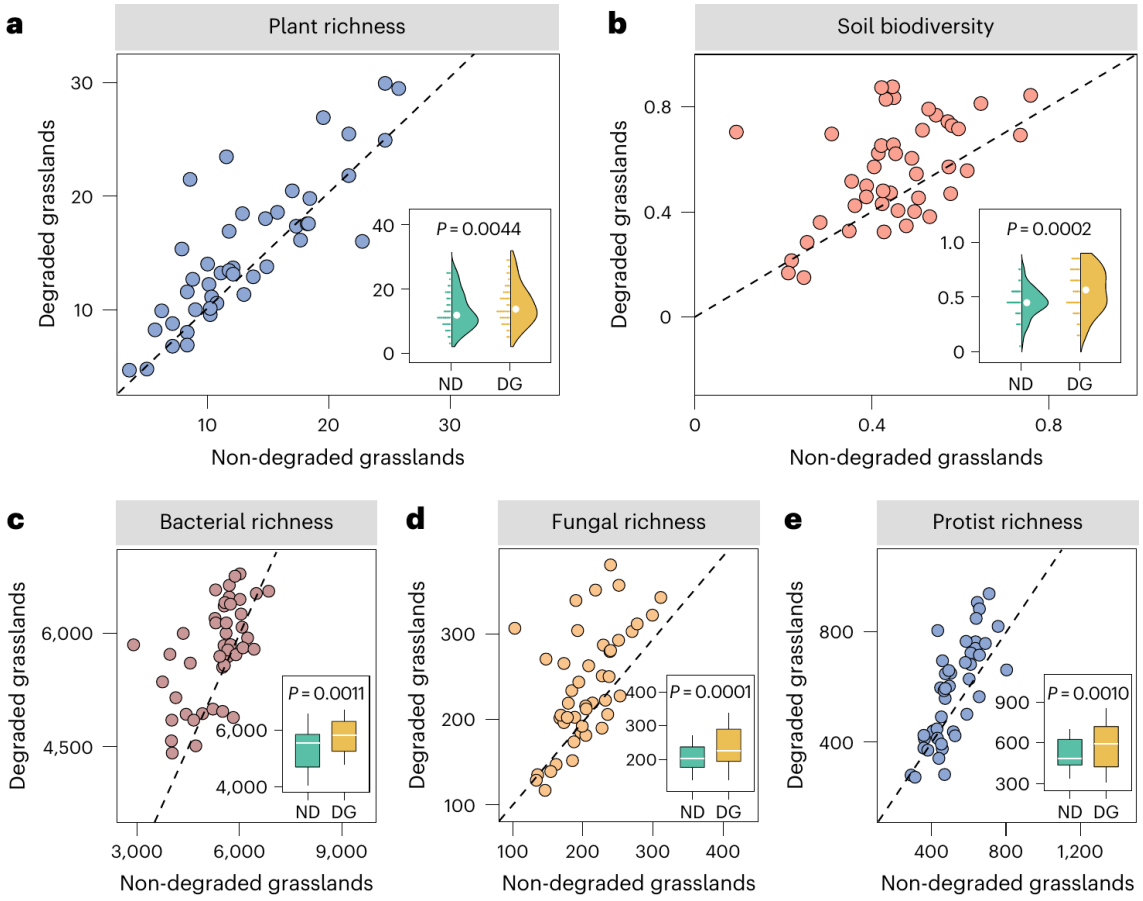


图 3

图 4｜非生物与生物因子对 EMF 直接和间接效应的结构方程模型

图注译文：a，非退化草地中非生物与生物因子影响 EMF 的路径。b，退化草地中非生物与生物因子影响 EMF 的路径。SEM 的构建依据见补充表 2。草地退化指数由植物群落盖度、组成和关键土壤参数综合构建，数值越高表示退化越严重。土壤生物多样性为细菌、真菌和原生生物标准化丰富度的平均值。实线箭头表示边缘显著关系（$P < 0.1$），蓝色箭头表示正效应，红色箭头表示负效应；黑色虚线箭头表示不显著关系（$P \geqslant 0.1$）。路径系数（箭头旁数字）为标准化回归权重，右上角括号内为未作多重比较校正的双侧 P 值。构建 SEM 时，草地类型（高寒草原、高寒草甸或沼泽化草甸）作为随机效应。SEM 的显著性采用 Fisher’s C 统计量检验。MAT，年均温；MAP，年降水量；R^2M 和 R^2C 分别为边际 R^2 和条件 R^2；AIC，赤池信息量准则。

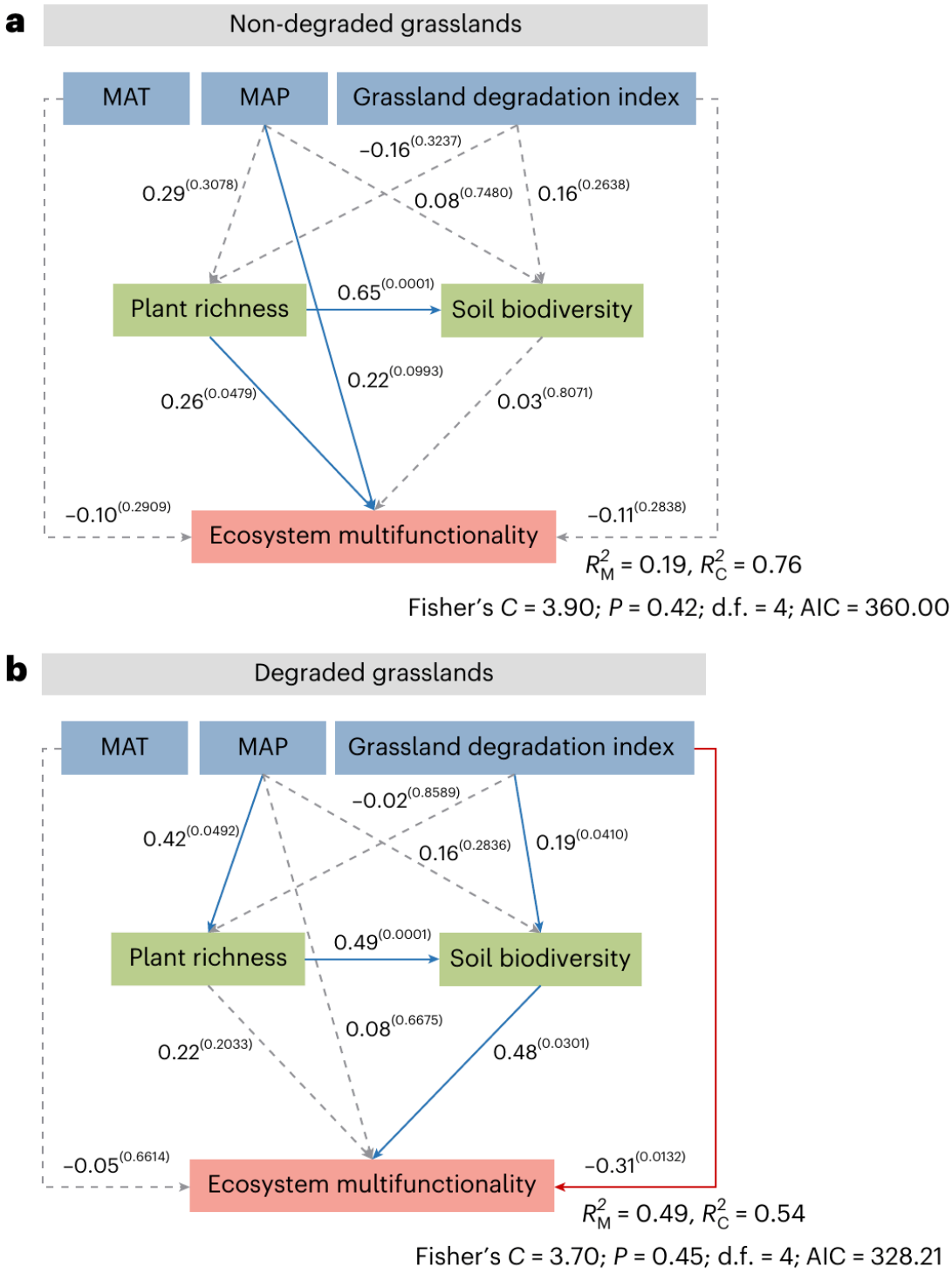


图 4

扩展数据图 1｜采样设计示意图

图注译文：在特定样点选择 3 个区组，每个区组内在非退化与退化草地各建立 1 个 30 × 30 m 样地；每个样地随机选取 3 个 1 × 1 m 样方进行植被调查并采集植物和土壤样品（9 个 0—10 cm 深度的土芯）。高程图来自 SRTM-DEM。非退化与退化草地的无人机影像对比显示，退化后植物生产力以及禾草和莎草（例如 S. purpurea 和 K. humilis）的比例下降，而杂类草（例如 L. nanum 和 S. chamaejasme）的比例上升。照片由李秦鲁于 2021 年 7 月在八宝镇（37.86° N，100.44° E，海拔 3 663 m）拍摄。ND，非退化草地；DG，退化草地。

扩展数据图 2｜非退化与退化草地生态系统多功能性（EMF）的比较

图注译文：a，平均法；b，多阈值法；c、d，基于 Hill 数的方法（c 为 q = 1，d 为 q = 2）。空心圆为样点水平的值。箱线图两端表示第 25 和第 75 四分位数，须线延伸至标准差的 1.5 倍（n = 44 个独立样点），箱内水平线为中位数。采用校正环境协变量的线性混合模型在 44 个样点上对非退化与退化草地进行比较；气候和土壤因子作为协变量，样点和草地类型作为随机因子。报告的双侧 P 值未进行多重比较校正，详细 F 统计量见补充表 1。

扩展数据图 3｜非退化与退化草地植物群落的比较

图注译文：a，禾草和莎草盖度；b，杂类草盖度。虚线表示中位数，实线表示各样点的值（n = 44 个独立样点）。采用校正环境协变量的线性混合模型在 44 个样点上对非退化与退化草地进行比较（禾草和莎草盖度：$F_{1,46.72} = 276.01$，$P = 3.10 \times 10^{-21}$；杂类草盖度：$F_{1,44.72} = 52.66$，$P = 4.40 \times 10^{-9}$；双侧 P 值未进行多重比较校正）。气候和土壤因子作为协变量，样点和草地类型作为随机因子。

扩展数据图 4｜非退化与退化草地富营养型与寡营养型细菌相对多度的差异

图注译文：a，富营养型细菌；b，寡营养型细菌。箱线图两端表示第 25 和第 75 四分位数，须线延伸至标准差的 1.5 倍（n = 44 个独立样点），箱内水平线为中位数，空心圆表示各样点的值。采用校正环境协变量的线性混合模型在 44 个样点上对非退化与退化草地进行比较（富营养型细菌：$F_{1,51.14} = 5.69$，$P = 0.0209$；寡营养型细菌：$F_{1,51.01} = 6.46$，$P = 0.0141$；双侧 P 值未进行多重比较校正）。气候和土壤因子作为协变量，样点和草地类型作为随机因子。富营养型与寡营养型细菌的划分如下：寡营养型包括 Acidobacteriota、Actinobacteriota、Planctomycetota、Chloroflexi、Verrucomicrobiota 和 Cyanobacteria；富营养型包括 Firmicutes、Gemmatimonadota、Bacteroidota 和 Proteobacteria。富营养型细菌通常生长快、资源获取能力强，而寡营养型细菌倾向于生长缓慢、资源保守。

扩展数据图 5｜非退化与退化草地克隆植物与非克隆植物盖度的差异

图注译文：a，克隆植物；b，非克隆植物。箱内水平线为中位数，空心圆表示各样点的值（n = 44 个独立样点）。采用校正环境协变量的线性混合模型在 44 个样点上对非退化与退化草地进行比较（克隆植物盖度：$F_{1,47.77} = 265.38$，$P = 3.89 \times 10^{-21}$；非克隆植物盖度：$F_{1,44.67} = 39.42$，$P = 1.24 \times 10^{-7}$；双侧 P 值未进行多重比较校正）。气候和土壤因子作为协变量，样点和草地类型作为随机因子。

扩展数据图 6｜非退化与退化草地土壤生物多样性与植物丰富度的关系

图注译文：土壤生物多样性为细菌、真菌和原生生物三类群丰富度标准化后的平均值。采用线性混合模型（n = 44 个独立样点）确定土壤生物多样性与植物丰富度之间的联系，草地类型（高寒草原、高寒草甸或沼泽化草甸）作为随机因子（非退化草地：$F_{1,42} = 27.68$，$P = 4.55 \times 10^{-6}$；退化草地：$F_{1,41.71} = 24.97$，$P = 1.09 \times 10^{-5}$；双侧 P 值未进行多重比较校正）。阴影区为 95% 置信区间，空心圆为各样点的值。在考虑环境协变量（气候和土壤因子）后，土壤生物多样性仍与植物丰富度呈显著关联。

扩展数据图 7｜非退化与退化草地毒杂草盖度的差异

图注译文：箱线图两端表示第 25 和第 75 四分位数，须线延伸至标准差的 1.5 倍，空心圆表示各样点的值（n = 44 个独立样点）。采用校正环境协变量的线性混合模型在 44 个样点上对非退化与退化草地进行比较

（$F_{1,48.06} = 34.34$，$P = 4.08 \times 10^{-7}$；双侧 P 值未进行多重比较校正）。气候和土壤因子作为协变量，样点和草地类型作为随机因子。

扩展数据图 8｜非退化与退化草地植物和微生物群落均匀度的比较

图注译文：a，植物均匀度；b，细菌均匀度；c，真菌均匀度；d，原生生物均匀度。箱线图两端表示第 25 和第 75 四分位数，须线延伸至标准差的 1.5 倍（n = 44 个独立样点），箱内水平线为中位数，空心圆表示各样点的值。采用校正环境协变量的线性混合模型在 44 个样点上对非退化与退化草地进行比较（植物：$F_{1,48.52} = 143.60$，$P = 4.15 \times 10^{-16}$；细菌：$F_{1,42.24} = 11.05$，$P = 0.0018$；真菌：$F_{1,48.86} = 4.45$，$P = 0.0400$；原生生物：$F_{1,50.95} = 0.25$，$P = 0.6211$；双侧 P 值未进行多重比较校正）。气候和土壤因子作为协变量，样点和草地类型作为随机因子。

扩展数据图 9｜非退化与退化草地微生物种间凝聚力的比较

图注译文：a，微生物正凝聚力；b，微生物负凝聚力。箱线图两端表示第 25 和第 75 四分位数，须线延伸至标准差的 1.5 倍（n = 44 个独立样点），空心圆表示各样点的值，箱内水平线为中位数。采用校正环境协变量的线性混合模型在 44 个样点上对非退化与退化草地进行比较（正凝聚力：$F_{1,49.67} = 24.93$，$P = 7.71 \times 10^{-6}$；负凝聚力：$F_{1,41.20} = 0.11$，$P = 0.7464$；双侧 P 值未进行多重比较校正）。气候和土壤因子作为协变量，样点和草地类型作为随机因子。

扩展数据图 10｜非退化与退化草地微生物群落组成的比较

图注译文：a，细菌群落组成；b，真菌群落组成；c，原生生物群落组成。图中数据为门水平微生物的相对多度。置换多元方差分析表明，草地退化后细菌、真菌和原生生物的群落组成均发生显著变化（均 $P < 0.05$）。采用校正环境协变量的线性混合模型在 44 个样点上对各微生物类群的相对多度进行比较；气候和土壤因子作为协变量，样点和草地类型作为随机因子。加号（+）和减号（−）分别表示该微生物类群在草地退化后显著增加或减少。报告的双侧 P 值均未进行多重比较校正。

三、思维导图

论文思维导图：草地退化如何改变生物多样性—生态系统多功能性关系

Grassland degradation alters plant and soil biodiversity–multifunctionality relationships | Nature Plants 2025, 11(12): 2487–2497



- **① 研究背景**
  - 人为活动与气候变化快速改变生物多样性
  - 生物多样性支撑生产力、土壤碳储与碳排放
  - BEF 关系强度可随环境改变，即使多样性不变
  - 现有证据多来自小尺度人工控制实验
  - 土壤生物多样性长期被忽视
- **② 目的与假设**
  - 核心问题：中度退化如何影响功能、多样性与二者关系？
  - H1 退化损害生态系统整体功能
  - H2 退化可促进或降低生物多样性
  - H3 多样性—EMF 关系可增强或减弱
- **③ 研究方法**
  - 青藏高原高寒草地：44 样点 / 792 样方 / 2 600 km 样带
  - 非退化与退化配对观测（空间代替时间）

- 20 项功能指标 → 加权 EMF（3 种算法互证）
- 植物丰富度 + 细菌/真菌/原生生物 ASV → 综合土壤生物多样性
- 线性混合模型 + 结构方程模型（SEM）

- **④ 研究结果**
  - 单项功能平均下降 20.3%，EMF 0.21 → 0.15
  - 植物丰富度 +2 种；综合土壤生物多样性 0.45 → 0.56
  - 植物丰富度 → EMF：0.26 → 0.22（不显著）
  - 土壤生物多样性 → EMF：0.03 → 0.48
  - 机制：克隆植物↓、毒杂草↑、pH↑、正凝聚力↑、Gemmatimonadota↑
- **⑤ 结论与意义**
  - 中度退化呈「功能降、多样性升」的反向格局
  - 支撑 EMF 的重心由地上植物多样性转向地下土壤生物多样性
  - 退化草地恢复评估应把地下生物多样性作为关键指标
  - 局限：相关不等于因果，需双因子控制实验验证

四、摘要翻译

一、英文原文

Biodiversity is known to promote ecosystem multifunctionality (EMF), but how grassland degradation influences the relationship between biodiversity and EMF remains unclear. Here, using paired observations at 44 sites (a total of 792 sampling quadrats) along a 2,600 km transect, we test how moderate grassland degradation influences 20 surrogates of ecosystem functions, EMF, plant richness, soil bacterial, fungal and protist richness, and biodiversity–EMF relationships in Tibetan alpine grasslands. Our results reveal significant declines in individual ecosystem functions and EMF with moderate grassland degradation. By contrast, both plant richness and integrated soil biodiversity exhibit significant increases. The structural equation models analyses show that following degradation, the effect of soil biodiversity on EMF strengthens, whereas that of plant richness weakens. These findings offer large-scale empirical evidence that moderate grassland degradation can amplify both soil biodiversity and its functional importance, emphasizing the key role of below-ground biodiversity in supporting ecosystem functioning in degraded grasslands.

二、中文参考译文

生物多样性已知能够促进生态系统多功能性（EMF），但草地退化如何影响生物多样性与 EMF 之间的关系，目前仍不清楚。

本研究沿一条 2 600 km 长的样带，在青藏高原高寒草地的 44 个样点（合计 792 个采样样方）开展配对观测，检验中度草地退化如何影响 20 项生态系统功能替代指标、EMF、植物丰富度、土壤细菌/真菌/原生生物丰富度以及生物多样性—EMF 关系。

结果表明，中度草地退化使各项生态系统功能和 EMF 均显著下降；与之相反，植物丰富度和综合土壤生物多样性却显著上升。

结构方程模型分析显示，退化之后土壤生物多样性对 EMF 的作用增强，而植物丰富度的作用减弱。

这些发现提供了大尺度实证证据，表明中度草地退化可同时放大土壤生物多样性及其功能重要性，凸显了地下生物多样性在支撑退化草地生态系统功能中的关键作用。

> 附记：PDF 版在正文之后附原论文完整 PDF（24 页，原样保留）；Word 版按提交要求不含该附录。

附：原论文完整 PDF（24 页）

以下页面为原论文 PDF 原样并入：保留原始页面尺寸、字体与图表排版，未作任何重新排版；页码从原论文第 1 页重新开始。

nature plants

Article

https://doi.org/10.1038/s41477-025-02147-x

Grassland degradation alters plant and soil biodiversity–multifunctionality relationships

Received: 15 October 2024

Accepted: 3 October 2025

Published online: 10 November 2025

Check for updates

Xiaoxia Gao[1,2,11], Dianye Zhang[1,2,11], Yunfeng Peng[1,2], Josep Peñuelas[3,4], Yann Hautier[5], Michel Loreau[6,7], Yaping Niu[1,2,8], Shiting Yao[1,2,9], Zan Wu[1,2], Qinlu Li[1,2], Lina Zhou[1,2], Yang Liu[1,2], Xuning Liu[1,2], Bin Wei[1,2,8], Shuqi Qin[1,2], Yutong Song[1,2,8], Luyao Kang[1,2], Lin Jiang[10], Shaopeng Wang[7] & Yuanhe Yang[1,2,8] ✉

Biodiversity is known to promote ecosystem multifunctionality (EMF), but how grassland degradation influences the relationship between biodiversity and EMF remains unclear. Here, using paired observations at 44 sites (a total of 792 sampling quadrats) along a 2,600 km transect, we test how moderate grassland degradation influences 20 surrogates of ecosystem functions, EMF, plant richness, soil bacterial, fungal and protist richness, and biodiversity–EMF relationships in Tibetan alpine grasslands. Our results reveal significant declines in individual ecosystem functions and EMF with moderate grassland degradation. By contrast, both plant richness and integrated soil biodiversity exhibit significant increases. The structural equation models analyses show that following degradation, the effect of soil biodiversity on EMF strengthens, whereas that of plant richness weakens. These findings offer large-scale empirical evidence that moderate grassland degradation can amplify both soil biodiversity and its functional importance, emphasizing the key role of below-ground biodiversity in supporting ecosystem functioning in degraded grasslands.

Anthropogenic activities and climate change are driving unprecedented changes in biodiversity[1,2]. Given the central role of biodiversity in sustaining ecosystem functioning[3], such shifts may fundamentally affect key ecosystem functions including plant productivity, soil carbon (C) storage and C emission rates, ultimately influencing the overall ecosystem multifunctionality (EMF)[4,5]. The indirect impact of changes in biodiversity on ecosystem functioning may rival or even exceed the direct effects of anthropogenic activities and climate change[6,7]. Moreover, the strength of the biodiversity–ecosystem functioning (BEF) relationships can vary under changing environmental conditions[8,9], even when biodiversity remains constant. Nevertheless, empirical evidence on how BEF relationships respond to real-world environmental changes remains scarce, with most current knowledge coming from biodiversity manipulation experiments conducted at small spatial scales[8–10]. Consequently, it remains uncertain whether the positive BEF relationships persist across natural ecosystems facing the intensified human pressures and climate change.

[1]State Key Laboratory of Forage Breeding-by-Design and Utilization; Key Laboratory of Vegetation and Environmental Change, Institute of Botany, Chinese Academy of Sciences, Beijing, China. [2]China National Botanical Garden, Beijing, China. [3]CSIC, Global Ecology Unit CREAF-CSIC-UAB, Barcelona, Spain. [4]CREAF, Cerdanyola del Vallès, Catalonia, Spain. [5]Ecology and Biodiversity Group, Department of Biology, Utrecht University, Utrecht, The Netherlands. [6]Theoretical and Experimental Ecology Station, CNRS, Moulis, France. [7]Institute of Ecology, College of Urban and Environmental Science, and State Key Laboratory for Vegetation Structure, Function and Construction (VegLab), Peking University, Beijing, China. [8]University of Chinese Academy of Sciences, Beijing, China. [9]College of Agriculture and Animal Husbandry, Qinghai University, Xining, China. [10]School of Biological Sciences, Georgia Institute of Technology, Atlanta, GA, USA. [11]These authors contributed equally: Xiaoxia Gao, Dianye Zhang. ✉e-mail: yhyang@ibcas.ac.cn

As anthropogenic activities and climate change intensify, there is a growing urgency to elucidate how environmental changes alter biodiversity and the BEF relationships across natural ecosystems. Theoretically, biodiversity may increase if environmental changes promote interspecific facilitation[11], enhance environmental heterogeneity[12] or reduce the abundance of species that monopolize resources[13]. Conversely, biodiversity may decline due to the intensified interspecific competition[14] or habitat loss[15], processes that frequently lead to species exclusion. Moreover, environmental changes can strengthen or weaken BEF relationships by enhancing or reducing the complementarity effect, because interspecific facilitation and complementarity improve community resource-use efficiency[9,16]. Environmental changes can also influence BEF relationships via other community attributes, such as species composition and evenness[17]. Particularly, when species turnover exacerbates the differences in functions provided by individual species, the positive effect of biodiversity on EMF may strengthen markedly, even if species richness remains unchanged[18]. However, current understanding of how environmental changes influence the relationship between ecosystem functioning and soil biodiversity remains limited. To date, most research has focused primarily on plant diversity[8,9], despite that soil biodiversity is increasingly recognized as a fundamental regulator of terrestrial ecosystem functioning[19]. Yet, soil communities themselves are vulnerable to anthropogenic activities and climate change[20]. This highlights a pressing need for large-scale empirical studies exploring how environmental changes influence the associations of ecosystem functioning with both above- and below-ground biodiversity in natural ecosystems.

Grasslands rank among the most extensive terrestrial ecosystems and are frequently subjected to degradation. Globally, ~49% of grasslands have undergone some degree of degradation, primarily due to anthropogenic disturbances such as overgrazing, overexploitation or climate change[21]. The Tibetan Plateau hosts the world's largest alpine grassland ecosystem, where degradation has accelerated in recent decades, with the moderate degradation stage now representing the most widespread form[22]. This degradation has often been linked to substantial changes in soil environmental conditions, ecosystem functioning and the biodiversity and composition of both plant and microbial communities[23–25]. Consequently, the Tibetan Plateau provides a unique, large spatial-scale natural setting for investigating how environmental changes influence BEF relationships. It has been reported that following grassland degradation, there is a notable decline in plant productivity. Meanwhile, the cover of highly productive grasses and sedges, which are resource-monopolizing clonal plants[26,27], decreases, while the cover of forbs increases[24,25]. Grassland degradation can also alter microbial community composition and interspecific interactions[23]. Considering these points, we hypothesize that (1) grassland degradation impairs the overall ecosystem functioning; (2) grassland degradation can promote biodiversity by providing additional niche space for the colonization of other species or decrease biodiversity following severe habitat destruction[21,25]; (3) biodiversity–EMF relationships may strengthen or weaken depending on how grassland degradation alters interspecific interactions and community composition.

To test these hypotheses, we conducted a field survey in paired non-degraded and degraded grasslands at 44 sites which were all located in the transition zone between non-degraded and degraded grasslands (Fig. 1). Grassland degradation status was assessed based on a comprehensive grassland degradation index (GDI) that integrated plant community cover, composition and key soil parameters. All degraded landscapes included in this study were classified as moderately degraded based on this index (Methods). At each site, three blocks were set up, each containing both non-degraded and degraded landforms (Extended Data Fig. 1). Within each block, a 30 m × 30 m plot was demarcated in both non-degraded and degraded grasslands. From each plot, three randomly selected 1 m × 1 m quadrats were used for vegetation surveys and collection of plant and soil samples. We measured 20 indicators of 9 ecosystem functions related to plant productivity; soil water holding capacity; pools of soil C, nitrogen (N) and phosphorus (P); C hydrolases; N hydrolases; phosphatase; and oxidases for each quadrat (Methods). Based on 16S and 18S ribosomal RNA gene amplicon sequencing, we determined both above- and below-ground biodiversity, that is, species richness of plant, bacteria, fungi and protists. In total, our study comprised 792 sampling quadrats (44 sites × 2 degradation levels × 3 blocks × 3 quadrats), encompassing ~16,000 observations of ecosystem functions and ~5 million biodiversity records (averaging ~14, 5,500, 220 and 550 records for plant, soil bacteria, fungi, and protists within each quadrat). This extensive dataset provides a robust foundation to enhance our mechanistic understanding of whether and how BEF relationships shift during grassland degradation.

Reduced ecosystem function upon grassland degradation

Our results showed that most individual ecosystem functions decreased with grassland degradation ($P < 0.05$; Fig. 2a and Supplementary Table 1), supporting our first hypothesis. The average magnitude of the decline in individual ecosystem functions was 20.3 ± 2.5% (hereafter, data are shown as mean ± standard error). EMF, calculated based on a weighted approach[28], also decreased markedly from 0.21 ± 0.02 to 0.15 ± 0.01 following degradation ($P = 0.0001$; Fig. 2b). These results were consistent across alternative EMF metrics, including averaged EMF[28], multiple-threshold EMF[29] and the EMF based on Hill numbers[30] (Extended Data Fig. 2). The decrease in EMF under grassland degradation can be attributed to several factors. First, the decline in EMF upon grassland degradation is primarily driven by livestock grazing. In fact, the degraded alpine grasslands involved in the study experience overgrazing[24]. Herbivore grazing and trampling directly damages vegetation, leading to a substantial reduction in above- and below-ground plant biomass. This decline in plant-derived organic matter inputs corresponds to diminished soil C and N pools, accompanied by reduced rates of organic matter decomposition. These changes collectively underpin the observed deterioration in EMF.

Second, the decline in EMF is associated with alterations of the plant and soil microbial communities. Grassland degradation typically leads to remarkable alterations in plant and microbial community composition[23,24]. Specifically, the relative abundance of grasses and sedges decreased, whereas that of forbs increased in degraded grasslands (Extended Data Fig. 3). Forbs are typically less productive than grasses and sedges in alpine grasslands[26], so the expansion of forbs tends to decrease EMF. Moreover, grassland degradation favours microbes that are less efficient in organic matter decomposition and nutrient turnover. For example, degradation increased the proportion of slow-growing, resource-conservative oligotrophic bacteria[31] (Extended Data Fig. 4), which may further lead to the lower EMF observed in degraded grasslands.

Third, the weakened EMF may also be attributed to the alterations of physical processes, for example, soil erosion and evapotranspiration. Specifically, grassland degradation in alpine grasslands disrupts the above-ground vegetation and below-ground mattic layer (consisting of a dense root mat[32]; Supplementary Fig. 1). The surface vegetation and mattic layer serve essential functions in decelerating water flow, preventing soil erosion and enhancing soil water holding capacity[32]. The destruction of these protective layers intensifies evapotranspiration and soil erosion and further exacerbates the decline of EMF in alpine grasslands. In addition, the enhanced compaction of soil from overgrazing[24] can restrict the penetration of oxygen, consequently reducing soil organic matter decomposition and negatively impacting EMF.

Grassland degradation increases plant richness and soil biodiversity

Our results revealed that moderate degradation significantly promoted plant species richness by 2.0 ± 0.5 species across the 44 sites

https://doi.org/10.1038/s41477-025-02147-x

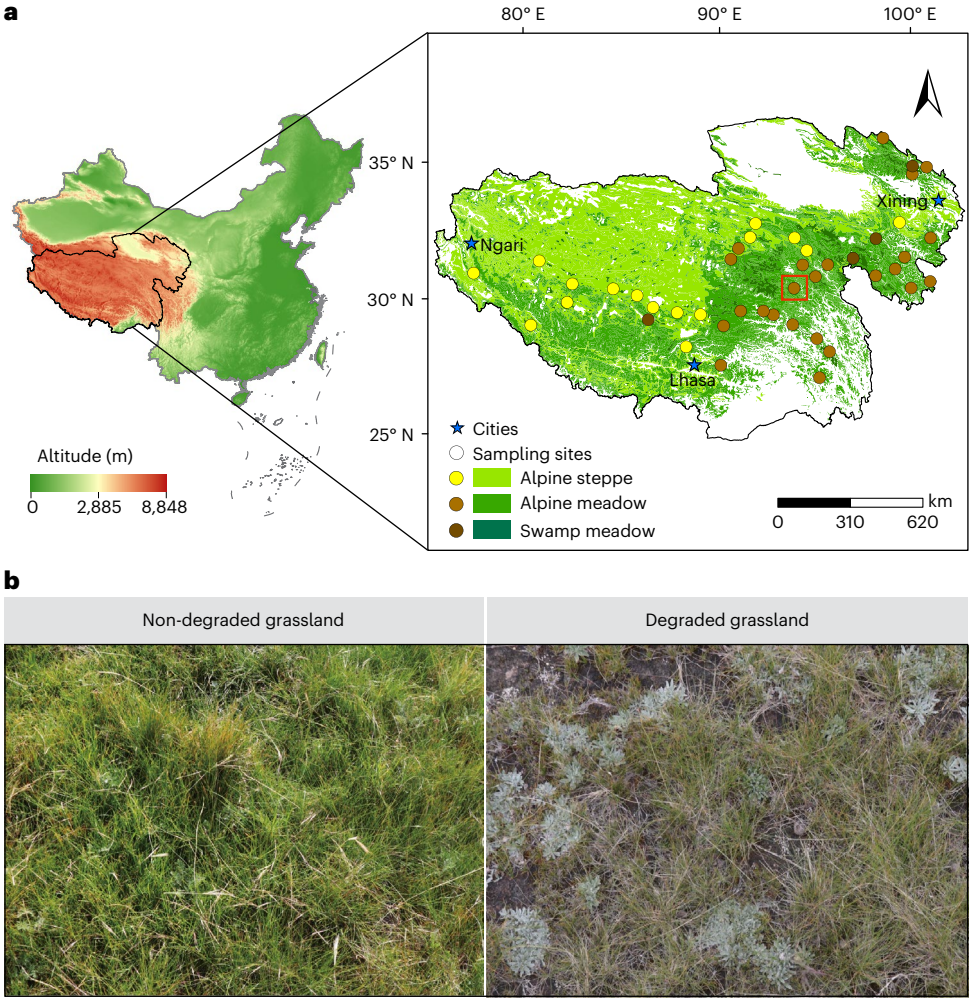


Fig. 1 | Sampling sites and vegetation community of non-degraded and degraded grasslands. a, Distributions of the 44 sampling sites in Tibetan alpine grasslands. **b**, Images of contrasting non-degraded and degraded grasslands show that plant productivity and the proportion of grasses and sedges (for example, *S. purpurea* and *K. humilis*) decreases, while the proportion of forbs (for example, *Leontopodium nanum* and *Stellera chamaejasme*) increases upon degradation. Photographs were taken in Sahuteng Town (32.91° N, 95.20° E, altitude 4,109 m; marked with a red box in **a**) in August 2021 by Xiaoxia Gao. National boundary layer in **a** from the Standard Map Service Website (https://cloudcenter.tianditu.gov.cn/administrativeDivision, approval number GS(2024)0650). Elevation data are from the Shuttle Radar Topography Mission-Digital Elevation Model[95] and vegetation data are from a digitalized map of China's vegetation, scaled at 1:1,000,000 (ref. 53).

(non-degraded versus degraded: 13.2 ± 0.9 versus 15.1 ± 1.0; $P = 0.0044$; Fig. 3a). The following two reasons may account for the observed increase in plant species richness: First, the reduction in the proportion of clonal plants enhances community diversity. In non-degraded alpine grasslands, dominant clonal species such as *Kobresia pygmaea*, *K. tibetica* and *Stipa purpurea* are able to monopolize above-ground light and below-ground nutrients through their dense ramets and unique resource-sharing strategies (interconnected ramets of a single genet can share photosynthates and nutrients via rhizomes or stolons[27]), thereby impeding the colonization and growth of other species. It follows that, in degraded conditions, the reduction in clonal plant cover ($P < 0.001$; Extended Data Fig. 5) is likely to provide additional niche space for the colonization of other plant species and thus enhance plant species richness.

Second, increased plant species richness may be linked to the alteration of environmental heterogeneity. Environmental heterogeneity is widely recognized as a fundamental driver of biodiversity, with heightened heterogeneity facilitating available habitat space for species with different niches[12]. As mentioned above, the degradation in alpine grasslands is largely attributable to overgrazing[21,24], and herbivore activities such as foraging, trampling and excretion typically increase environmental heterogeneity (Supplementary Fig. 2). This amplified environmental heterogeneity promotes species coexistence and augments plant richness in degraded grasslands. Nevertheless, it should be noted that, although moderate degradation (as in our study) can enhance plant richness, severe and extreme degradation have been shown to lead to biodiversity loss[24,25].

Similar to plant richness, we found that moderate grassland degradation augmented soil biodiversity by analysing amplicon sequence variants (ASVs) for soil bacteria, fungi and protists (Fig. 3b–e). The richness of soil bacteria, fungi and protists increased from 5,309.3 ± 127.4, 204.8 ± 6.7 and 520.2 ± 18.3 in non-degraded grasslands to 5,757.0 ± 97.9, 238.4 ± 10.1 and 581.8 ± 27.4 in degraded grasslands (all $P < 0.05$; Fig. 3c–e), respectively. The integrated soil biodiversity (mean biodiversity across the three taxa after min–max standardization[33]) also significantly increased from 0.45 ± 0.02 to 0.56 ± 0.03 across the 44 sites upon degradation ($P = 0.0002$; Fig. 3b). These increases in soil biodiversity following moderate degradation may be attributable to alterations in plant richness and soil physicochemical conditions. First, elevated plant richness likely supplies a broader

https://doi.org/10.1038/s41477-025-02147-x

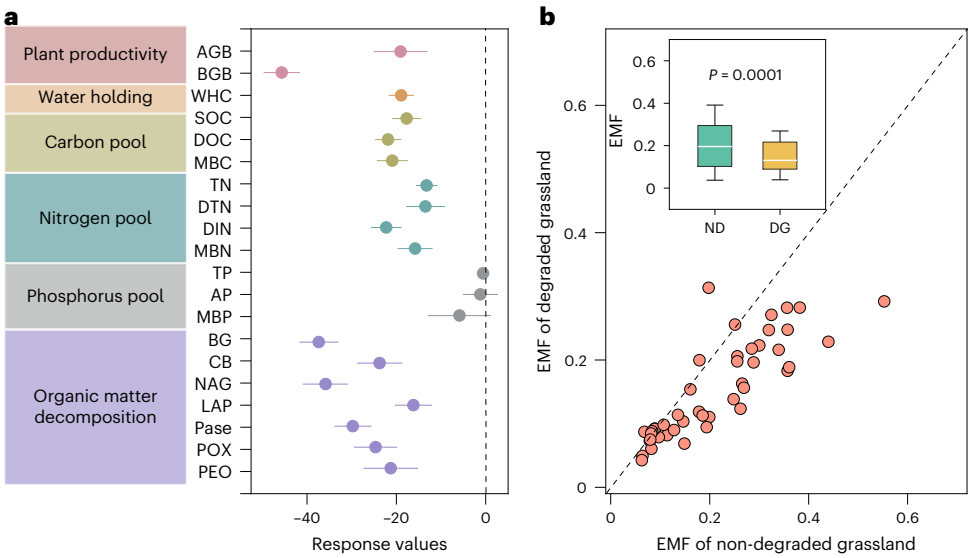


Fig. 2 | Responses of ecosystem functions to grassland degradation. **a**, The individual ecosystem functions' responses to grassland degradation. The response values are calculated as $(F_{DG} - F_{ND})/F_{ND} \times 100\%$, where F_{DG} is the value of the corresponding functions in degraded grasslands (DG), and F_{ND} is the value of corresponding functions in non-degraded grasslands (ND). The dots and the horizontal line represent means ± standard error ($n = 44$ independent sites). **b**, Comparison of EMF in non-degraded and degraded grasslands ($n = 44$ independent sites). The points (main panel) are the EMF values derived from the weighted approach[28] at the site level, and the dashed line is the 1:1 line. The ends of the box plot (insert panel) denote the 25th and 75th quartiles; whiskers extend to 1.5 times the standard deviation; the horizontal line inside each box shows the median value. Linear mixed models with a correction for environmental covariates were used to conduct statistical comparisons of individual functions and EMF between non-degraded and degraded grasslands. Climate and soil factors were treated as covariates, site and grassland type (alpine steppe, alpine meadow or swamp meadow) were treated as random factors. The reported two-sided *P* value was not corrected for multiple comparisons, and detailed *F*-statistics are presented in Supplementary Table 1. AGB, above-ground biomass; BGB, below-ground biomass; WHC, soil water holding capacity; SOC, soil organic carbon, DOC, dissolved organic carbon; MBC, microbial biomass carbon; TN, total nitrogen; DTN, dissolved total nitrogen; DIN, dissolved inorganic nitrogen; MBN, microbial biomass nitrogen; TP, total phosphorus; AP, available phosphorus; MBP, microbial biomass phosphorus; BG, β-1,4-glucosidase; CB, β-1,4-cellobiosidase; NAG, β-1,4-*N*-acetylglucosaminidase; LAP, leucine aminopeptidase; Pase, phosphatase; POX, polyphenol oxidases; PEO, peroxidase.

variety of root exudates and litter inputs, which can mitigate interspecific competition and support the coexistence of more diverse soil microbial communities[34]. In line with this point, our results showed significantly positive relationships between soil biodiversity and plant richness in both non-degraded and degraded grasslands ($P < 0.001$; Extended Data Fig. 6). Thus, soil biodiversity enhances as plant species richness increases following degradation.

Second, shifts in soil physicochemical conditions, such as pH, are also key drivers of soil biodiversity[35]. Previous studies suggest that, within a specific pH range, from acidic to weakly alkaline, soil biodiversity generally increases with soil pH[36]. Our results are consistent with this pattern, as shown by the higher soil pH observed in degraded grasslands (Supplementary Fig. 3), which may contribute to the enhanced soil biodiversity. The underlying mechanisms can be attributed to the fact that low pH accelerates the leaching of soil base cations, such as calcium ions and magnesium ions, that are essential for biological growth[37]. Furthermore, reduced pH can increase the mobilization of toxic heavy metals, including aluminium and manganese[38], posing additional threats to microbial survival. In addition, the increased soil environmental heterogeneity within degraded grassland (Supplementary Fig. 2) probably also fosters the coexistence of soil microorganisms, thereby promoting soil biodiversity[39].

Altered biodiversity–multifunctionality relationships following grassland degradation

Based on the structural equation model (SEM), we assessed the relative contributions of climate factors (mean annual temperature and precipitation), grassland degradation intensity, plant richness and soil biodiversity to EMF for both non-degraded and degraded grasslands (Fig. 4). The results showed that grassland degradation directly reduced EMF and also indirectly influenced EMF through biodiversity. In non-degraded grasslands, the standardized path coefficient of plant richness on EMF was 0.26 ($P = 0.0479$), while that in degraded grasslands was 0.22 ($P = 0.2033$). Conversely, the standardized effect of soil biodiversity on EMF increased from 0.03 ($P = 0.8071$) in non-degraded grasslands to 0.48 ($P = 0.0301$) in degraded grasslands (Fig. 4). These findings indicated that grassland degradation weakened the relationship between plant richness and EMF but strengthened the relationship between soil biodiversity and EMF.

Our finding about microbial diversity being unrelated to EMF in non-degraded grasslands (Fig. 4a) conflicts with previous studies that state that both plant richness and soil biodiversity exhibit significant positive effects on ecosystem functions across Tibetan alpine grasslands[40]. One possible explanation is that our analyses account for key confounding factors, including covariate effects (climate factors and GDI) and the random effect associated with grassland type (Supplementary Fig. 4)[41]. It is worth noting that when data were pooled across degradation states, we observed a significantly positive biodiversity–EMF relationship for plants, but not for soil biota (Supplementary Fig. 4b), even though grassland degradation reduced EMF yet promoted biodiversity. This pattern aligns with the trends observed in non-degraded grasslands. These results reflect that the effects of grassland degradation on EMF and biodiversity are less than their spatial variations across the study sites.

The observed shift in the dominant driver of EMF from plant richness in non-degraded grasslands to soil biodiversity in degraded grasslands (Fig. 4) is supported by previous studies reporting that the determinants of EMF transition from above- to below-ground diversity under harsh environmental conditions[42,43]. Given that plant production serves as the foundation of EMF, plant richness positively influences EMF in non-degraded grasslands by affecting matter and energy inputs[42]. Meanwhile, microbes in Tibetan alpine grasslands

https://doi.org/10.1038/s41477-025-02147-x

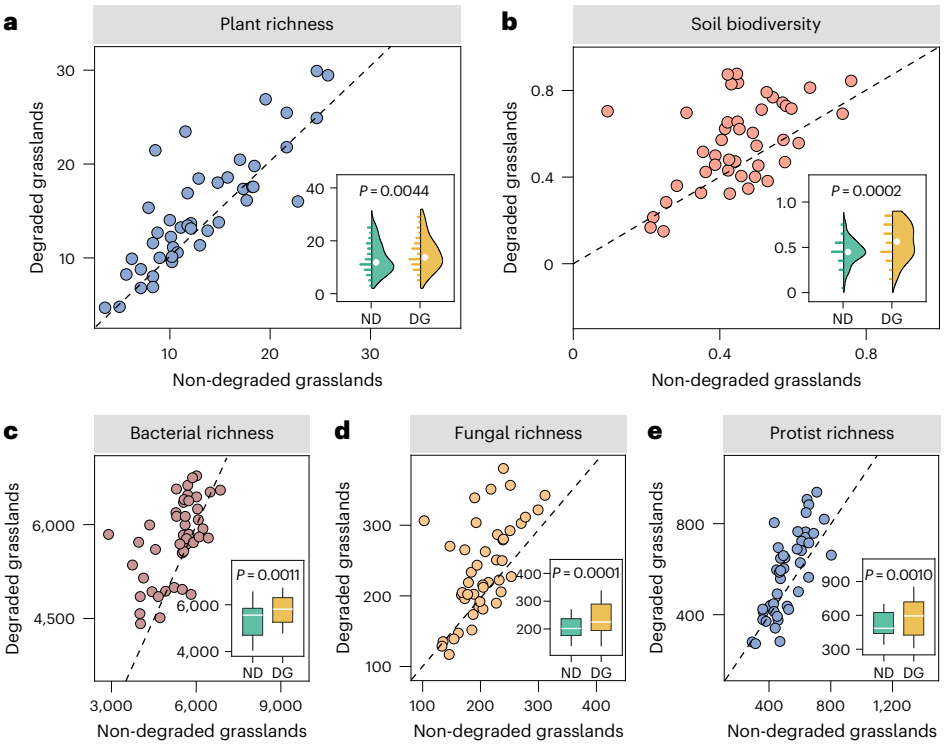


Fig. 3 | Comparisons of plant richness and soil biodiversity in non-degraded and degraded grasslands. a, Change in plant richness following grassland degradation. **b**–**e**, Changes in integrated soil biodiversity (**b**), and bacterial (**c**), fungal (**d**) and protist (**e**) richness following grassland degradation. The points (main panel) are the values for each site, and the dashed line in each panel is the 1:1 line. The white dots in insert panels in **a** and **b** represent the median values, and the points on the left-hand side show the distribution of data ($n = 44$ independent sites). The ends of the box in insert panels in **c**–**e** denote the 25th and 75th quartiles, and whiskers extend to 1.5 times the standard deviation; the horizontal line inside each box shows the median value ($n = 44$ independent sites). Plant richness was calculated as the mean number of species across the nine quadrats in each site, whereas the richness of soil bacteria, fungi and protists was determined as the mean number of amplicon sequence variants. Soil biodiversity is the mean of the standardized richness across the bacteria, fungi and protists[33,73]. Linear mixed models with a correction for environmental covariates were used to conduct statistical comparisons of biodiversity metrics between non-degraded and degraded grasslands. Climate and soil factors were treated as covariates, while site and grassland type (alpine steppe, alpine meadow or swamp meadow) were treated as random factors. ND, non-degraded grasslands; DG degraded grasslands. All the reported two-sided *P* values were not corrected for multiple comparisons, and detailed *F*-statistics are presented in Supplementary Table 1.

exhibit functional redundancy across species[44]. Collectively, only plant richness significantly affects EMF in non-degraded grasslands. By contrast, plant-derived resources decline in degraded grasslands, which enhances the dependence of ecosystem functioning on microbial decomposers[42,43]. Accordingly, soil biodiversity plays a critical role in degraded grasslands by regulating decomposition and nutrient transformation processes, thereby affecting EMF.

We further investigated the specific mechanisms driving the differential changes in above- and below-ground biodiversity–EMF relationships. These differences may be attributed to the divergent responses of interspecific interactions and community compositions to grassland degradation between plants and soil biota. For plant communities, the proportion of poisonous weeds (for example, *S. chamaejasme*; Supplementary Fig. 5) significantly increased in degraded grasslands (Extended Data Fig. 7). Poisonous weeds can inhibit the growth of neighbouring plants through the exudation of allelochemicals such as coumarins, flavonoids and phenolic compounds[45]. This suggests a probable intensification in interspecific competition but decline in complementarity effect (interspecific facilitation and resource use complementarity[46]) during grassland degradation. Concurrently, as mentioned above, the proportion of highly productive dominant grasses and sedges declined (Extended Data Fig. 3), which were associated with enhanced plant community evenness (Extended Data Fig. 8) but decreased selection effect (highly productive species promote ecosystem functioning[46]). Collectively, the weakened plant richness–EMF relationship with degradation may be due to the declines complementarity effect (increased interspecific competition) and/or downward selection effect (reductions in high functioning dominants)[9,46], although further experimental validation is required to identify the exact mechanisms.

For soil biota, the enhanced soil biodiversity–EMF relationship following grassland degradation arises from the following two aspects. First, grassland degradation may promote the interspecific facilitation and resource use complementarity among soil biota. To illustrate this point, we assessed the alteration of the complementarity effect following grassland degradation by examining the interspecific cohesion derived from species co-occurrence patterns (detailed determination of microbial cohesion is outlined in Supplementary Note 1). Cohesion serves as a widely adopted proxy for microbial interactions, with positive cohesion indicating potential complementary interactions among taxa and negative cohesion suggesting competitive interactions[47]. Our results showed that, following grassland degradation, the positive cohesion among soil microorganisms increased ($P < 0.001$; Extended Data Fig. 9), while the negative cohesion did not show a significant change ($P = 0.7464$). These results suggest that degradation promotes facilitative interactions and complementary resource use among soil microorganisms, thereby reinforcing the biodiversity–EMF relationship in degraded grasslands.

Second, the alteration in soil biodiversity–EMF relationship may result from changes in microbial community composition and evenness. Grassland degradation altered microbial community composition, notably increasing the relative abundance of Gemmatimonadota

https://doi.org/10.1038/s41477-025-02147-x

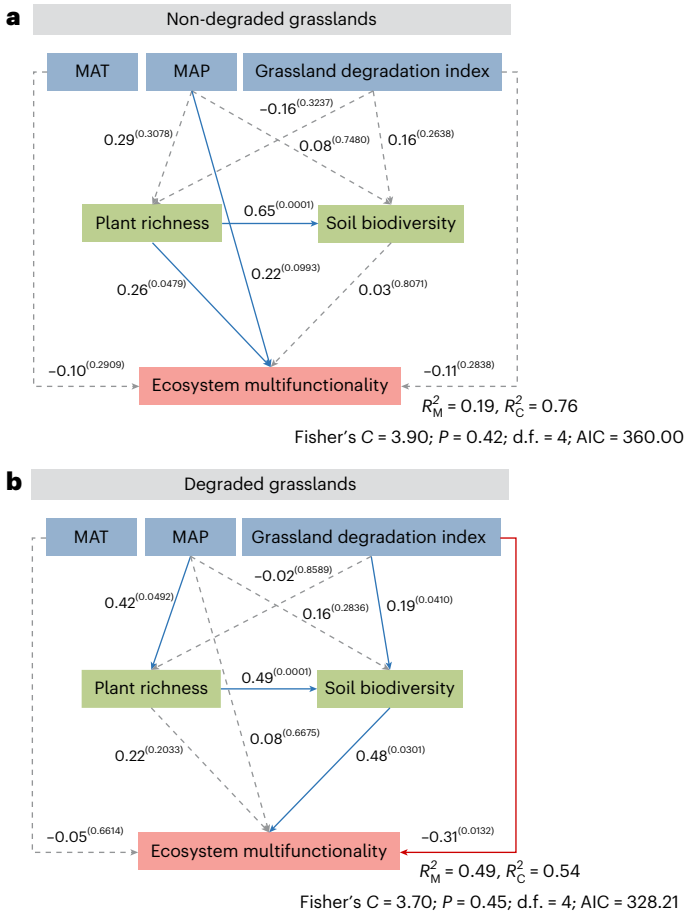


Fig. 4 | SEMs illustrating the direct and indirect effects of abiotic and biotic factors on EMF. a, Pathways of abiotic and biotic factors affecting EMF in non-degraded grasslands. **b**, Pathways of abiotic and biotic factors affecting EMF in degraded grasslands. The rationale of the SEM is shown in Supplementary Table 2. Grassland degradation index is constructed by integrating plant community cover, composition and key soil parameters, with higher values signifying more severe degradation. Soil biodiversity is the mean of the standardized richness across the bacteria, fungi and protists[33,73]. Solid arrows indicate marginal significant relationships ($P < 0.1$), with blue arrows representing positive effects and red arrows representing negative effects. Dashed black arrows denote non-significant relationships ($P \geq 0.1$). *P*ath coefficients (numbers adjacent to arrows) represent standardized regression weights, and values in top-right parentheses are the two-sided *P* values with no adjustment for multiple comparisons. During the construction of the SEM, grassland type (alpine steppe, alpine meadow or swamp meadow) was treated as the random effect. The significance of the SEMs was test using Fisher's *C* statistics. MAT, mean annual temperature; MAP, mean annual precipitation; R^2_M and R^2_C marginal and conditional R^2; AIC, Akaike information criterion.

(Extended Data Fig. 10). This phylum is known to play a critical role in nitrogen metabolism and had the potential to accelerate nutrient cycling[48]. It is well established that a higher proportion of species that increase nutrient availability can enhance BEF relationships[49]. Thus, the rise in Gemmatimonadota abundance likely contributes to the strengthened soil biodiversity–EMF relationship in degraded grasslands. Along with the enrichment of Gemmatimonadota, microbial evenness also increased (Extended Data Fig. 8). Under this scenario, elevated community evenness can promote interspecific facilitation and resource use complementarity[50] and thus enhance soil biodiversity–EMF relationship in degraded grasslands. It is important to note that, although this study linked biodiversity and EMF based on the SEM (an analysis that has been widely used in this research field[40,42,51]), statistical correlations do not necessarily reflect true causal relationships. To more rigorously assess changes in the biodiversity–EMF relationship and elucidate underlying mechanisms, future studies should implement experimental manipulations through dual-factor experiments that systematically vary both degradation levels and biodiversity.

In summary, through a comprehensive large-scale field survey across Tibetan alpine grasslands, this study investigated the effects of grassland degradation on EMF, above- and below-ground biodiversity and their interrelationships. Our results showed a significant decrease in EMF, alongside notable increases in both plant species richness and soil biodiversity in moderately degraded grasslands. The relationship between soil biodiversity and EMF was more pronounced in degraded grasslands than in non-degraded ones, while the effect of plant richness on EMF weakened. These findings suggest that below-ground biodiversity plays a critical role in sustaining ecosystem functioning in degraded grasslands, an observation that is consistent with empirical evidence showing that management practices that aim to enhance soil biodiversity (for example, addition of microbial fertilizer[52]) can effectively restore ecosystem functioning in degraded grasslands. Although previous studies have indicated that environmental changes can strengthen the relationship between plant diversity and ecosystem functioning[8,9], we present large-scale evidence for the augmentation of the association between soil biodiversity and EMF following grassland degradation. This finding emphasizes the fact that alterations in below-ground biodiversity must be considered to achieve a more comprehensive understanding of how anthropogenic activities and climate change influence ecosystem functioning.

Methods

Study area and site description

This study was carried out on the Tibetan Plateau (Fig. 1a), which covers ~2.5×10^6 km^2. It is the world's largest and highest plateau with an average elevation exceeding 4,000 m above sea level[53]. Alpine grasslands cover 60% of the plateau and comprise alpine steppe, alpine meadow and swamp meadow. Alpine steppe displays relatively low levels of plant productivity and soil organic carbon content, and the primarily dominating species are *S. purpurea* and *Carex moorcroftii*[26,54,55]. By contrast, alpine meadow and swamp meadow have relatively high levels of plant productivity and soil organic carbon content[26,54,55]. The dominating species are *K. pygmaea* and *K. humilis* in alpine meadow and *K. tibetica* in swamp meadow[26,54,55]. Alpine grasslands provide forage for ~13 million yak and 50 million Tibetan sheep[56] that support the livelihoods of 5 million pastoralists and agropastoralists. Primarily due to overgrazing, ~40% of the alpine grasslands on the Tibetan Plateau have experienced degradation[22,24,57].

To assess the impacts of grassland degradation on plant richness, soil biodiversity and ecosystem functions, we conducted an extensive field survey across the Tibetan Plateau during the peak growing seasons (July to August) of 2021 and 2022. Our study used a paired sampling design, comparing non-degraded and degraded grasslands at 44 spatially distributed sites (Fig. 1a). Details concerning geographical information and sampling year are given in Supplementary Table 3. The climate factors were similar between the two sampling years (Supplementary Fig. 6), with R^2 values for 2021–2022 mean annual temperature and mean annual precipitation being 0.94 and 0.86, respectively. The 44 study sites comprised 16 alpine steppes, 24 alpine meadows and 4 swamp meadows and spanned a wide range of climatic conditions, with mean annual temperature ranging from −4.1 to 3.2 °C and mean annual precipitation from 233 to 941 mm. According to the World Reference Base for Soil Resources classification[58], the major soil types at the sites were Cambisols, Cryosols, Calcisols, Chernozems and Kastanozems.

All the sampling sites were located in the transition zone between non-degraded and degraded grasslands. Livestock grazing has been continuously practiced across the study area for at least 40 years, with a mean grazing intensity of 88.2 ± 7.7 sheep unit per km^2 (data extracted

from ref. 59). Apart from grazing, no other management actions, such as fertilization, irrigation and sowing were observed across our study area. Both the non-degraded and degraded grasslands were grazed, but the grazing management regime at the study sites permitted winter grazing only, with no grazing allowed during the summer (the season in which samples were collected). The uneven spatial pattern of grazing (for example, degraded grasslands were typically close to the entrance of the pasture and experienced heavier grazing pressure compared to the non-degraded areas) was the primary driver for the formation of distinct patches of non-degraded and degraded grasslands within a specific site[60].

Evaluation of grassland degradation

We assessed the degree of grassland degradation at each study site by using a comprehensive GDI. The GDI integrated plant community cover, composition and key soil parameters, which are widely recognized indicators of grassland degradation[21,61,62]. The formula used to calculate GDI was as follows:

$$\begin{aligned}\mathrm{GDI} = 1 - [&(0.5 \times \text{vegetation cover} + 0.5 \times \mathrm{NDVI}) \times 1/3 \\ &+ (0.5 \times 1/\text{relative cover of degeneration indicator species} \\ &+ 0.5 \times \text{relative cover of climax species}) \\ &\times 1/3 + (1/3 \times \text{soil moisture} + 1/3 \times 1/\text{bulk density} \\ &+ 1/3 \times 1/\text{soil pH}) \times 1/3]\end{aligned} \quad (1)$$

where NDVI is the normalized differential vegetation index determined by CM1000-NDVI meter (Beijing Yinchitech), degeneration indicator species are shown in Supplementary Table 4, climax species are grasses and sedges for steppe and meadow, soil moisture is measured gravimetrically, and soil bulk density is determined by dividing the oven-dried mass of soil core by its volume (100 cm^3). In principle, these parameters should be standardized against baseline values from undisturbed grasslands before GDI calculation. However, due to data limitations, undisturbed reference values were unavailable across the broad geographic scale. Given this situation, we established site-specific baselines by using the maximum observed value for each parameter across the non-degraded areas at each site[63]. The standardization for each site was performed using the following equation:

$$\mathrm{Parameter}_{\mathrm{standardized}} = \mathrm{Parameter}_{\mathrm{observed}} / \mathrm{Parameter}_{\mathrm{baseline}} \quad (2)$$

where $\mathrm{Parameter}_{\mathrm{standardized}}$ is the standardized value used for GDI computation, $\mathrm{Parameter}_{\mathrm{observed}}$ represents the measured data, and $\mathrm{Parameter}_{\mathrm{baseline}}$ denotes the maximum value of a given metric in any of the areas at a specific site in question.

According to the GDI-based classification system, a higher GDI indicates more intensive degradation. The grassland degradation can be then categorized into four distinct levels: non-degraded (0–0.25), moderately degraded (0.25–0.50), severely degraded (0.50–0.75) and extremely degraded (0.75–1.00)[62,64]. In this study, non-degraded grasslands exhibited GDI values ranging from 0.06 to 0.23, while degraded grasslands in our study area had values between 0.25 and 0.45 (Supplementary Fig. 7). According to the GDI-based classification, all our degraded grasslands were in the moderate degradation stage, which constitutes the most widespread form of grassland degradation across the Tibetan Plateau[22,24,57]. The GDI had no significant effect on plant richness in degraded grasslands, despite incorporating information on plant community cover and composition (Supplementary Fig. 8). Thus, the GDI-based classification system was considered objective and could be reliably used to explore the response of plant richness to grassland degradation.

Plant and soil sampling

At each site, three blocks that included both non-degraded and degraded landforms were selected (Extended Data Fig. 1). The blocks were spaced ~500 m apart. Within each block, a 30 m × 30 m plot was established in both non-degraded and degraded grasslands. In each block, the non-degraded and degraded plots were separated by approximate 55 m, ranging from 50 to 100 m. Subsequently, three 1 m × 1 m sampling quadrats were randomly positioned in each 30 m × 30 m plot within which to conduct vegetation surveys and collect plant and soil samples. Thus, our study comprised 792 replicate sampling quadrats.

During the vegetation investigation, we recorded total vegetation cover and the number and cover of each species present in each 1 m × 1 m quadrat. The sward was then gathered to ground level, and three root cores were collected using a stainless auger with an 8 cm diameter from the upper 30 cm of the soil profile where ~90% of alpine grassland roots are distributed[65,66]. We carefully rinsed the root material and identified live roots by colour, flexibility and the presence of root hairs[66]. The above- and below-ground plant material was dried at 65 °C and weighed to determine above- and below-ground biomass. After sampling the plant material, we collected nine soil cores (10 cm depth) from each plot using a stainless auger (3.5 cm diameter). Following collection, soil samples were sieved through a 2 mm mesh to remove gravel and root material, then homogenized to create composite samples for subsequent analyses.

Measurements of ecosystem functions and calculation of multifunctionality

We measured 20 surrogates of ecosystem functions related to plant productivity (above- and below-ground biomass), soil water holding capacity, pools of soil C (soil organic C, dissolved organic C, microbial biomass C), N (total N, total dissolved N, dissolved inorganic N, microbial biomass N) and P (total P, available P, microbial biomass P), as well as organic matter decomposition functions (C hydrolases: β-1,4-glucosidase, β-1,4-cellobiosidase; N hydrolases: β-1,4-N-acetylglucosaminidase, leucine aminopeptidase; phosphatase; oxidases: polyphenol oxidases and peroxidase) for each of the 792 quadrats.

Above- and below-ground biomass were measured using the procedure mentioned above. Soil water holding capacity was determined by re-wetting fresh soil to saturation, followed by drying at 105 °C for 24 h. Concentrations of soil total C and N were measured using an elemental analyser (Vario EL Cube, Elementar), and soil inorganic C was measured via a solid-state infrared carbon-sulfur analyser (Multi EA 4000, Analytik Jena AG); soil organic C was then determined by subtracting inorganic C from the total C in the soil. We determined soil dissolved organic C and dissolved total N content using a multi-N/C 3100 analyser (Multi N/C 3100, Analytik Jena AG) after extraction with 0.5 M K_2SO_4 and removal of inorganic carbon with HCl. Soil dissolved inorganic N (ammonium and nitrate) concentration was determined using a continuous flow analyser (AutoAnalyzer 3, SEAL Analytic) after extraction with 1 M KCl. Soil total P concentration was quantified using inductively coupled plasma optical emission spectrometry (iCAP 6300, Thermo Fisher Scientific) following high-pressure acid digestion. Soil available P concentration was measured using the molybdenum–antimony colorimetric method[67], following extraction with a 0.5 M $NaHCO_3$ solution. Soil microbial biomass C, N and P were measured using the chloroform fumigation method[68], following a 7 day pre-incubation at 15 °C (the average summer season temperature in the study area). Universal conversion factors of 0.45, 0.54 and 0.40 were used to calculate microbial biomass C, N and P, respectively[68–70].

For the analysis of hydrolase activity, we prepared soil slurries by mixing 2.75 g of fresh soil with 91 ml of buffer (0.05 M sodium acetate). The pH of the buffer was adjusted to correspond with that of the soil. We then added 150 µl of soil slurry and 50 µl of substrate to each well of black 96-well microplates. The specific substrates for β-1,4-glucosidase, β-1,4-cellobiosidase, β-1,4-N-acetylglucosaminidase, leucine aminopeptidase and phosphatase were 4-methylumbelliferone-β-D-glucoside, 4-methylumbelliferone-β-D-cellobioside, 4-methylumbelliferone-*N*-acetyl-β-D-glucosaminide, L-leucine-7-amino-4-methylcoumarin and

4-methylumbelliferone-phosphate, respectively. The 96-well microplates were placed in a 15 °C incubator for 3 h, and the fluorescence intensity of the mixture was then measured using a microplate reader (Synergy H1MF, BioTek Instruments). The excitation and emission wavelengths were 365 and 450 nm[71]. Hydrolase activities were calculated as nanomoles per gram dry soil per hour using the fluorescence intensity and standard curve[71]. To account for quenching effects, standard curves were established for soil slurry samples and standards (4-methylumbelliferone for β-1,4-glucosidase, β-1,4-cellobiosidase, β-1,4-*N*-acetylglucosaminidase and phosphatase, and 7-amino-4-methylcoumarin for leucine aminopeptidase). Oxidase activity was assayed by adding 50 µl of substrate (polyphenol oxidases: L-3,4-dihydroxy-phenylalanine; peroxidase: L-3,4-dihydroxy-phenylalanine combined with hydrogen peroxide)[71], 200 µl of soil slurries and 50 µl EDTA to wells of transparent 96-well microplates. The microplates were incubated at 15 °C for 42 h, and a microplate reader was used to measure absorbance at 450 nm. The oxidase activities were calculated as micromoles per gram dry soil per hour.

To calculate EMF, we first standardized each of the ecosystem functions using min–max standardization methods[29]. We then calculated the weighted EMF, using agglomerative cluster analysis to down-weight highly correlated functions, following the method described by ref. 28. In addition, we calculated the averaged EMF[29], multiple-threshold EMF[29] and the EMF based on Hill numbers[30] (detailed determinations of EMF are outlined in Supplementary Note 2). Given that the weighted EMF exhibited strong associations with the EMF calculated by other approaches (all $R^2 > 0.9$; Supplementary Fig. 9), we selected the EMF index derived from the weighted approach to conduct the subsequent analyses.

Determination of plant richness and soil biodiversity

We simultaneously assessed both plant richness and soil biodiversity. Plant richness was quantified as the total count of species present in each 1 m × 1 m quadrat. Soil biodiversity was assessed based on the ASVs for soil bacteria, fungi and protists. The species richness of soil bacteria, fungi and protists was estimated by the number of ASVs based on the package vegan v2.6-4 (ref. 72). The richness values for each taxonomic group were then standardized by the min–max standardization method[33,73]. The integrated soil biodiversity was calculated by averaging the standardized richness across the three groups (bacteria, fungi and protists)[33,73].

To determine the richness of soil microorganisms, we first extracted soil DNA using the FastDNA SPIN Kit (Qbiogene/MP Biomedicals). DNA quality was evaluated based on absorbance ratios of optical density at 260/280 nm (1.8-1.9) and 260/230 nm (1.7–2.0) measured using a spectrophotometer (NanoDrop 2000, Thermo Fisher Scientific). Amplicon sequencing was then carried out for the V3–V4 regions of bacterial 16S rRNA and the V9 region of eukaryotic 18S rRNA genes using the Illumina PE250 platform with primers 338 F (5′-ACTCCTACGGGAGGCAGCAG-3′) and 806 R (5′-GGACTACHVGGGTWTCTAAT-3′) for 16S[74,75] and Euk1391f (5′-GTACACCGCCCGTC-3′) and EukBr (5′-TGATCCTTCTGC AGGTTCACCTAC-3′) for 18S[76,77], respectively.

The bioinformatics processing involved several steps using USEARCH v11.0.667 (ref. 78) and VSEARCH v2.15.2 (ref. 79). Raw reads were initially trimmed to eliminate low-quality bases (average quality score < 20 within a 10 bp moving window, and minimum length < 50 bp). Then FLASH v1.2.11 (ref. 80) was used to merge the paired-end reads with at least 10 bp overlap and fewer than 20% mismatches. Effective sequences were then distinguished based on barcode and primer sequences. Further quality control measures involved discarding sequences shorter than 200 bp and those exceeding an expected error rate of 0.01 per sequence using the -fastx_filter function[81]. After quality control, sequences were dereplicated and denoised using the UNOISE3 algorithm[82] with USEARCH v11.0.667 (ref. 78), and chimeric sequences were removed. Sequences were assigned into ASVs at the 100% identity level, as ASVs provide effective error control and enhance the robustness of downstream analyses[83]. Taxonomic information for each representative sequence (the most abundant sequence within each ASV) was annotated with a confidence threshold of ≥0.8 using SILVA v138 (ref. 84) (16S rRNA gene, https://www.arb-silva.de/) and the NCBI Nucleotide Sequence Database[85] (18S rRNA gene, annotated using BLASTN v2.14.0+ with the best hit methods, https://ftp.ncbi.nlm.nih.gov/blast/db/). ASV abundance tables were rarefied to 31,514 sequences per sample for bacteria (16S rRNA gene), 6,237 for fungi (18S rRNA gene) and 6,088 for protists (18S rRNA gene) to ensure uniform sampling depth across soil biological communities, respectively. Eukaryotic taxa, excluding fungi, metazoan and Streptophyta, were classified as protists[73].

Determination of environmental variables

Along with ecosystem functions and biodiversity metrics, we determined a series of climate (mean annual temperature and precipitation) and soil factors (soil pH and moisture) as predictors of ecosystem functions[40,86]. Among these variables, the mean annual temperature and mean annual precipitation from 2001 to 2020 were obtained from the National Tibetan Plateau Data Center of China (http://data.tpdc.ac.cn)[87]. Soil pH was measured using PB-10 (Sartorius) in a 1:2.5 soil-to-deionized-water suspension. Soil moisture was measured gravimetrically by oven-drying soil samples at 105°C for 24 h.

Statistical analyses

Before the examination of shifts of biodiversity, ecosystem functions and their relationships upon grassland degradation, we averaged the values of each of the individual metrics across the 9 quadrats within each site. This procedure was carried out because the main aim of the study was to investigate how biodiversity–EMF relationships shift upon grassland degradation across broad spatial gradients, and ecosystem heterogeneity within sites was considerably lower than that observed among sites. Thus, averaging data from the 9 quadrats can improve site-level representativeness, reduce observation error and ensure statistical robustness. This analytical approach has been widely adopted in studies with a similar experimental design to ours[40,88].

The statistical analyses were then carried out in two steps using the above site-level data. First, the differences in individual ecosystem functions, EMF, plant richness, and soil biodiversity between non-degraded and degraded grasslands were assessed using linear mixed models with a correction for environmental covariates. The formula of the linear mixed models was as follows:

$$\begin{aligned} &Y \sim \text{Degradation} + \text{Mean annual temperature} \\ &+\text{Mean annual precipitation} + \text{Soil pH} \\ &+\text{Soil moisture} + (1|\text{Site}) + (1|\text{Grassland type}) \end{aligned} \quad (3)$$

where climate and soil factors were treated as covariates, and site and grassland type (alpine steppe, alpine meadow or swamp meadow) were treated as random factors (|). Residuals of the linear mixed models were tested for homoscedasticity and normality.

Second, we conducted the SEM to illustrate the effects of abiotic and biological factors on EMF. Before the construction of the SEM, we assessed the significance of the interaction effect between grassland degradation and biodiversity on EMF[9,16] using the following formula:

$$\begin{aligned} &\text{EMF} \sim \text{Degradation} \times \text{biodiversity} + \text{Mean annual temperature} \\ &+\text{Mean annual precipitation} + \text{Soil pH} \\ &+\text{Soil moisture} + (1|\text{Site}) + (1|\text{Grassland type}) \end{aligned} \quad (4)$$

where climate and soil factors were treated as covariates, and site and grassland type (alpine steppe, alpine meadow or swamp meadow) were treated as random factors. Our results showed that plant richness and soil biodiversity exhibited significant interaction effects

with grassland degradation on the EMF (all $P < 0.05$). Accordingly, we conducted separate SEM analyses for non-degraded and degraded grasslands, respectively.

The SEM considered (1) the direct effects of climate factors (mean annual temperature and precipitation), GDI, plant richness and soil biodiversity on EMF. (2) The indirect effects of climate factors on EMF via plant and soil biodiversity. We did not consider the effects of mean annual temperature on biodiversity metrics, because previous studies reported that mean annual precipitation rather than mean annual temperature was the primary driver of the spatial pattern of biodiversity across the Tibetan alpine grasslands[40,89]. Our data also confirmed that biodiversity metrics exhibited non-significant associations with mean annual temperature (all $P > 0.05$). (3) The indirect effects of GDI on EMF via plant and soil biodiversity. (4) The indirect effects of plant richness on EMF via soil biodiversity. For more details of the SEM, see Supplementary Table 2. During the construction of the SEM, grassland type was treated as the random effect. The standardized path coefficients derived from the SEM were used to explore whether the biodiversity–EMF relationships changed upon grassland degradation. The goodness of the SEM was assessed according to Fisher's C statistic, the Akaike information criterion and the whole-model P value[90]. The linear mixed model was conducted using the lme4 R package[91], and the SEM was carried out using the piecewiseSEM R package[90]. All statistical analyses were conducted using R 4.2.3 (ref. 92).

Reporting summary

Further information on research design is available in the Nature Portfolio Reporting Summary linked to this article.

Data availability

Data used in this study are available from the figshare data repository https://doi.org/10.6084/m9.figshare.30119233 (ref. 93). The sequence data generated in this study have been deposited in the Genome Sequence Archive in National Genomics Data Center, China National Center for Bioinformation https://ngdc.cncb.ac.cn/bioproject/browse/PRJCA046361 (ref. 94). Source data are provided with this paper.

References

1. Keck, F. et al. The global human impact on biodiversity. *Nature* **641**, 395–400 (2025).
2. Blowes, S. A. et al. The geography of biodiversity change in marine and terrestrial assemblages. *Science* **366**, 339–345 (2019).
3. van der Plas, F. Biodiversity and ecosystem functioning in naturally assembled communities. *Biol. Rev.* **94**, 1220–1245 (2019).
4. Weiskopf, S. R. et al. Biodiversity loss reduces global terrestrial carbon storage. *Nat. Commun.* **15**, 4354 (2024).
5. Hautier, Y. et al. Local loss and spatial homogenization of plant diversity reduce ecosystem multifunctionality. *Nat. Ecol. Evol.* **2**, 50–56 (2018).
6. Hooper, D. U. et al. A global synthesis reveals biodiversity loss as a major driver of ecosystem change. *Nature* **486**, 105–108 (2012).
7. Tilman, D., Reich, P. B. & Isbell, F. Biodiversity impacts ecosystem productivity as much as resources, disturbance, or herbivory. *Proc. Natl Acad. Sci. USA* **109**, 10394–10397 (2012).
8. Pichon, N. A. et al. Nitrogen availability and plant functional composition modify biodiversity-multifunctionality relationships. *Ecol. Lett.* **27**, e14361 (2024).
9. Hong, P. et al. Biodiversity promotes ecosystem functioning despite environmental change. *Ecol. Lett.* **25**, 555–569 (2022).
10. Garcia, F. C., Bestion, E., Warfield, R. & Yvon-Durocher, G. Changes in temperature alter the relationship between biodiversity and ecosystem functioning. *Proc. Natl Acad. Sci. USA* **115**, 10989–10994 (2018).
11. McIntire, E. J. & Fajardo, A. Facilitation as a ubiquitous driver of biodiversity. *New Phytol.* **201**, 403–416 (2014).
12. Stein, A., Gerstner, K. & Kreft, H. Environmental heterogeneity as a universal driver of species richness across taxa, biomes and spatial scales. *Ecol. Lett.* **17**, 866–880 (2014).
13. Koerner, S. E. et al. Change in dominance determines herbivore effects on plant biodiversity. *Nat. Ecol. Evol.* **2**, 1925–1932 (2018).
14. Armstrong, R. A. & McGehee, R. Competitive exclusion. *Am. Nat.* **115**, 151–170 (1980).
15. Horváth, Z., Ptacnik, R., Vad, C. F. & Chase, J. M. Habitat loss over six decades accelerates regional and local biodiversity loss via changing landscape connectance. *Ecol. Lett.* **22**, 1019–1027 (2019).
16. Moi, D. A. et al. Human pressure drives biodiversity–multifunctionality relationships in large Neotropical wetlands. *Nat. Ecol. Evol.* **6**, 1279–1289 (2022).
17. Maestre, F. T., Castillo-Monroy, A. P., Bowker, M. A. & Ochoa-Hueso, R. Species richness effects on ecosystem multifunctionality depend on evenness, composition and spatial pattern. *J. Ecol.* **100**, 317–330 (2012).
18. Mori, A. S., Isbell, F. & Cadotte, M. W. Assessing the importance of species and their assemblages for the biodiversity ecosystem multifunctionality relationship. *Ecology* **104**, e4104 (2023).
19. Bardgett, R. D. & van der Putten, W. H. Belowground biodiversity and ecosystem functioning. *Nature* **515**, 505–511 (2014).
20. Tibbett, M., Fraser, T. D. & Duddigan, S. Identifying potential threats to soil biodiversity. *PeerJ* **8**, e9271 (2020).
21. Bardgett, R. D. et al. Combatting global grassland degradation. *Nat. Rev. Earth Environ.* **2**, 720–735 (2021).
22. Li, C., de Jong, R., Schmid, B., Wulf, H. & Schaepman, M. E. Changes in grassland cover and in its spatial heterogeneity indicate degradation on the Qinghai-Tibetan Plateau. *Ecol. Indic.* **119**, 106641 (2020).
23. Du, Y. et al. Core microbes regulate plant-soil resilience by maintaining network resilience during long-term restoration of alpine grasslands. *Nat. Commun.* **16**, 3116 (2025).
24. Zhou, H. et al. Alpine grassland degradation and its restoration in the Qinghai-Tibet Plateau. *Grasses* **2**, 31–46 (2023).
25. Zhang, W., Xue, X., Peng, F., You, Q. & Hao, A. Meta-analysis of the effects of grassland degradation on plant and soil properties in the alpine meadows of the Qinghai-Tibetan Plateau. *Glob. Ecol. Conserv.* **20**, e00774 (2019).
26. Zhang, J., Wang, J., Chen, W., Li, B. & Zhao, K. *Vegetation of Xizang (Tibet)* (Science, 1988).
27. Song, M., Dong, M. & Jiang, G. Importance of clonal plants and plant species diversity in the Northeast China Transect. *Ecol. Res.* **17**, 705–716 (2002).
28. Manning, P. et al. Redefining ecosystem multifunctionality. *Nat. Ecol. Evol.* **2**, 427–436 (2018).
29. Byrnes, J. E. K. et al. Investigating the relationship between biodiversity and ecosystem multifunctionality: challenges and solutions. *Methods Ecol. Evol.* **5**, 111–124 (2014).
30. Byrnes, J. E. K., Roger, F. & Bagchi, R. Understandable multifunctionality measures using Hill numbers. *Oikos* **2023**, e09402 (2023).
31. Stone, B. W. G. et al. Life history strategies among soil bacteria-dichotomy for few, continuum for many. *ISME J.* **17**, 611–619 (2023).
32. Zhang, G., Yang, F. & Long, H. Save the life-sustaining mattic layer on the Qinghai-Tibetan Plateau. *Innov* **4**, 100418 (2023).
33. Wagg, C., Bender, S. F., Widmer, F. & van der Heijden, M. G. Soil biodiversity and soil community composition determine ecosystem multifunctionality. *Proc. Natl Acad. Sci. USA* **111**, 5266–5270 (2014).

34. Lange, M. et al. Plant diversity increases soil microbial activity and soil carbon storage. *Nat. Commun.* **6**, 6707 (2015).
35. Fierer, N. & Jackson, R. B. The diversity and biogeography of soil bacterial communities. *Proc. Natl Acad. Sci. USA* **103**, 626–631 (2006).
36. Kamble, P. N., Gaikwad, V. B., Kuchekar, S. R. & Bååth, E. Microbial growth, biomass, community structure and nutrient limitation in high pH and salinity soils from Pravaranagar (India). *Eur. J. Soil Biol.* **65**, 87–95 (2014).
37. Tibbett, M. et al. Long-term acidification of pH neutral grasslands affects soil biodiversity, fertility and function in a heathland restoration. *Catena* **180**, 401–415 (2019).
38. Tian, Q. et al. A novel soil manganese mechanism drives plant species loss with increased nitrogen deposition in a temperate steppe. *Ecology* **97**, 65–74 (2016).
39. Li, Y. et al. Environmental heterogeneity and dispersal limitation simultaneously determine the spatial scaling of different microbial functional groups. *Sci. Total Environ.* **885**, 163854 (2023).
40. Jing, X. et al. The links between ecosystem multifunctionality and above- and belowground biodiversity are mediated by climate. *Nat. Commun.* **6**, 8159 (2015).
41. Dee, L. E. et al. Clarifying the effect of biodiversity on productivity in natural ecosystems with longitudinal data and methods for causal inference. *Nat. Commun.* **14**, 2607 (2023).
42. Hu, W. et al. Aridity-driven shift in biodiversity-soil multifunctionality relationships. *Nat. Commun.* **12**, 5350 (2021).
43. Zhang, M. et al. Experimental impacts of grazing on grassland biodiversity and function are explained by aridity. *Nat. Commun.* **14**, 1–8 (2023).
44. Qin, S. et al. Temperature sensitivity of permafrost carbon release mediated by mineral and microbial properties. *Sci. Adv.* **7**, eabe3596 (2021).
45. Zhang, Z. et al. Don't judge toxic weeds on whether they are native but on their ecological effects. *Ecol. Evol.* **10**, 9014–9025 (2020).
46. Loreau, M. & Hector, A. Partitioning selection and complementarity in biodiversity experiments. *Nature* **412**, 72–76 (2001).
47. Herren, C. M. & McMahon, K. D. Cohesion: a method for quantifying the connectivity of microbial communities. *ISME J.* **11**, 2426–2438 (2017).
48. Xun, W. B. et al. Specialized metabolic functions of keystone taxa sustain soil microbiome stability. *Microbiome* **9**, 1–15 (2021).
49. Wright, A. J., Wardle, D. A., Callaway, R. & Gaxiola, A. The overlooked role of facilitation in biodiversity experiments. *Trends Ecol. Evol.* **32**, 383–390 (2017).
50. Filstrup, C. T., King, K. B. & McCullough, I. M. Evenness effects mask richness effects on ecosystem functioning at macro-scales in lakes. *Ecol. Lett.* **22**, 2120–2129 (2019).
51. Noulèkoun, F. et al. Contrasting ecological mechanisms mediate the impact of land conversion on ecosystem multifunctionality. *Funct. Ecol.* **39**, 783–798 (2025).
52. Gu, S. et al. Microbial and chemical fertilizers for restoring degraded alpine grassland. *Biol. Fertil. Soils* **59**, 911–926 (2023).
53. Editorial Committee for Vegetation Map of China. *Vegetation Atlas of China* (Science, 2001).
54. Ding, J. et al. Decadal soil carbon accumulation across Tibetan permafrost regions. *Nat. Geosci.* **10**, 420–424 (2017).
55. Wang, Y. F. et al. Vegetation structural shift tells environmental changes on the Tibetan Plateau over 40 years. *Sci. Bull.* **68**, 1928–1937 (2023).
56. Dong, S., Zhang, Y., Shen, H., Li, S. & Xu, Y. Overview of the third pole's grasslands. in *Grasslands on the Third Pole of the World: Structure, Function, Process, and Resilience of Social-Ecological Systems* 31–72 (Springer, 2023).
57. Sun, J. et al. Nature-based solutions can help restore degraded grasslands and increase carbon sequestration in the Tibetan Plateau. *Commun. Earth Environ.* **5**, 154 (2024).
58. IUSS Working Group. *International Soil Classification System for Naming Soils and Creating Legends for Soil Maps*. World Soil Resources Reports (Food and Agriculture Organization of the United Nations, 2015).
59. Liu, B. *Actual Livestock Carrying Capacity Estimation Product in Qinghai-Tibet Plateau (2000–2019)* (National Tibetan Plateau/Third Pole Environment Data Center, 2021); https://doi.org/10.11888/Ecolo.tpdc.271513
60. Che, R. et al. Degraded patch formation significantly changed microbial community composition in alpine meadow soils. *Soil. Till. Res.* **195**, 104426 (2019).
61. Wen, L. et al. The construction of grassland degradation index for alpine meadow in Qinghai-Tibetan Plateau. *Procedia Environ. Sci.* **2**, 1966–1969 (2010).
62. Zhang, H., Chen, W., Dong, L. & Wang, W. Grassland degradation amplifies the negative effect of nitrogen enrichment on soil microbial community stability. *Glob. Change Biol.* **30**, e17217 (2024).
63. Zheng, H. et al. The implementation of ecological protection in Inner Mongolia has slowed down grassland degradation. *Fundam. Res.* https://doi.org/10.1016/j.fmre.2024.10.006 (2024).
64. Bastida, F., Luis Moreno, J., Teresa, H. & García, C. Microbiological degradation index of soils in a semiarid climate. *Soil Biol. Biochem.* **38**, 3463–3473 (2006).
65. Li, X. J. et al. Root biomass distribution in alpine ecosystems of the northern Tibetan Plateau. *Environ. Earth Sci.* **64**, 1911–1919 (2011).
66. Yang, Y., Fang, J., Ji, C. & Han, W. Above- and belowground biomass allocation in Tibetan grasslands. *J. Veg. Sci.* **20**, 177–184 (2009).
67. Olsen, S. R. *Estimation of Available Phosphorus in Soils by Extraction with Sodium Bicarbonate* (US Department of Agriculture, 1954).
68. Vance, E. D., Brookes, P. C. & Jenkinson, D. S. An extraction method for measuring soil microbial biomass C. *Soil Biol. Biochem.* **19**, 703–707 (1987).
69. Hedley, M. J., Stewart, J. W. B. & Chauhan, B. S. Changes in inorganic and organic soil phosphorus fractions induced by cultivation practices and by laboratory incubations. *Soil Sci. Soc. Am. J.* **46**, 970–976 (1982).
70. Brookes, P. C., Landman, A., Pruden, G. & Jenkinson, D. S. Chloroform fumigation and the release of soil nitrogen: a rapid direct extraction method to measure microbial biomass nitrogen in soil. *Soil Biol. Biochem.* **17**, 837–842 (1985).
71. German, D. P. et al. Optimization of hydrolytic and oxidative enzyme methods for ecosystem studies. *Soil Biol. Biochem.* **43**, 1387–1397 (2011).
72. Oksanen, J. et al. vegan: Community ecology package. R package version 2.6-4 https://CRAN.R-project.org/package=vegan (2010).
73. Delgado-Baquerizo, M. et al. Changes in belowground biodiversity during ecosystem development. *Proc. Natl Acad. Sci. USA* **116**, 6891–6896 (2019).
74. Finkel, O. M. et al. A single bacterial genus maintains root growth in a complex microbiome. *Nature* **587**, 103–108 (2020).
75. Zhang, Y. et al. Temperature fluctuation promotes the thermal adaptation of soil microbial respiration. *Nat. Ecol. Evol.* **7**, 205–213 (2023).
76. Ramirez, K. S. et al. Biogeographic patterns in below-ground diversity in New York City's Central Park are similar to those observed globally. *Proc. R. Soc. B* **281**, 20141988 (2014).
77. Amaral-Zettler, L. A., McCliment, E. A., Ducklow, H. W. & Huse, S. M. A method for studying protistan diversity using massively parallel sequencing of V9 hypervariable regions of small-subunit ribosomal RNA genes. *PLoS ONE* **4**, e6372 (2009).

78. Edgar, R. C. Search and clustering orders of magnitude faster than BLAST. *Bioinformatics* **26**, 2460–2461 (2010).
79. Rognes, T., Flouri, T., Nichols, B., Quince, C. & Mahé, F. VSEARCH: a versatile open source tool for metagenomics. *PeerJ* **4**, e2584 (2016).
80. Magoč, T. & Salzberg, S. L. FLASH: fast length adjustment of short reads to improve genome assemblies. *Bioinformatics* **27**, 2957–2963 (2011).
81. Caporaso, J. G. et al. QIIME allows analysis of high-throughput community sequencing data. *Nat. Methods* **7**, 335–336 (2010).
82. Edgar, R. C. UPARSE: highly accurate OTU sequences from microbial amplicon reads. *Nat. Methods* **10**, 996–998 (2013).
83. Callahan, B. J., McMurdie, P. J. & Holmes, S. P. Exact sequence variants should replace operational taxonomic units in marker-gene data analysis. *ISME J.* **11**, 2639–2643 (2017).
84. Quast, C. et al. The SILVA ribosomal RNA gene database project: improved data processing and web-based tools. *Nucleic Acids Res.* **41**, 590–596 (2013).
85. Federhen, S. The NCBI Taxonomy database. *Nucleic Acids Res.* **40**, 136–143 (2012).
86. Delgado-Baquerizo, M. et al. Multiple elements of soil biodiversity drive ecosystem functions across biomes. *Nat. Ecol. Evol.* **4**, 210–220 (2020).
87. Yang, K. et al. *A High-Resolution Near-Surface Meteorological Forcing Dataset for the Third Pole Region* (TPMFD, 1979–2022) (National Tibetan Plateau/Third Pole Environment Data Center, 2023); https://doi.org/10.11888/Atmos.tpdc.300398
88. Delgado-Baquerizo, M. et al. Global homogenization of the structure and function in the soil microbiome of urban greenspaces. *Sci. Adv.* **7**, eabg5809 (2021).
89. Cheng, C. et al. Plant species richness on the Tibetan Plateau: patterns and determinants. *Ecography* **1**, e06265 (2023).
90. Lefcheck, J. S. piecewiseSEM: piecewise structural equation modelling in R for ecology, evolution, and systematics. *Methods Ecol. Evol.* **7**, 573–579 (2016).
91. Bates, D., Mächler, M., Bolker, B. & Walker, S. Fitting linear mixed-effects models using lme4. *J. Stat. Softw.* **67**, 1–48 (2015).
92. R Core Team *R: A Language and Environment for Statistical Computing* (R Foundation for Statistical Computing, 2023).
93. Gao, X. et al. Grassland degradation alters plant and soil biodiversity–multifunctionality relationships. *figshare* https://doi.org/10.6084/m9.figshare.30119233 (2025).
94. Gao, X. Grassland degradation alters plant and soil biodiversity-multifunctionality relationships. *National Genomics Data Center, China National Center for Bioinformation* https://ngdc.cncb.ac.cn/bioproject/browse/PRJCA046361 (2025).
95. Jarvis, A., Reuter, H. I., Nelson, A. & Guevara, E. Hole-filled SRTM for the globe Version 4. *CGIAR-CSI SRTM 90m Database* http://srtm.csi.cgiar.org (2008).

Acknowledgements

The authors thank Z. Tang (Institute of Ecology, College of Urban and Environmental Science, Peking University), B. Schmid (Remote Sensing Laboratories, Department of Geography, University of Zurich) and N. A. Pichon (Swiss Federal Institute for Forest, Snow and Landscape Research WSL, Birmensdorf, Switzerland) for their comments and suggestions on the manuscript. This study was financially supported by the Strategic Priority Research Program of Chinese Academy of Sciences (XDA26020201, Y.Y.), the National Natural Science Foundation of China (32588202, Y.Y.; 32425004, Y.Y.; 32301501, X.G.) and the New Cornerstone Science Foundation through the XPLORER PRIZE (Y.Y.).

Author contributions

Y.Y. conceived the idea. Y.Y., D.Z. and X.G. designed the research. Y.P. and Y.Y. designed the field sampling. Y.P., X.G., Q.L., Z.W., Y.N., S.Y. and X.L. performed field samplings. X.G., Z.W., L.Z., Y.N., Y.L. and S.Y. performed the experiments. X.G. and D.Z. analysed the data. X.G., D.Z. and Y.Y. wrote the paper with inputs from J.P., Y.H., M.L., S.W., L.J., B.W., S.Q., Y.S. and L.K.

Competing interests

The authors declare no competing interests.

Additional information

Extended data is available for this paper at https://doi.org/10.1038/s41477-025-02147-x.

Supplementary information The online version contains supplementary material available at https://doi.org/10.1038/s41477-025-02147-x.

Correspondence and requests for materials should be addressed to Yuanhe Yang.

Peer review information *Nature Plants* thanks Eric Allan, Ling Wang and the other, anonymous, reviewer(s) for their contribution to the peer review of this work.

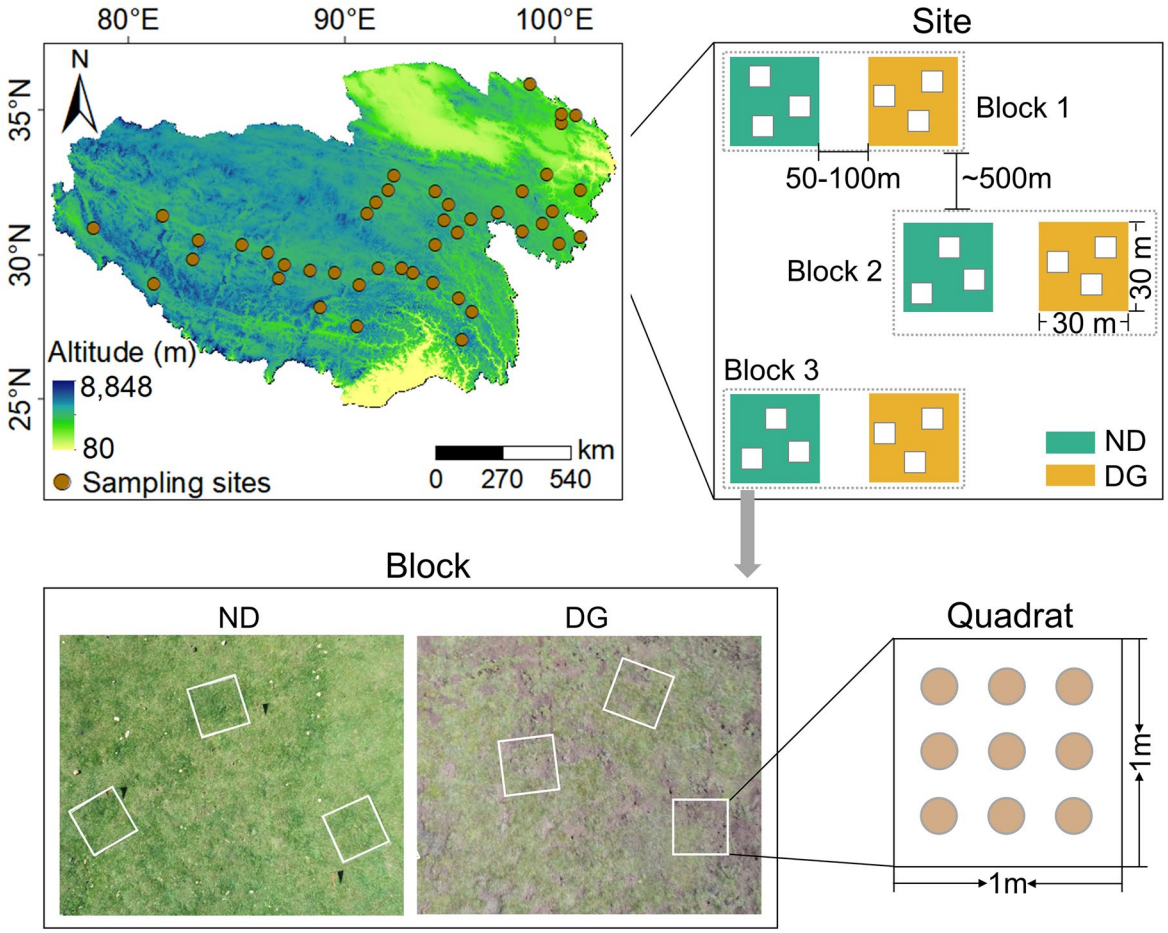
Reprints and permissions information is available at www.nature.com/reprints.

Publisher's note Springer Nature remains neutral with regard to jurisdictional claims in published maps and institutional affiliations.

Springer Nature or its licensor (e.g. a society or other partner) holds exclusive rights to this article under a publishing agreement with the author(s) or other rightsholder(s); author self-archiving of the accepted manuscript version of this article is solely governed by the terms of such publishing agreement and applicable law.

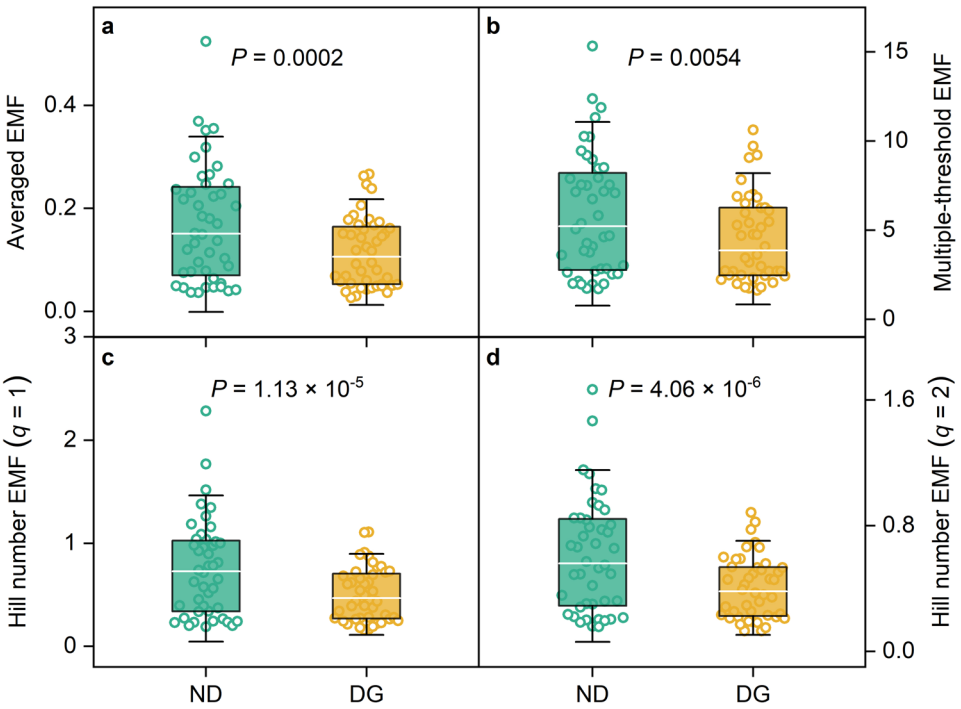
© The Author(s), under exclusive licence to Springer Nature Limited 2025

https://doi.org/10.1038/s41477-025-02147-x



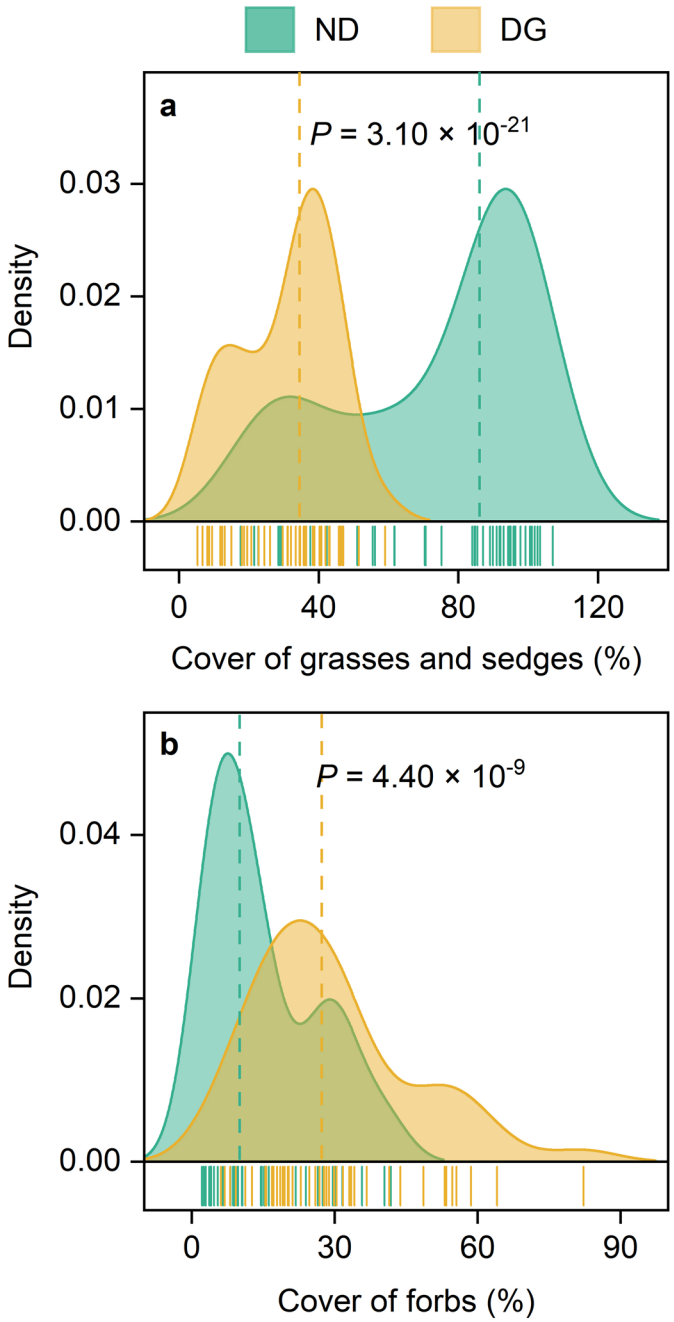
Extended Data Fig. 1 | Schematic diagram of the sampling design. At a specific site, three blocks were selected, and within each block a 30 × 30 m plot was established in both non-degraded and degraded grasslands. Within each plot, three 1 × 1 m quadrats were randomly chosen to conduct vegetation surveys and collect plant and soil samples (9 soil cores at 0-10 cm depth). Altitude map derived from the Shuttle Radar Topography Mission (SRTM)-Digital Elevation Model (DEML)[95]. Drone images of contrasting non-degraded and degraded grasslands show that plant productivity and the proportion of grasses and sedges (for example, *S. purpurea* and *K. humilis*) decreases while the proportion of forbs (for example, *L. nanum* and *S. chamaejasme*) increases upon degradation. Photos were captured by Qinlu Li in Babao Town (37.86°N, 100.44°E, altitude 3663 m), July 2021. ND, non-degraded grasslands; DG, degraded grasslands.

https://doi.org/10.1038/s41477-025-02147-x



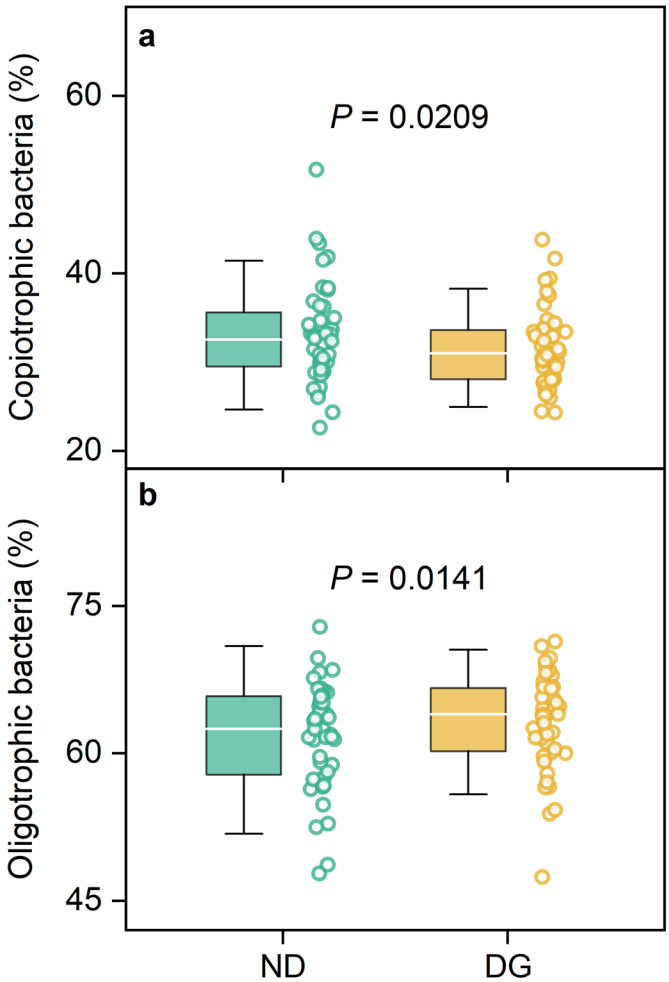
Extended Data Fig. 2 | Comparisons of ecosystem multifunctionality (EMF) between non-degraded (ND) and degraded grasslands (DG). a, Averaged approach; **b**, multiple-threshold approach; **c**, **d**, hill-number based approaches when $q = 1$ (**c**) and $q = 2$ (**d**). The open circles shown are the site-level values. The ends of a box denote the 25th and 75th quartiles, and whiskers extend to 1.5 times the standard deviation ($n = 44$ independent sites). The horizontal line within each box represents the median value. Linear mixed models with a correction for environmental covariates were employed to conduct statistical comparisons between non-degraded and degraded grasslands across the 44 sites. Climate and soil factors were treated as covariates, site and grassland type (alpine steppe, alpine meadow or swamp meadow) were treated as random factors. All the reported two-sided *P* values were not corrected for multiple comparisons, and detailed *F*-statistics were presented in Supplementary table 1.

https://doi.org/10.1038/s41477-025-02147-x



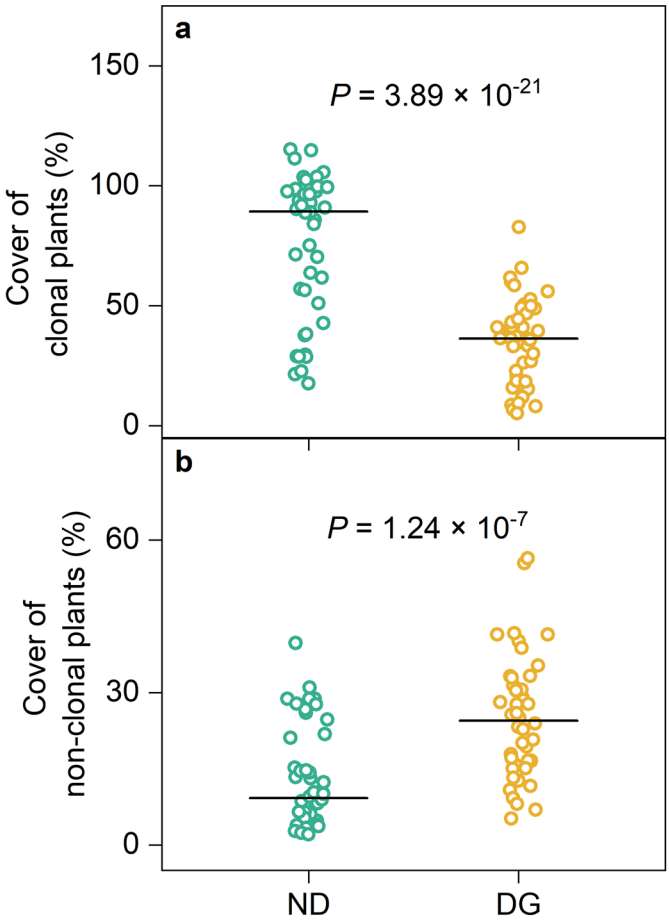
Extended Data Fig. 3 | Comparisons of plant community in non-degraded (ND) and degraded grasslands (DG). a, Cover of grasses and sedges; **b**, cover of forbs. The dashed lines indicate median values; solid lines represent the values for each site ($n = 44$ independent sites). Linear mixed models with a correction for environmental covariates were employed to conduct statistical comparisons between non-degraded and degraded grasslands across the 44 sites (cover of grasses and sedges: $F_{1,46.72} = 276.01$, $P = 3.10 \times 10^{-21}$; cover of forbs: $F_{1,44.72} = 52.66$, $P = 4.40 \times 10^{-9}$; the two-sided P values were not corrected for multiple comparisons). Climate and soil factors were treated as covariates, site and grassland type (alpine steppe, alpine meadow or swamp meadow) were treated as random factors.

https://doi.org/10.1038/s41477-025-02147-x



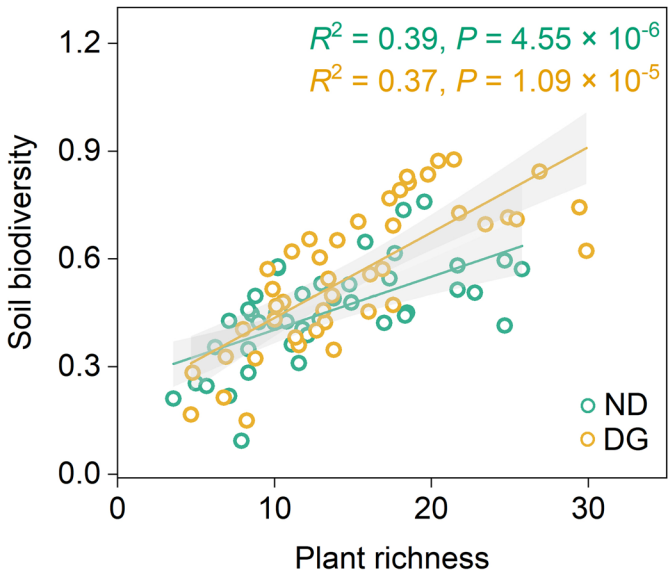
Extended Data Fig. 4 | Differences in the relative abundance of copiotrophic and oligotrophic bacteria between non-degraded (ND) and degraded grasslands (DG). a, Copiotrophic bacteria; **b**, oligotrophic bacteria. The ends of a box denote the 25th and 75th quartiles, and whiskers extend to 1.5 times the standard deviation ($n = 44$ independent sites). The horizontal line within each box represents the median value. The open circles represent the values for each site. Linear mixed models with a correction for environmental covariates were employed to conduct statistical comparisons between non-degraded and degraded grasslands across the 44 sites (copiotrophic bacteria: $F_{1,51.14} = 5.69$, $P = 0.0209$; oligotrophic bacteria: $F_{1,51.01} = 6.46$, $P = 0.0141$; the two-sided P values were not corrected for multiple comparisons). Climate and soil factors were treated as covariates, site and grassland type (alpine steppe, alpine meadow or swamp meadow) were treated as random factors. The demarcations of copiotrophic and oligotrophic bacteria were as follows[31], oligotrophs: Acidobacteriota, Actinobacteriota, Planctomycetota, Chloroflexi, Verrucomicrobiota, Cyanobacteria; copiotrophs: Firmicutes, Gemmatimonadota, Bacteroidota, Proteobacteria. Copiotrophic bacteria are generally fast-slowing and resource acquisitive, while oligotrophic bacteria tend to be slow-growing and resource conservative[31].

https://doi.org/10.1038/s41477-025-02147-x



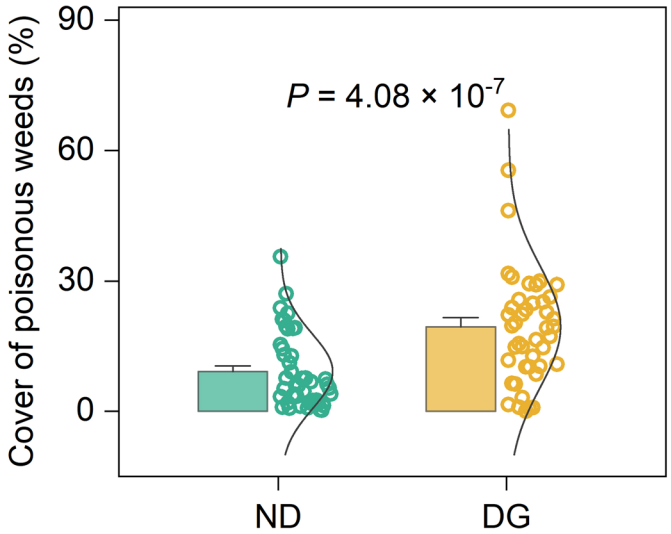
Extended Data Fig. 5 | Differences in cover of clonal and non-clonal plants in non-degraded (ND) and degraded grasslands (DG). a, Clonal plants; **b**, non-clonal plants. The horizontal line within each box represents the median value; the open circles represent the values for each site ($n = 44$ independent sites). Linear mixed models with a correction for environmental covariates were employed to conduct statistical comparisons between non-degraded and degraded grasslands across the 44 sites (cover of clonal plants: $F_{1,47.77} = 265.38$, $P = 3.89 \times 10^{-21}$; cover of non-clonal plants: $F_{1,44.67} = 39.42$, $P = 1.24 \times 10^{-7}$; the two-sided P values were not corrected for multiple comparisons). Climate and soil factors were treated as covariates, site and grassland type (alpine steppe, alpine meadow or swamp meadow) were treated as random factors.

https://doi.org/10.1038/s41477-025-02147-x



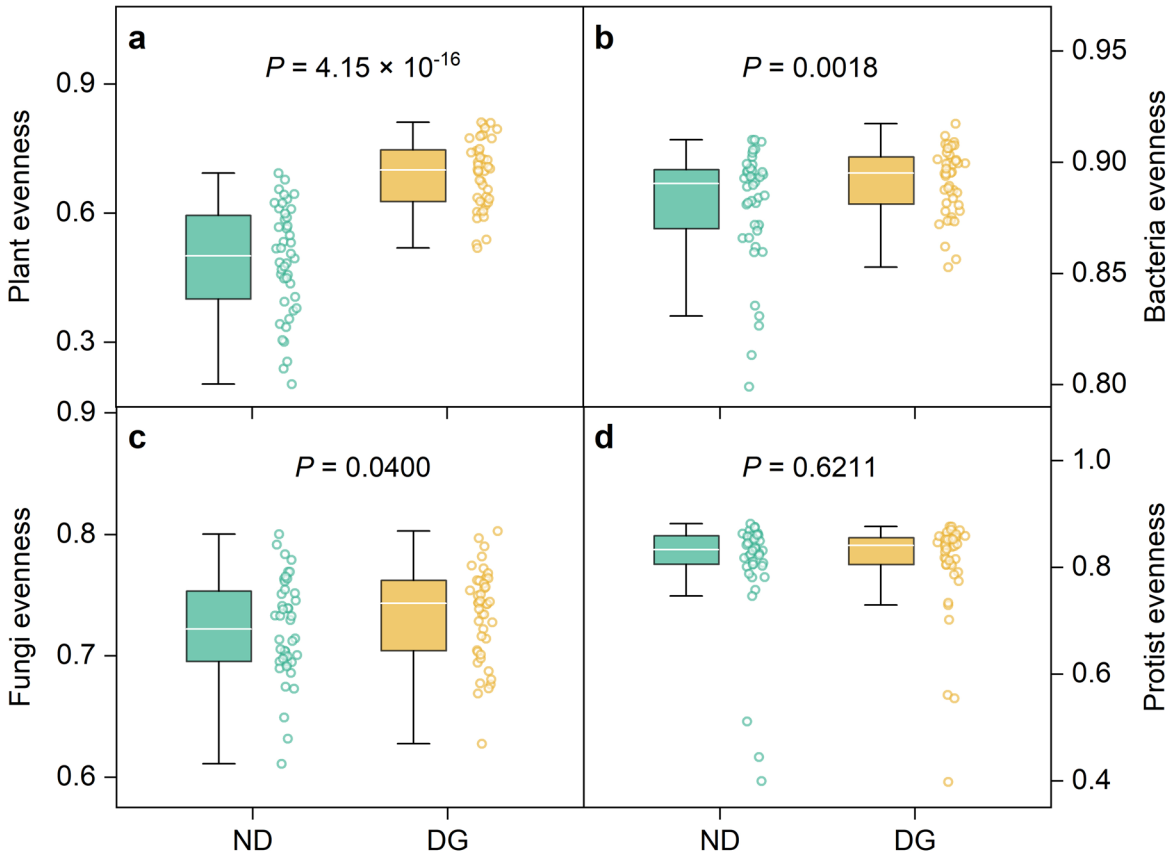
Extended Data Fig. 6 | Relationships between soil biodiversity and plant richness in non-degraded (ND) and degraded grasslands (DG). Soil biodiversity was calculated by averaging biodiversity across the three taxa (soil bacteria, fungi and protists) after standardization[33,73]. Linear mixed models (n = 44 independent sites) were used to determine the linkages between soil biodiversity and plant richness, with grassland type (alpine steppe, alpine meadow or swamp meadow) being treated as the random factor (non-degraded grasslands: $F_{1,42}$ = 27.68, P = 4.55 × 10^{-6}; degraded grasslands: $F_{1,41.71}$ = 24.97, P = 1.09 × 10^{-5}; the two-sided P values were not corrected for multiple comparisons). Shaded areas are the 95% confidence intervals; the open circles are the values for each site. Soil biodiversity still exhibited significant linkages with plant richness when considering the environmental covariates (climate and soil factors).

https://doi.org/10.1038/s41477-025-02147-x



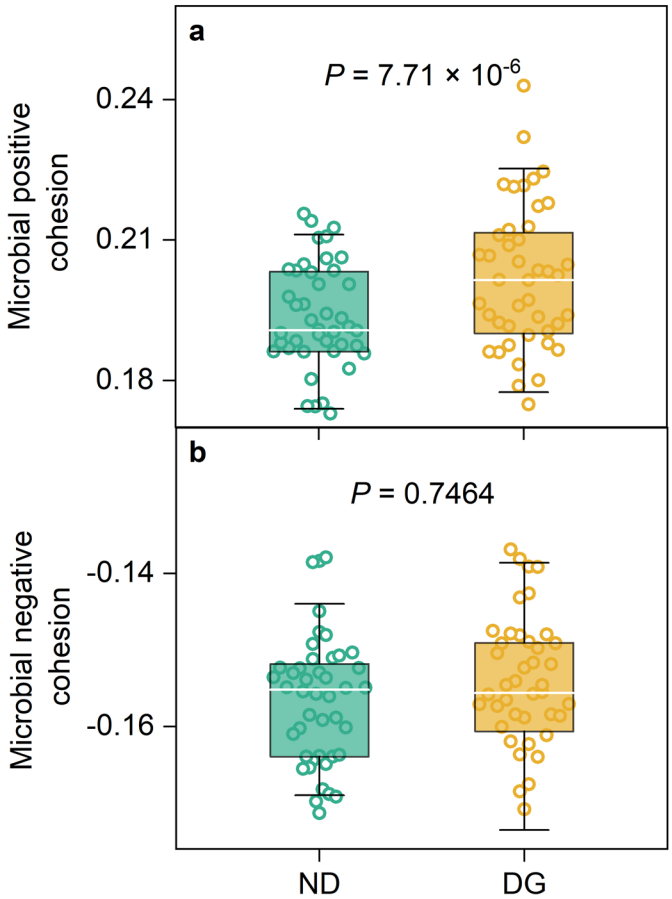
Extended Data Fig. 7 | Differences in cover of poisonous weeds in non-degraded (ND) and degraded grasslands (DG). The ends of a box denote the 25th and 75th quartiles, and whiskers extend to 1.5 times the standard deviation. The open circles represent the values for each site ($n = 44$ independent sites). Linear mixed models with a correction for environmental covariates were employed to conduct statistical comparisons between non-degraded and degraded grasslands across the 44 sites ($F_{1,48.06} = 34.34$, $P = 4.08 \times 10^{-7}$; the two-sided P value was not corrected for multiple comparisons). Climate and soil factors were treated as covariates, site and grassland type (alpine steppe, alpine meadow or swamp meadow) were treated as random factors.

https://doi.org/10.1038/s41477-025-02147-x



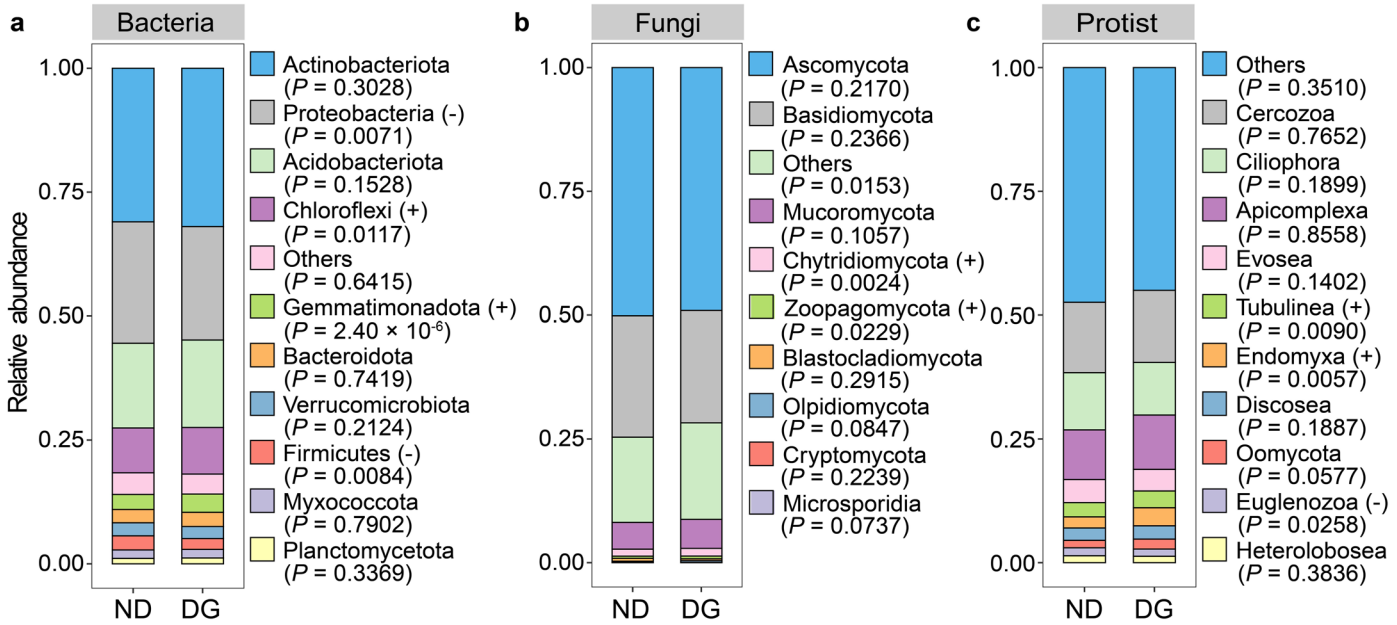
Extended Data Fig. 8 | Comparisons of plant and microbial community evenness between non-degraded (ND) and degraded grasslands (DG). **a**, Plant evenness; **b**, bacteria evenness; **c**, fungi evenness; **d**, protist evenness. The ends of a box denote the 25th and 75th quartiles, and whiskers extend to 1.5 times the standard deviation ($n = 44$ independent sites). The horizontal line within each box represents the median value. The open circles represent the values for each site. Linear mixed models with a correction for environmental covariates were employed to conduct statistical comparisons between non-degraded and degraded grasslands across the 44 sites (plant: $F_{1,48.52} = 143.60$, $P = 4.15 \times 10^{-16}$; bacteria: $F_{1,42.24} = 11.05$, $P = 0.0018$; fungi: $F_{1,48.86} = 4.45$, $P = 0.0400$; protist: $F_{1,50.95} = 0.25$, $P = 0.6211$; the two-sided P values were not corrected for multiple comparisons). Climate and soil factors were treated as covariates, site and grassland type (alpine steppe, alpine meadow or swamp meadow) were treated as random factors.

https://doi.org/10.1038/s41477-025-02147-x



Extended Data Fig. 9 | Comparisons of microbial interspecific cohesion between non-degraded (ND) and degraded grasslands (DG). a, Microbial positive cohesion; **b**, microbial negative cohesion. The ends of a box denote the 25th and 75th quartiles, and whiskers extend to 1.5 times the standard deviation ($n = 44$ independent sites). The open circles represent the values for each site, the horizontal line within each box represents the median value. Linear mixed models with a correction for environmental covariates were employed to conduct statistical comparisons between non-degraded and degraded grasslands across the 44 sites (positive cohesion: $F_{1,49.67} = 24.93$, $P = 7.71 \times 10^{-6}$; negative cohesion: $F_{1,41.20} = 0.11$, $P = 0.7464$; the two-sided P values were not corrected for multiple comparisons). Climate and soil factors were treated as covariates, site and grassland type (alpine steppe, alpine meadow or swamp meadow) were treated as random factors.

https://doi.org/10.1038/s41477-025-02147-x



Extended Data Fig. 10 | Comparisons of microbial community composition between non-degraded (ND) and degraded grasslands (DG). a, Bacterial community composition; **b**, fungal community composition; **c**, protist community composition. Data shown in this figure are the relative abundance of microbes at the level of phylum. Community composition of bacteria, fungi and protist all exhibited significant changes following degradation according to permutational multivariable analysis of variance (all $P < 0.05$). Linear mixed models with a correction for environmental covariates were employed to conduct statistical comparisons of the relative abundance of each microbial group between non-degraded and degraded grasslands across the 44 sites. Climate and soil factors were treated as covariates, site and grassland type (alpine steppe, alpine meadow or swamp meadow) were treated as random factors. The plus (+) and minus (-) signs denote that microbial taxa significantly increase or decrease, respectively, following grassland degradation. All the reported two-sided *P* values were not corrected for multiple comparisons.

nature portfolio

Corresponding author(s): Yuanhe Yang

Last updated by author(s): Sep 24, 2025

Reporting Summary

Nature Portfolio wishes to improve the reproducibility of the work that we publish. This form provides structure for consistency and transparency in reporting. For further information on Nature Portfolio policies, see our Editorial Policies and the Editorial Policy Checklist.

Statistics

For all statistical analyses, confirm that the following items are present in the figure legend, table legend, main text, or Methods section.

n/a	Confirmed	
☐	☒	The exact sample size (*n*) for each experimental group/condition, given as a discrete number and unit of measurement
☐	☒	A statement on whether measurements were taken from distinct samples or whether the same sample was measured repeatedly
☐	☒	The statistical test(s) used AND whether they are one- or two-sided *Only common tests should be described solely by name; describe more complex techniques in the Methods section.*
☐	☒	A description of all covariates tested
☐	☒	A description of any assumptions or corrections, such as tests of normality and adjustment for multiple comparisons
☐	☒	A full description of the statistical parameters including central tendency (e.g. means) or other basic estimates (e.g. regression coefficient) AND variation (e.g. standard deviation) or associated estimates of uncertainty (e.g. confidence intervals)
☐	☒	For null hypothesis testing, the test statistic (e.g. *F*, *t*, *r*) with confidence intervals, effect sizes, degrees of freedom and *P* value noted *Give P values as exact values whenever suitable.*
☒	☐	For Bayesian analysis, information on the choice of priors and Markov chain Monte Carlo settings
☒	☐	For hierarchical and complex designs, identification of the appropriate level for tests and full reporting of outcomes
☐	☒	Estimates of effect sizes (e.g. Cohen's *d*, Pearson's *r*), indicating how they were calculated

Our web collection on statistics for biologists contains articles on many of the points above.

Software and code

Policy information about availability of computer code

Data collection	No software was used in this study for data collection.
Data analysis	The following softwares were used to analyse data and draw pictures: R4.2.3, Origin Pro 2021, Arcgis 10.5

For manuscripts utilizing custom algorithms or software that are central to the research but not yet described in published literature, software must be made available to editors and reviewers. We strongly encourage code deposition in a community repository (e.g. GitHub). See the Nature Portfolio guidelines for submitting code & software for further information.

Data

Policy information about availability of data

All manuscripts must include a data availability statement. This statement should provide the following information, where applicable:

- Accession codes, unique identifiers, or web links for publicly available datasets
- A description of any restrictions on data availability
- For clinical datasets or third party data, please ensure that the statement adheres to our policy

We have uploaded the data used in this study in Figshare (https://doi.org/10.6084/m9.figshare.30119233). The swquence data has been deposited in GSA-CNCB-NGDC (https://ngdc. cncb.ac.cn/gsa/) under the accession mumber PRJCA046361.

Research involving human participants, their data, or biological material

Policy information about studies with human participants or human data. See also policy information about sex, gender (identity/presentation), and sexual orientation and race, ethnicity and racism.

Reporting on sex and gender	No human research participants.
Reporting on race, ethnicity, or other socially relevant groupings	No human research participants.
Population characteristics	No human research participants.
Recruitment	No human research participants.
Ethics oversight	No human research participants.

Note that full information on the approval of the study protocol must also be provided in the manuscript.

Field-specific reporting

Please select the one below that is the best fit for your research. If you are not sure, read the appropriate sections before making your selection.

☐ Life sciences ☐ Behavioural & social sciences ☒ Ecological, evolutionary & environmental sciences

For a reference copy of the document with all sections, see nature.com/documents/nr-reporting-summary-flat.pdf

Ecological, evolutionary & environmental sciences study design

All studies must disclose on these points even when the disclosure is negative.

Study description	Based on observations of paired non-degraded and degraded grasslands at 44 sites along a 2600 km transect, we found that the effect of soil biodiversity on ecosystem multifunctionality strengths, whereas that of plant richness weakensupon grassland degradation in Tibetan alpine grasslands.
Research sample	The field survey was carried out in the transitional zones between non-degraded and degraded grasslands. The degradation status of the grasslands was assessed based on a comprehensive grassland degradation index, which integrated plant community cover, composition, and key soil parameters. According to the grassland degradation index, all the degraded grasslands in this study were in the moderate degradation category.
Sampling strategy	At each site, three blocks were set up, with each block containing both non-degraded and degraded landforms. Within each block, we laid out a 30 × 30 m plot in both non-degraded and degraded grasslands. Three 1 × 1m quadrats were randomly chosen from each quadrat to conduct vegetation surveys and collect plant and soil samples.
Data collection	Four types of data were used in our analyses: ecosystem functions, plant diversity, soil biodiversity and climate and soil environment parameters. Of them, twenty surrogates of ecosystem functions related to soil water availability, plant biomass, pools of soil carbon, nitrogen, and phosphorus, as well as organic matter decomposition were measured by X.G., Z.W., L.Z., Y.N., Y.L. and S.Y. following the standard methods. Plant diversity was recorded during the field survey by X.G. Soil biodiversity was measured in Shanghai Majorbio Bio-pharm Technology Co., Ltd. (Shanghai, China), and analyzed by X.G.. Climate parameters were obtained from the National Tibetan Plateau Data Center of China (http://data.tpdc.ac.cn), and soil environment parameters were measured by X.G., Z.W. and S.Y..
Timing and spatial scale	The field survey was conducted in the peak growing period (July and August) of 2021 and 2022. The spatial scale of the study spans 2600 km.
Data exclusions	No data were excluded from the analyses.
Reproducibility	The study design, sampling method, lab measurements, and statistics are depicted in detail. All data and codes for reproducing the results will be available upon publication.
Randomization	Three 1 × 1 m plots were randomly chosen within each 30 × 30 m quadrats during the field survey.
Blinding	Not relevant because data collection and analysis were conducted using standardized protocols, minimizing the potential for observer bias or influence on the conclusions.

Did the study involve field work? ☒ Yes ☐ No

Field work, collection and transport

Field conditions	The mean annual temperature varied from -4.1 to 3.2 °C and mean annual precipitation varied from 233 to 941 mm across the studied 119 sites.
Location	The longitude spanned from 80.5°E to 101.5°E, the latitude spanned from 29.6°N to 38.8°N, the altitude spanned from 3432 to 4914 m across the studied 44 sites.
Access & import/export	The study site can be easily reached by cars, and the soil samples collected were transferred to the laboratory as soon as possible.
Disturbance	We minimized the disturbance to soil profile by using small size of soil corer during sampling.

Reporting for specific materials, systems and methods

We require information from authors about some types of materials, experimental systems and methods used in many studies. Here, indicate whether each material, system or method listed is relevant to your study. If you are not sure if a list item applies to your research, read the appropriate section before selecting a response.

Materials & experimental systems

n/a	Involved in the study
☒	☐ Antibodies
☒	☐ Eukaryotic cell lines
☒	☐ Palaeontology and archaeology
☒	☐ Animals and other organisms
☒	☐ Clinical data
☒	☐ Dual use research of concern
☒	☐ Plants

Methods

n/a	Involved in the study
☒	☐ ChIP-seq
☒	☐ Flow cytometry
☒	☐ MRI-based neuroimaging

Plants

Seed stocks	No seed stocks.
Novel plant genotypes	No novel plant genotypes.
Authentication	No authentication.